

# WiMAX for Smart Grid Applications and the Influence of Impulsive Noise

Oana Neagu

A Thesis  
In  
The Department  
of  
Electrical and Computer Engineering

Presented in Partial Fulfillment of the Requirements  
for the Degree of Master of Applied Science at  
Concordia University  
Montréal, Québec, Canada

October 2015

© Oana Neagu, October 2015

**CONCORDIA UNIVERSITY**  
**SCHOOL OF GRADUATE STUDIES**

This is to certify that the thesis prepared

By: Oana Neagu

Entitled: “WiMAX for Smart Grid Applications and the Influence of Impulsive Noise”

and submitted in partial fulfillment of the requirements for the degree of

**Master of Applied Science**

Complies with the regulations of the University and meets the accepted standards with respect to originality and quality.

Signed by the final Examining Committee:

\_\_\_\_\_ Chair  
Dr. R. Raut

\_\_\_\_\_ Examiner  
Dr. Y. R. Shayan

\_\_\_\_\_ Examiner  
Dr. A. Youssef

\_\_\_\_\_ Supervisor  
Dr. W. Hamouda

Approved by \_\_\_\_\_  
Chair of Department or Graduate Program Director

\_\_\_\_\_ 2015 \_\_\_\_\_  
Dean of Faculty

# Abstract

In order to adapt the power grid to today's level of electricity consumption, growing investments are made in a smart power grid. The employment of this novel architecture brings advantages such as efficiency of energy production and consumption, availability and reliability of the service, scalability, self-healing grid, environment friendly, consumer participation in electricity production with harvested energy through solar panels and wind turbines. The rising power demand curve can be restrained by a smart implementation of the new electrical power grid. The smart grid brings out an additional layer that will interconnect and manage all the generation, transmission and distribution sectors of the power grid. Many other features will be brought by the smart grid that will improve its reliability and efficiency and will lead towards renewable and sustainable energy development. In this thesis, we analyze the performances of a smart grid in which the communication layer is implemented using Worldwide Interoperability for Microwave Access (WiMAX) communication technology. Parameters such as throughput, network capacity, packet loss, latency are studied by analyzing the traffic model generated by using several applications in the Distribution Area Network (DAN) of the Smart Grid. The applications whose traffic was simulated using OPNET are the following four: metering and pricing, electrical car, video surveillance and voice support for workforce. The capacity of a base station in the distribution area network is obtained for each smart grid application individually as well as for the combined traffic of all applications. Furthermore, this thesis also discusses the effects of the impulsive noise over the communication layer. An Orthogonal Frequency Division Multiplexing (OFDM) structure using WiMAX physical layer characteristics was simulated with and without the influence of impulsive noise using MATLAB. The results highlighted the effects of the impulsive noise over performances such as

bit error rate, packet error rate, throughput and the overall capacity of the network. For a better understanding, the outcomes are presented with and without the presence of impulsive noise.

# Acknowledgement

First and foremost, I would like to express my gratitude to my supervisor, Dr. Walaa Hamouda for offering me the chance of being part of his research team. Being a thesis master student under his supervision was a great learning experience that stood out from everything else at Concordia University. I was introduced to a new research topic, guided with great patience, support and availability and for all this I am grateful. The great team that I had in the Communication Lab, was a source of inspiration for me.

Secondly, I would like to extend my gratitude to Prof. Giovanni Beltrame, from École Polytechnique de Montréal, who introduced me to the Canadian education system, by accepting me in 2012 as an intern in the MIST Lab. I would like to thank him for that and for the way in which he guided me throughout the program.

I was fortunate to have the support of my friends and family. I would like to thank my parents and sister for their everlasting support and love. My parents encouraged me and supported me in obtaining my goal, even though at the beginning it seemed very far away and hard to achieve.

Furthermore, I would like to express my greatest and deepest appreciation to my “Canadian family”, Fam. Mihi. They helped me throughout this journey by offering me a place that felt like home, acted as both friends and parents, and gave me great support and advice when I needed it.

Finally, I would like to thank my partner, Alexandru, for being next to me throughout this journey with great love and encouragement.

# Contents

Abstract .....	iii
Acknowledgement .....	v
Contents .....	vi
List of Figures .....	ix
List of Tables .....	xii
Acronyms .....	xiv
List of Symbols .....	xvii
Chapter 1 Introduction .....	1
1.1 Motivation .....	3
1.2 Thesis Contribution .....	3
1.3 Thesis Outline .....	4
Chapter 2 Background .....	6
2.1 Traditional Power Grid .....	8
2.2 Power Grid Challenges .....	10
2.3 Smart Grid .....	11
2.3.1 Smart Meters .....	13
2.3.2 Communication Layer .....	14

2.4 WiMAX Specifications .....	16
2.4.1 Introduction .....	16
2.4.2 Characteristics .....	17
2.4.3 FDD, TDD .....	20
2.4.4 Physical Layer .....	20
2.4.5 OFDM.....	25
2.5 OPNET .....	32
2.6 Impulsive Noise.....	34
2.6.1 Literature Review .....	35
2.6.2 Characteristics of the Impulsive Noise.....	36
Chapter 3 Smart Grid Applications.....	40
3.1 Metering and Pricing Application .....	41
3.2 Video Surveillance .....	45
3.3 Electrical Car Application.....	47
3.4 Voice Application for Workforce.....	48
3.5 Comparative Analysis between Applications.....	49
3.5.1 Packet Loss Performance.....	49
3.5.2 Latency Performance.....	51
3.6 Simulations.....	52
3.6.1 Constant Distribution of Applications' Profiles.....	53
3.6.2 Random Distribution of Applications' Profiles .....	55
3.6.3 Single Collector .....	55
3.6.4 Multiple Collectors.....	59
Chapter 4 Effects of Impulsive Noise over the Communication Layer.....	62
4.1 Applications Requirements .....	63

4.2 Simulations Results .....	65
4.2.1 BER Performance .....	66
4.2.2 PER Performance .....	74
4.2.3 Throughput Performance .....	79
4.2.4 Capacity of the Base Station.....	82
4.2.5 Throughput Performance for Fixed traffic .....	82
Chapter 5 Conclusions and Future Work .....	84
5.1 Conclusions .....	84
5.2 Future work .....	85
Chapter 6 Resources .....	87



# List of Figures

Figure 2.1 Supply and demand of primary and secondary electricity (Canada) [1] .....	7
Figure 2.2 Total Electricity Demand in Canada (2013) [2] .....	7
Figure 2.3 The classic view of the power grid [4] .....	9
Figure 2.4 Population projected by Statistics Canada along with the electricity requirement for residential usage [1]. .....	10
Figure 2.5 Typical daily power consumption on a Wednesday in Ontario .....	12
Figure 2.6 Information flow in the Smart Grid.....	13
Figure 2.7 Conceptual System Architecture for the Smart Grid [13] .....	15
Figure 2.8 Distributed and adjacent subcarrier allocation [23].....	22
Figure 2.9 OFDMA versus OFDM: sub-channels and sub-carriers [23].....	25
Figure 2.10 Transmitter for OFDM-WiMAX System [26].....	26
Figure 2.11 Impulsive Channel system.....	28
Figure 2.12 Receiver for OFDM-WiMAX System [26].....	29
Figure 2.13 The Application Model Hierarchy [33] .....	32
Figure 2.14 Impulsive Noise Amplitude .....	38
Figure 3.1 Smart Grid Infrastructure between NAN and DAN .....	41
Figure 3.2 Metering and Pricing application message transmission.....	43
Figure 3.3 Throughput (kbps) generated by 1 collector which uses the Metering and Pricing Application over 1 hour .....	44
Figure 3.4 Capacity performance when Metering and Pricing application is employed (UPLINK) .....	44

Figure 3.5 Capacity performance when Video Surveillance application is employed .....	46
Figure 3.6 Capacity performance when Electric Car application is employed.....	48
Figure 3.7 Capacity performance when Voice application is employed.....	49
Figure 3.8 Packet Loss Performance when the number of collectors is increased .....	50
Figure 3.9 Latency performance when different applications are employed.....	51
Figure 3.10 Throughput Performance for 1 Collector over 15 minutes, when all the applications are using the same constant start-time distribution.....	53
Figure 3.11 Throughput Performance for up to 6 collectors over 1 hour, when all the applications have the same start time.....	54
Figure 3.12 Network Topology of 1 Collector: 1 node which aggregates the information from 4000 smart meters, 4 nodes- Voice Application, 6 nodes- Electrical Car Application, 1 node - Video Application. ....	55
Figure 3.13 Throughput (Mbps) of 1 collector over 1 hour simulation.....	56
Figure 3.14. Throughput of all applications from 1 collector over 1 hour simulation: a) Metering + Pricing Application, b) Video Surveillance Application, c) Voice Application, d) Electric Car Application.....	58
Figure 3.15 Network topology for 9 collectors.....	59
Figure 3.16 Throughput performance for different number of collectors over 1 hour simulation	60
Figure 3.17 Throughput performance vs Number of Collectors, random traffic.....	60
Figure 3.18 a)Packet loss ratio performance, random traffic b)Latency performance, random traffic.....	61
Figure 4.1 BER vs $Eb/N_0$ , SIR= -15dB, Electrical Car Application.....	68
Figure 4.2 BER vs $Eb/N_0$ , SIR= -10dB, Electrical Car Application.....	69
Figure 4.3 BER vs $Eb/N_0$ , SIR=-5dB, Electrical Car Application.....	69
Figure 4.4 BER vs $Eb/N_0$ , SIR=-15dB, Metering Application .....	70
Figure 4.5 BER vs $Eb/N_0$ , SIR=-10dB, Metering Application .....	70
Figure 4.6 BER vs $Eb/N_0$ , SIR=-5dB, Metering Application .....	71
Figure 4.7 BER vs $Eb/N_0$ , SIR=-15dB, Video Surveillance Application .....	71
Figure 4.8 BER vs $Eb/N_0$ , SIR=-10dB, Video Surveillance Application .....	72
Figure 4.9 BER vs $Eb/N_0$ , SIR=-5dB, Video Surveillance Application .....	72
Figure 4.10 BER vs $Eb/N_0$ , SIR=-15dB, Voice Application.....	73

Figure 4.11 BER vs $E_b/N_0$ , SIR=-10dB, Voice Application .....	73
Figure 4.12 BER vs $E_b/N_0$ , SIR=-5dB, Voice Application .....	74
Figure 4.13 PER vs $E_b/N_0$ , $p=0.001$ , Electrical Car Application .....	75
Figure 4.14 PER vs $E_b/N_0$ , $p=0.0001$ , Electrical Car Application .....	76
Figure 4.15 PER vs $E_b/N_0$ , $p=0.001$ , Metering Application .....	76
Figure 4.16 PER vs $E_b/N_0$ , $p=0.0001$ , Metering Application .....	77
Figure 4.17 PER vs $E_b/N_0$ , $p=0.001$ , Video Surveillance Application .....	77
Figure 4.18 PER vs $E_b/N_0$ , $p=0.0001$ , Video Surveillance Application .....	78
Figure 4.19 PER vs $E_b/N_0$ , $p=0.001$ , Voice Application .....	78
Figure 4.20 PER vs $E_b/N_0$ , $p=0.0001$ , Voice Application .....	79
Figure 4.21 Throughput Performance vs $E_b/N_0$ for AWGN and Impulsive Noise Channels for the Electrical Car Applications .....	80
Figure 4.22 Throughput Performance vs $E_b/N_0$ for AWGN and Impulsive Noise Channels for the Metering Application .....	80
Figure 4.23 Throughput Performance vs $E_b/N_0$ for AWGN and Impulsive Noise Channels for Video Surveillance Application .....	81
Figure 4.24 Throughput Performance vs $E_b/N_0$ for AWGN and Impulsive Noise Channels for Voice Application .....	81
Figure 4.25 Number of collectors for each application that can be supported by the Base Station (AWGN and Impulsive Noise) when the start time is fixed .....	82
Figure 4.26 Number of collectors that can be supported by the Base Station (AWGN and Impulsive Noise) when all applications are sending information in the same time. ....	83

# List of Tables

Table 2.1 Comparison of different communication standards [21] .....	17
Table 2.2 WiMAX Frequency bands [19].....	18
Table 2.3 WiMAX Scheduling Services [20] .....	19
Table 2.4 WiMAX Physical Layers [23].....	21
Table 2.5 OFDMA Scalability Parameters [20].....	23
Table 2.6 Supported Codes and Modulation [20].....	23
Table 2.7 Mobile WiMAX Physical Layer Data Rates with PUSC Sub-Channel [20] .....	24
Table 2.8 Parameters of the Gaussian and Bernoulli distribution [46]:.....	38
Table 3.1 Metering and Pricing Application Configuration [21].....	42
Table 3.2 Video Surveillance Application Configuration [21] .....	46
Table 3.3 Electric Car Application Configuration [21].....	47
Table 3.4 Voice Application Configuration [21].....	48
Table 3.5 Base station and subscriber stations configuration .....	52
Table 3.6 WiMAX configuration parameters.....	52
Table 3.7 Distribution of subscriber stations in one neighborhood .....	56
Table 4.1 System Attributes .....	64
Table 4.2 Subcarrier Allocations for the employed applications .....	65
Table 4.3 BER values when $E_b/N_0=8$ dB, $p=0.0005$ and the gain of BER between the results with AWGN and Impulsive noise .....	67
Table 4.4 Uplink Packet sizes for all applications .....	74
Table 4.5 PER, $E_bN_0 = 12dB$ , SIR=-15dB $p=0.001$ and $p=0.0001$ .....	75

Table 4.6 Maximum number of Collectors for fixed start-time distribution ..... 83

# Acronyms

ACORD	Appliance Coordination
AMC	Adaptive Modulation and Coding
AMI	Advanced Metering Infrastructure
AWGN	Additive White Gaussian Noise
BB-PLC	Broadband over Power Line
BE	Best Effort
BER	Bit Error Rate
BS	Base Station
CC	Convolutional Code
CCP	Condition Plans
CTC	Convolutional Turbo Code
DAN	Distribution Area Network
DL	Downlink
DSL	Digital Subscriber Line
EMU	Energy Management Unit
ertPS	Extended Real-Time Polling Service
ESI	Energy Service Interface
FDD	Frequency Division Multiplexing
FDMA	Frequency Division Multiplexing Access
FFT	Fast Fourier Transform
FTP	File Transfer Protocol

FUSC	Fully Used Subchannelization
GPRS	General Packet Radio Service
IFFT	Inverse Fast Fourier Transform
iHEM	in-Home Energy Management
IN	Impulsive Noise
IPT	Interpolling Time
LOS	Line of Sight
LTE	Long Term Evolution
MAC	Media Access Control
MAN	Metropolitan Area Network
MIMO	Multiple Input Multiple Output
NAN	Neighborhood Area Network
NB-PLC	Narrowband Power Line Communication
NC	Network Coding
NLOS	Non Line of Sight
NoNC	Non-Network Coding
nrtPL	Non-Real-Time Polling Service
OFDM	Orthogonal Frequency Division Multiplexing
OFDMA	Orthogonal Frequency Division Multiplexing Access
PDF	Probability Density Function
PER	Packet Error Rate
PHEV	Plug-in Hybrid Electrical Vehicle
PHY	Physical Layer
PLC	Power Line Communication
PMF	Probability Mass Function
PUSC	Partially Used Subchannelization
QAM	Quadrature Amplitude Modulation
QoS	Quality of Service
QPSK	Quadrature Phase Shift Keying
RTP	Real Time Plans
rtPS	Real-Time Polling Service

SIR	Signal to Interference Ratio
SNR	Signal to Noise Ratio
SUI	Stanford University Interim Channel Model
TCP	Transmission Control Protocol
TDD	Time Division Multiplexing
TDMA	Time Division Multiplexing Access
TOU	Time of Use
UDP	User Datagram Protocol
UGS	Unsolicited Grant Service
UL	Uplink
UMTS	Universal Mobile Telecommunications system Networks
WAN	Wide Area Network
WiMAX	Worldwide Interoperability for Microwave Access
WirelessHUMAN	Wireless High-speed Unlicensed Metropolitan Area Network
WirelessMAN-OFDM	Wireless Metropolitan Area Network Orthogonal Frequency Division Multiplexing
WirelessMAN-OFDMA	Wireless Metropolitan Area Network Orthogonal Frequency Division Multiplexing Access
WirelessMAN-SC	Wireless Metropolitan Area Network Single Carrier
WirelessMAN-SCa	Wireless Metropolitan Area Network Single Carriers Access
WSN	Wireless Sensor Networks



# List of Symbols

$X_s(\omega)$	Duration of the sth OFDM symbol, frequency domain
$\tilde{x}_s(t)$	Duration of the sth OFDM symbol, time domain
$\Xi_{T_u}$	Unity amplitude rectangular pulse of duration $T_u$
$\tilde{s}(t)$	Transmitted complex baseband signal
$s(t)$	Carrier frequency
$f_x(x)$	Probability density function
$\sigma_m^2$	Noise variance
$P_r$	Probability mass function
$\mu$	Gaussian mean
$\sigma_\omega^2$	Gaussian variance
$\phi_g(\omega_1)$	Gaussian characteristic function
$\phi_b(\omega_2)$	Bernoulli Characteristic Function
$\sigma_i^2$	Impulsive noise variance
$\phi_{In}(\omega_1, \omega_2)$	Impulsive Noise Characteristic Function
$\phi_{Nt}(\omega_1, \omega_2)$	Total Noise Characteristic Function
$\sigma_a^2$	variance of the signal
$\sigma_i^2$	variance of the impulsive noise
$A$	Impulse index
$b$	Real Bernoulli process
DL	Downlink
$E[X]$	Expected value

$E_b/N_0$	the energy per bit to noise power spectral density ratio
$F_p$	Sampling frequency
$g$	Complex Gaussian process
$I_n$	Impulsive noise
$N$	AWGN noise
$n$	packet size
$N_{fft}$	FFt size
$p$	Probability of having "failure"
$p$	Bernoulli mean
$q$	Probability of "success"
$R$	Received signal
$S$	Transmitted signal
$SIR$	Signal to interference ratio
$T_b$	Useful symbol time
$T_g$	Guard time
$T_s$	OFDMA symbol duration
$T_s$	Mean impulse duration
$T_u$	Subcarrier duration
$UL$	Uplink
$\nu_t$	Mean impulse rate
$\Delta\omega$	Subcarrier spacing

# Chapter 1

## Introduction

The growth of electricity consumption, as well as the extensive usage of electrical devices on a daily basis forced the energy companies to review their power grids. The power transmission grids in US & Canada were mostly developed in the 60s and 70s. Ever since, the population in North America has doubled and in other continents like Latin America even tripled. The statistics anticipate a world population of 11.5 billion people by 2060 as compared with today's seven billion. The same trend is followed by the world's consumption of electricity, which will require tripling its capacity of energy generation to meet customer's needs.

Significant power failures occurred all over the world in the late 90s and early 2000s, caused either by natural causes such as lightnings, storms, solar storms or due to bad judgment calls. These massive shutdowns left millions of people spread over large areas without electricity. For example, 97 million people were left without electricity for almost five hours after lightning hit a power substation in 1999 in Sao Paulo, Brazil. In 2003, the worst North American blackout triggered a cascade of power failures that left 50 million people in the dark for more than a day in USA and Canada. During the same year the Italian blackout took place after a malfunction on the Swiss and French power transmission lines that were supplying the country. These three countries have an electricity agreement based on electricity exchange which helps manage peak demands.

In 2006, an imprudence of a German company lead to a power outage that affected 10 million people in Germany, France, Italy and Spain.

A renovation of the power grid is thus necessary, and an increasing number of countries are investing significant resources to be a step ahead. Major investments in smart grids around the world are done primarily in the industrialized countries such as US, Canada, China, Brazil, South Korea and countries from Western Europe. Globally, in 2014, \$14.9 billion were invested in the smart grid, from which more than half were oriented towards distribution automation. Many financial reports estimate a rapid growth of the global smart grid market with a cumulative amount of \$400billion investments worldwide by 2020. These numbers are offered by the Global Smart Grid Technologies Research, which also places China to be the largest market for implementation.

Smart grid applications and implementations are constantly developing in order to best suit different geographical areas with specific needs. For example, countries with extreme weather conditions and high life standards like Canada will use more than a third of the generated power to cover residential needs. In China, although the population is significant, 70% of its power production is geared towards industrial usage, while the residential consumption is around 15%.

The major innovation brought by the smart grid is the communications layer. This will make the reception of real time information possible covering all consumption sectors, and will thus permit the concurrent adjustment and distribution of power production and distribution. The communication layer will act as a lattice linking all the power grids' segments together, aiding the management and creation of a centralized information system. Many researches are focused on developing new and innovative ways of implementing the smart grid, whereas other are using the existing infrastructure to build the smart grid upon it. The wireless implementation is seen as a more beneficial solution for long term usage, but other hybrid implementations, combining Power Line Communications (PLC) and wireless technologies are also intensively studied. In general, the communication technologies that are researched upon worldwide are the following: fiber optic or copper cables, Narrowband Power Line Communication (NB-PLC) for Neighborhood Area Networks (NAN) and Broadband Power Line (BB-PLC) carrier for DAN,0 private wireless networks using WiMAX or public wireless networks using General Packet Radio Service (GPRS), Long Term Evolution (LTE) or WiMAX providers.

## 1.1 Motivation

The way the information is managed from the customers to the utility station and backwards has a great impact on the overall performance of the smart grid's communication layer. The data collection needs to follow a certain protocol, whether the information will be collected from customers on a periodic basis or from different services that are increasing the grid's reliability, such as video surveillance or voice support for workforce.

Another aspect that is influencing the quality of the wireless transmitted information is the presence of impulsive noise near the power substations. Hydro-Québec released a series of measurements using different wireless communication technologies at different voltage substations. A high interference of the signal was observed in the presence of metallic structures such as power substations.

This thesis analyzes the traffic generated by different consumers in the power grid. The data traffic is labeled under different applications, such as: metering and pricing updates, video surveillance, electrical car and voice support for workforce. The capacity of WiMAX base-stations, under certain parameters, is analyzed in order to determine how many NANs a base station can collect from. Lastly, the capacity of the substations is examined with and without the presence of impulsive noise.

## 1.2 Thesis Contribution

The main contributions of this thesis are summarized as follows:

- The study of the WiMAX standard for the smart grid applications along with the design, implementation and simulations of the network topology in OPNET, for which four smart grid applications were developed using appropriate characteristics and requirements.
- The results obtained after simulating the WiMAX network layer used to implement the smart grid applications can be divided into the following categories: throughput analysis, total capacity of the base station for fixed and random traffic, latency and packet loss.

- The effects of the impulsive noise were observed during the OFDM implementations. The physical layer was simulated using WiMAX characteristics specific to each smart grid application. The simulations were performed comparatively with Additive White Gaussian Noise (AWGN) and Impulsive Noise channels.
- The results obtained after simulating the OFDM physical layer in MATLAB provided information concerning the Bit Error Rate (BER) for all applications, Packer Error Rate (PER), throughput and the total capacity of the base station.

### **1.3 Thesis Outline**

The remaining chapters in this thesis are organized as follows:

#### Chapter 2

This chapter introduces the necessary theoretical concepts for the production and interpretation of the results from Chapter 3 and Chapter 4. Several questions relating to the smart grid are answered throughout pertaining to definitions, characteristics, pros and cons, possible implementation of the communication layer, the specifications of the WiMAX standard, physical layer definition, OFDM, and implementation of WiMAX in the smart grid.

#### Chapter 3

This chapter provides insight into the applications used to analyze the capacity of the base stations from the DAN. In this section, the WiMAX network layer that is used to implement the communication settings of the smart grid by using OPNET is thoroughly described. Throughout the chapter, the following four applications are designed, simulated and analyzed: the metering and pricing, voice, video surveillance and electrical car. The main performances investigated are the throughput, packet loss ratio and the latency of the applications. Individual and comparative reports were provided for a comprehensive understanding of the results.

## Chapter 4

This chapter focuses on the impulsive noise definition in the context of wireless networks. Literature concerning this subject is reviewed, portraying the effects of impulsive noise on different wireless communication standards. The physical layer of the WiMAX standard is simulated therein using MATLAB. The implementation of the OFDM physical layer is done individually for each application and it follows the data traffic requirements. The simulations will provide results for the BER performance for all applications, PER, throughput performance and total capacity of the base station.

## Chapter 5

Lastly, Chapter 5 presents conclusions and the suggested future works.

# Chapter 2

## Background

The electricity generation in Canada in 2015 has increased significantly from the 90's, in order to meet the growing demands. The Canadian sources of energy are mostly renewable, such as water and nuclear, while a small percentage is based on fossil fuels. The latter is considered secondary energy since it is produced using primary energy resources such as coal, natural gas and oil. Hydroelectricity covers 59% of the total amount of electricity generated in Canada, where provinces such as Quebec, Ontario, Labrador, Manitoba have a water energy production of almost 90% [1]. Also Canada ranks 3<sup>rd</sup> after China and Brazil in global hydroelectricity generation. The increase in power demand is due to the population growth, greater usage of household and industrial appliances, as well as rapid changes in temperatures, with extremely cold winters and humid hot summers.

Figure 2.1 displays the total supply and demand of primary and secondary electricity for the last decade in Canada. The total demand of electricity includes the following sectors: industrial, residential, transportation, agriculture, public administration and commercial. The enhancing consumption trend can be clearly observed. The usage of electricity in Canada alternates from year to year as a result of the frequent variations in temperature. A significant amount of electricity is consumed by heating devices during winter and air conditioners during summer. From 1995 to 2013, the Canadian people required an additional 402.691Twh to fulfill their requirements, which



represents an increase of 21.19% in comparison with the required amount of electricity in 1995 [2]. In consequence, Canadian consumption increases yearly with an average of 23Twh [2].

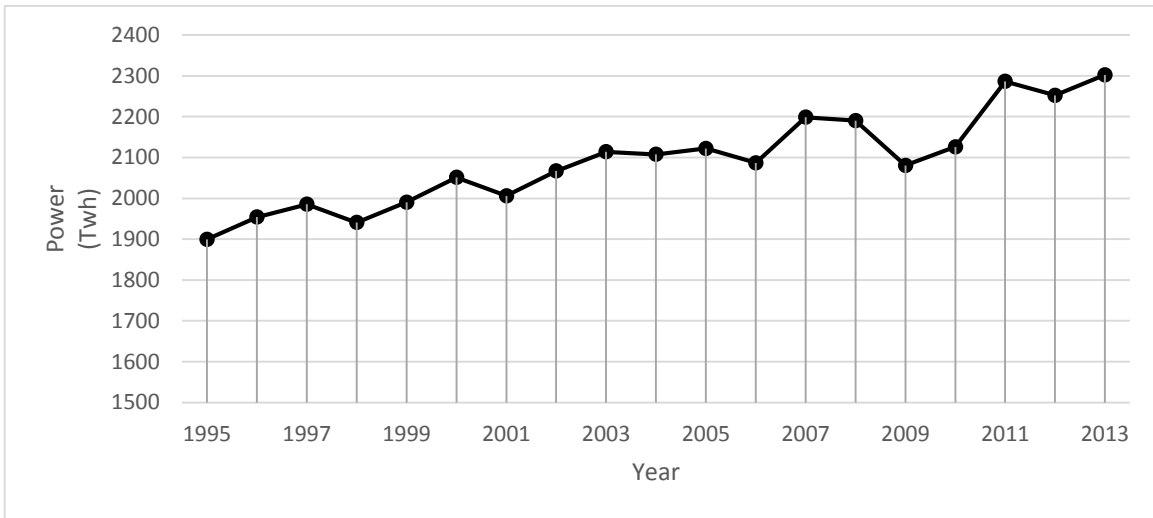


Figure 2.1 Supply and demand of primary and secondary electricity (Canada) [1]

Figure 2.2 displays the total electricity demand in Canada divided by sectors. As expected, the industrial, residential and commercial sectors represent major consumption components. In 2013, the industrial sector used 39% from the total annual consumption representing 510.99TWh [2]. The total demand of electricity in Canada registered an average yearly increase of 1.2%. This value can vary from sector to sector, for example in 2012, the residential consumption was higher than 2013 with 2.3% but in the same time the industrial demand increased with 1.9% along with the commercial sector [2].

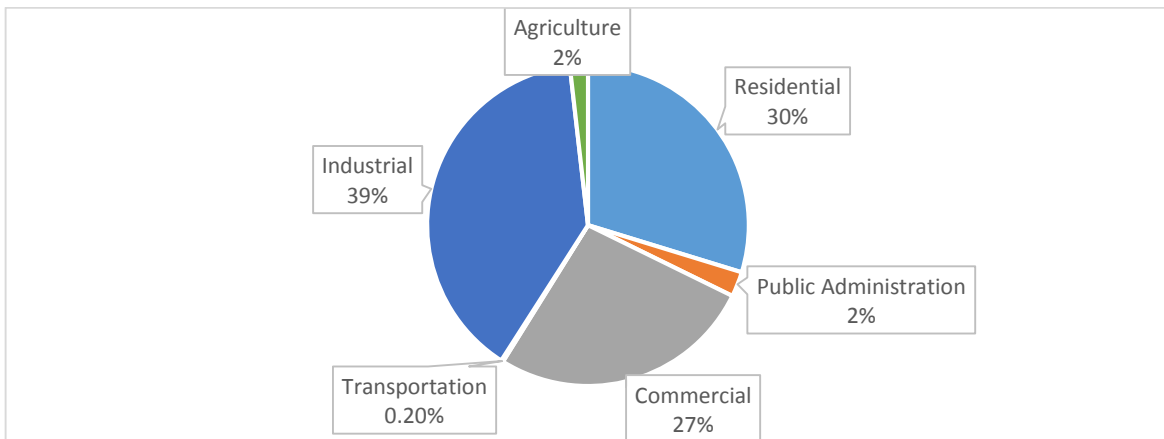


Figure 2.2 Total Electricity Demand in Canada (2013) [2]

## 2.1 Traditional Power Grid

The traditional power grid system is a centralized and unidirectional system where the power flows to the consumer from the power generation and distribution station [3].

The classic power grid includes elements of electricity production as well as distribution infrastructure. The path in the power grid starts with the bulk generation plant that consists of large power generation stations able to produce hundreds of Megawatts. The transmission network transports electricity to denser consumer population and is able to carry hundreds of Kilovolts. The distribution network is considered a low voltage network in the order of tens of Kilovolts, since the power electricity is stepped-down between the transmission lines segment and the distribution segment. In the consumption area, the voltage is stepped down again to the service voltage required and a digital meter is installed to measure the amount of power consumed for billing purposes.

The notion of information exchange between the utility station and residential area does not exist, nor is it limited in the traditional power grid and the energy efficiency is quite low. In the absence of real-time information regarding electricity demand, the generation station is either underused or overused, hence the multiple blackouts occurring during the past years. The customer is not accommodated to have an active participation, since, for example, he/she is not able to introduce his/her own electricity production through solar panels or wind turbines into the power grid. Figure 2.3 provides a graphical display of the traditional power grid and identifies the different segments.

A major issue of the traditional power grid is its low level of security. The grid is not able to detect in real-time failures or a possible threats on the transmission lines. It requires human presence to acknowledge the geographic failure point on the transmission lines. The emergence of Wireless Sensor Networks (WSN) in the grid are seen as a method to upgrade the grid, by offering real-time information concerning weather, possible video-surveillance, the present state of transmission lines and many other applications.

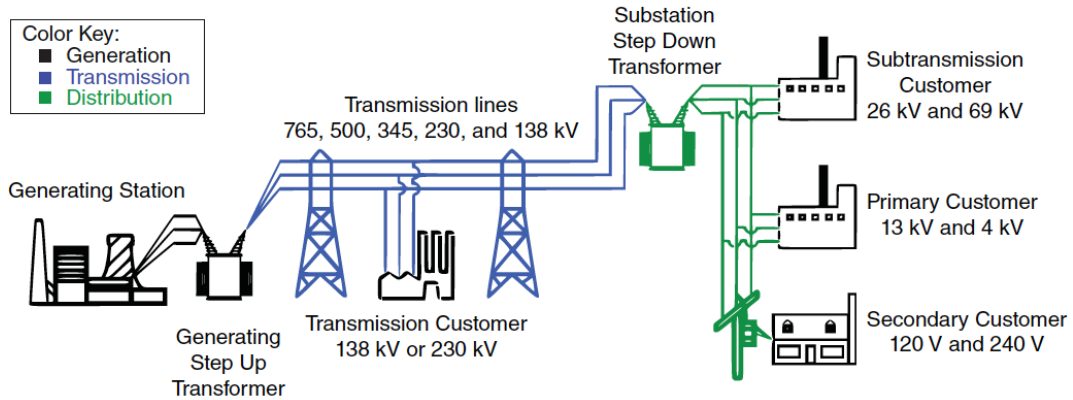


Figure 2.3 The classic view of the power grid [4]

In [5], the proposed model is bringing the WSN into homes by creating an in-Home Energy Management (iHEM) application that uses WSNs. This management model will employ smart appliances with communication capabilities, a WSN and a central Energy Management Unit (EMU). EMU communicates with the smart meter periodically and receives information on the updated price. The customer has the final say in deciding whether the appliances are used or not at that specific time. In [6], WSN is used in a synchronization scheme for appliances using an in-home WSN that reduces the cost of energy consumption called Appliance Coordination (ACORD). In the smart grid, the cost of energy will be linked to time ranges that are considered peak time. Thus, customers will have to adapt their habits in order to keep their energy consumption under control. The appliances communicate with the EMU that schedules the customer's request such that on-peak hours are avoided for cost reduction purposes. By using the ACORD scheme, the user will be able to turn on the appliance at any hour regardless of the peak time, and the EMU will make the decision according to the price rates received from the utility. Thus keeping consumption to a minimum without too much interference with the customers' needs [6]. The work [7] presents the possible advantages and disadvantages that can be brought by WSN in Smart Grid.

## 2.2 Power Grid Challenges

The current power grid faces several challenges of which we can note the growing demand of electricity, the necessity of having wider range coverage for the transmission networks, popular demand for incorporation of renewable energy, a more efficient power generation and distribution and higher security for the grid's segments.

The growing population and their future needs is the most relevant factor that challenges the delivery capacity of the current power grid. Statistics Canada projects a population increase of almost 25% in the following 20 years [8]. Considering the current power consumption per individual in Canada, the power capacity requirements from Figure 2.4 are expected in the following years. The power production capacity is also complemented by the reliability requirement. Electricity has a crucial role in civilization and has become an indispensable necessity for both residential and industrial sectors. The Canadian grid was mainly built between the '60s and '80s [9]. The natural resources from provinces such as Quebec, Manitoba and British Columbia allowed the exploitation of hydropower at relatively low costs. After the 80', the investments in Canada's electrical grid ceased [1]. The current hydro facilities are able to support the needs of a larger population but they need to be renovated and improved with smart technologies able to increase efficiency. In order to achieve these goals, Conference Board of Canada projected an investment of \$350billion in the next 20 years [1].

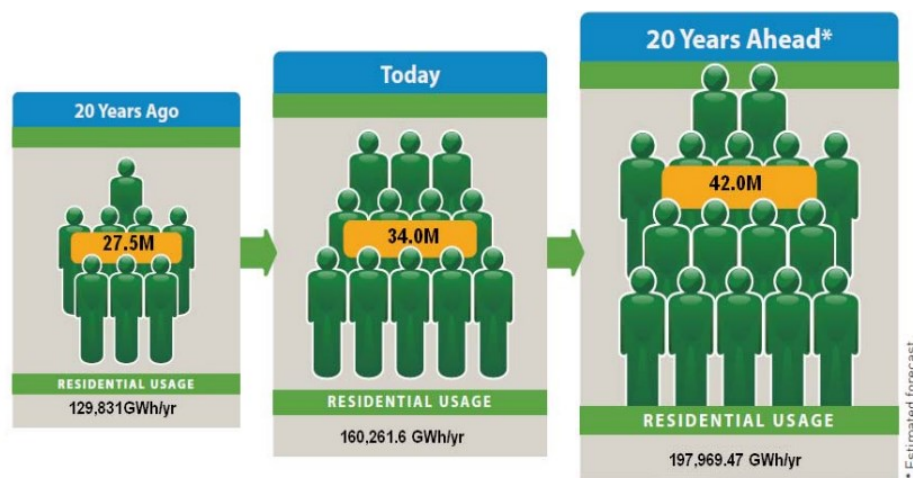


Figure 2.4 Population projected by Statistics Canada along with the electricity requirement for residential usage [1].

## 2.3 Smart Grid

Governments and utility companies are making efforts to modernize the current power grid to meet the demands of the 21<sup>st</sup> century. The new grid is expected to have a more efficient energy production and consumption, to provide two-way flow of information, improve energy storage, buildings and vehicles efficiency, immersion of renewable sources of energy, reduce greenhouse gas, the whole while being scalable and self-healable [5].

The implementation of the smart grid came as a necessity to manage a higher demand of electricity, provided that natural resources such as coal, gas and nuclear energy are limited. The employment of this novel architecture brings advantages such as efficiency of energy production and consumption, availability and reliability of the service, scalability, self-healing grid, environment friendly where consumers can participate in the production with energy harvested through solar panels and wind turbines.

The concept of smart grid pledges to accommodate renewable energy such as solar and wind with a more efficient management of resources and distribution. Consumers will become active components of the grid able to control their consumption according to the price they are paying. They will be able to produce and sell the energy made by their solar panels or wind turbines to the utility company.

The smart grid takes elements from the classical power grid and adapts them to the system's requirements. Compared to the classical grid, the bulk generation plant will include production of energy from various resources. The transmission segment addresses transportation of the produced energy to the distribution component. These sources can be (1) renewable and variable such as solar and wind; (2) non-variable such as hydro and geothermal; or (3) non-renewable, non-variable such as nuclear, coal and gas [7].

The transmission network equally accommodates the possibility of energy generation and storage. The distribution component provides energy to customers, power generation and storage. Furthermore, the consumers will be able to generate and store electricity that will be provided to the central energy utility company. To achieve this, the residence need to be equipped with a smart meter, an Energy Service Interface (ESI), and smart appliances. The distribution network connects

the smart meters and other smart devices, managing and controlling them through a two-way wireless or wireline communication network. The operation component has to monitor and interact with most aspects of the grid. It uses a two-way network to connect to substations, customer's households and other devices. The operations domain is the component that processes ongoing information and makes decisions. The market segment also has to manage and coordinate from a commercial perspective. Finally, the service provider is responsible with billing, emergency issues, installation and maintenance [7].

Many countries are researching and investing in a more reliable power grid, able to incorporate renewable energy and to make use of existing resources more efficiently. In Ontario, Canada, almost every home and small business is equipped with smart meters that employ the Time of Use (TOU) algorithm to assess the amount of electricity used by consumers. Figure 2.5 presents the drastic improvement in terms of power consumption obtained after implementing smart meters and TOU algorithm in Ontario. With more control in its hands, the consumer is able to actively respond to price signals and system conditions by increasing or reducing their electricity consumption. In the USA, the initiative became a federal program in 2007 under the supervision of the Department of Energy's Office of Electricity Delivery and Energy Reliability. Through the American Recovery and Reinvestment Act of 2009 under the management of the aforesaid U.S. Department, massive sums are spent in renewing the American power grid. Large investments are equally made in the European Union were the Energy European Commission projects that 72% of consumers will have a smart meter for electricity and 40% for gas by 2020.

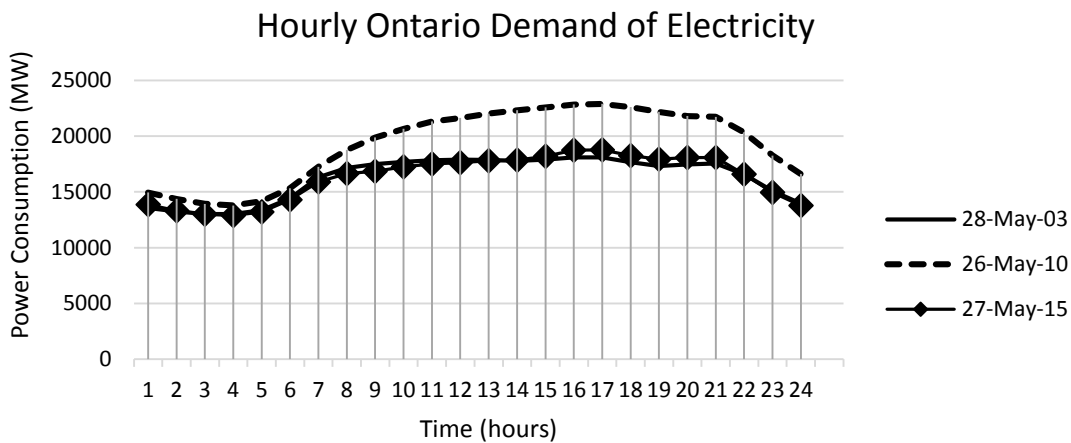


Figure 2.5 Typical daily power consumption on a Wednesday in Ontario

### 2.3.1 Smart Meters

At the consumer end, a smart meter will be installed to communicate with the utility company through Advanced Metering Infrastructure (AMI). By using the smart meter, the customer will have access to updated information regarding the demand and the price of electricity at that specific time, while the supplier will have information regarding the consumption in specific neighborhood depending on the network topology.

The timeline of the information route in the smart grid is outlined in Figure 2.6. The smart meter collects the information on a periodic time base. A wireless collection point will be present in every NAN, whose information will be taken over by a substation in the DAN. These wireless towers will facilitate the exchange of information between the customer and the utility station. The electricity company will be able to assess the supply and demand. Depending on these values, the station will send price updates through the same network back at the user. As such, the user will be able to better manage his/her financial planning depending on the billing algorithm used by the utility station.

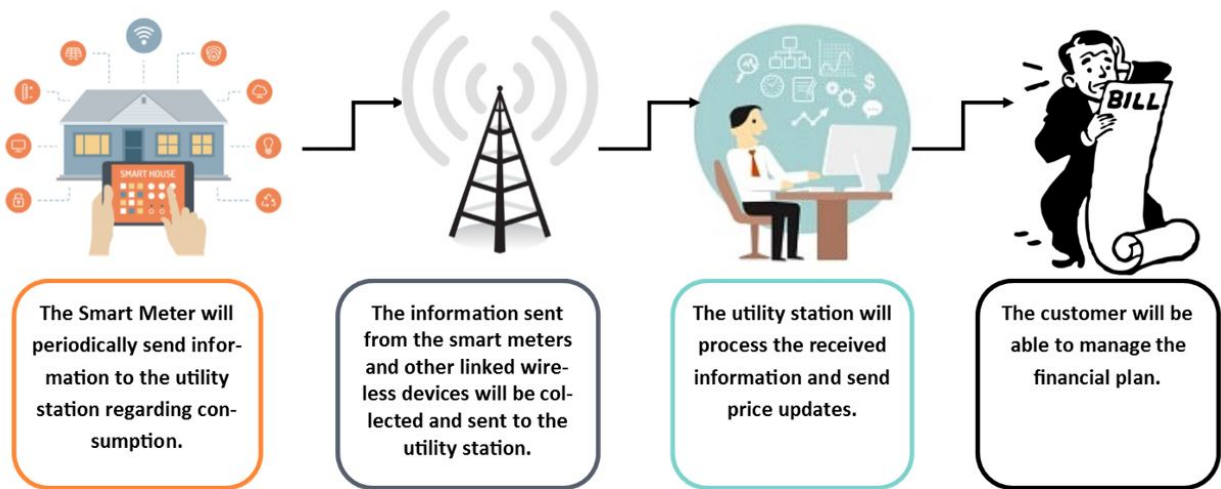


Figure 2.6 Information flow in the Smart Grid

By having a two-way communication channel, the utility station will be able to receive information on consumer's electrical usage, manage load control, monitor for electrical faults and support appliance level reporting [10].

Smart meters can use different pricing algorithms such as Time of Use (TOU), the Critical Condition Plans (CCP), and the Real Time Plans (RTP). Hydro-One, the company that delivers electricity across the Canadian province of Ontario uses the TOU billing scheme. This algorithm sets fixed prices for peak hours, mid-peak and off peak depending on the time of week days, weekends and holidays, the two latter of which are considered to be off peak. As expected, peak hours are at the time when consumers are home, between 7:00 AM and 11:00 AM and 5:00 PM to 7:00 PM, and are billed more than the rest of the day. CCP increases the price in some critical conditions, for example in cold countries where the temperature drops under a certain value. In RTP, the price varies according to the real time supply and demand [11].

The authors of [12] offer a comprehensive description of the smart meter integration in the electrical grid and of the customer's benefits after they have been integrated in the grid.

### **2.3.2 Communication Layer**

A very large traffic of data in the network is expected along with the introduction of the communication layer, which collects data from the consumer and forwards it to the utility company. At the same time, the purpose of employing a smart grid is to manage the resources more efficiently and not to add new consumers. Employing a communication layer that is based on the WiMAX standard could be a solution to deal with the bottle-neck effect that will emerge once all smart meters and wireless devices associated with the Smart Grid will start sending information to the utility station.

Transforming the consumer into an active part of the structure of the smart grid requires an exchange of information between himself and the utility company. In order to support this feature of the smart grid, the corresponding segments of the communication layer must be adapted to the power system layer. In Figure 2.7 we can observe the associated power segments to the communication segments. The houses are assumed to be "smart", having appliances able to transmit information to the local smart meter regarding consumption.

The implementation of the smart grid will however bring several challenges, starting with the way data flows from the utility company to the customer and vice versa. The downlink traffic



will be unicast or multicast. Unicast traffic means that the information sent by the utility company is focused on a single destination. Multicast traffic entails the simultaneous transmission of information from the transmitter to a group of destinations. The uplink traffic will be converge cast, meaning that the company will receive information from multiple destinations at the same time. This will produce a communication bottleneck at the receiver, which will slow down the process or even stop it. In [13], the solution found to this problem was to implement the Random Linear Network Coding (NC) algorithm. This implies combining several original packets of data into coded packets that allow a decreased number of transmissions. The implementation of NC at the NAN ensures diversity, as the packets are dispersed throughout the network over space and time. By using the solution provided in [13], a higher level of security is achieved since in the case of an attack, the coded packets can only be intercepted, but cannot be decoded. It was observed that by using NC a high reliability link is achieved.

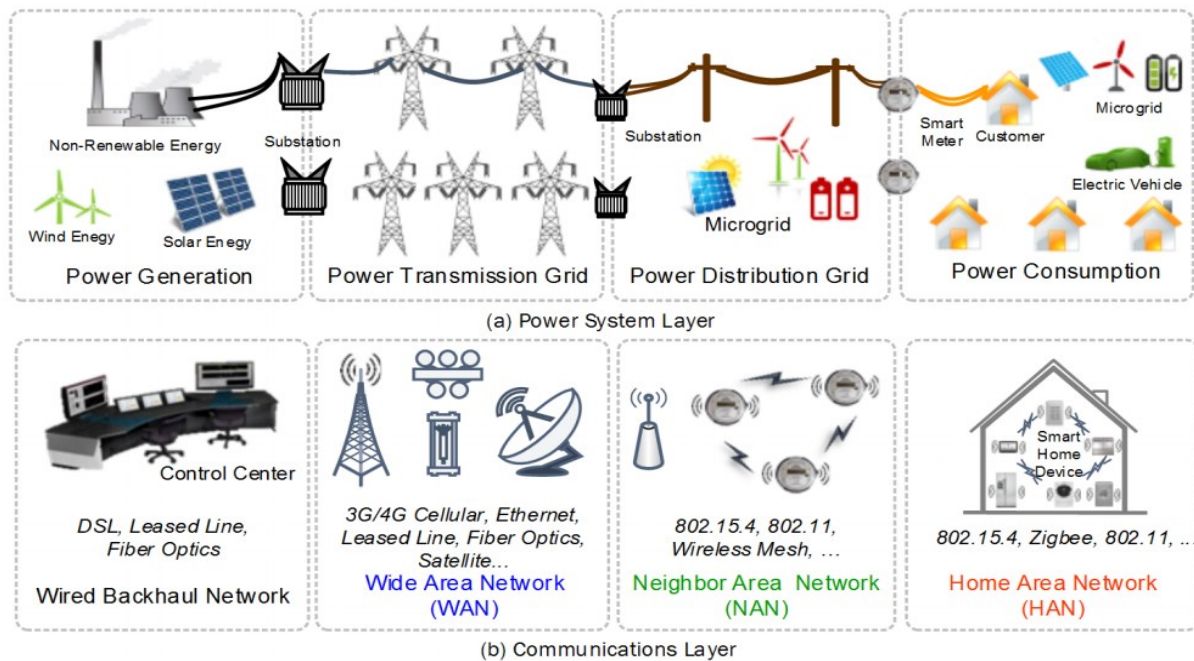


Figure 2.7 Conceptual System Architecture for the Smart Grid [13]

PLC is considered in many works a good way to implement the communication layer in the smart grid's distribution network. The authors in [14] analyze the effects of noise in the PLC for smart metering. The impulsive noise in the PLC is a substantial issue, due to connecting and disconnecting electrical devices. This noise affects the quality of the communication link. Another

disadvantage brought by this implementation is the reliability of the network in case of a power failure. This implementation requires a back-up plan that will offer energy availability in case of a power outage. The work in [14] describes also the quality trades to be performed for a more effective cost.

Another solution found for implementing the Smart Grid's communication layer is provided in [15], as a hybrid combination between PLC and WiMAX. In [15], the authors propose an implementation of the last mile with PLC and WiMAX for the backhaul network. The solution seems very appealing since the infrastructure for PLC is already in place, but as in [14] the drawback of such implementation is the link reliability. Another hybrid implementation is presented in [16] where a combination between WiMAX and WLAN is used to implement the network that provides connectivity between smart meters and utility company.

[17], [18] are presenting several communication technologies that could be used to employ different segments of the communication layer such as: Zigbee for the HAN, different cellular networks for a wider coverage such as 2G, 2.5G, 3G, WiMAX and LTE, PLC and DSL for the long-haul communication.

## **2.4 WiMAX Specifications**

### **2.4.1 Introduction**

WiMAX is based on the standard IEEE 802.16 and stands for Worldwide Interoperability for Microwave Access [19]. IEEE 802.16 provides fixed and mobile broadband access in telecommunication. The released standard IEEE 802.16e offers support for mobile applications while IEEE.802.16d is geared towards fixed wireless point-to-point and point-to-multipoint links. The IEEE Computer Society and the IEEE Microwave Theory and Techniques Society developed IEEE Standard for Air Interface for Broadband Wireless Access Systems [19] which offers a detailed assessment over the WiMAX specifications, including MAC and physical layer specifications for both fixed and mobile WIMAX systems.

WiMAX was built especially for communications in Metropolitan Area Networks (MAN) as it offers very high transmission rates at a larger range than other wireless protocols. WiMAX

was developed at a time when there was substantial interest in a technology that could provide an alternative for the wired communication through DSL (Digital Subscriber Line) for broadband access [19]. The advantages delivered by the IEEE 802.16 over other communication technologies are the following [19]:

- Quick deployment when some areas are hard to reach for wired technologies;
- Overcome the physical limitation of wired technologies;
- Reasonable cost;
- Broadband access services for a wide selection of devices;
- High data speed: being able to reach an optimal speed of 70Mbps;
- Range of coverage much larger than other wireless infrastructure 50km;

Although the technical specifications of WiMAX confirm very high coverage areas, over 30 miles radius with a single base station, this is only possible in ideal conditions with line-of-sight areas (LOS) and no real-time traffic and negligible attenuation. A single base station with a coverage radius of 4, 5 miles can provide high speed connectivity without LOS (NLOS) and in real time conditions. The range can go up to 10 miles if LOS is provided [20].

### 2.4.2 Characteristics

In comparison to other communication technologies, WiMAX along with LTE, provide better features for a reasonable cost compared with the PLC. The technologies presented in Table 2.1, DSL, BB-PLC, Universal Mobile Telecommunications System Network (UMTS), WiMAX and LTE are found in many research papers as viable implementations of the communication layer.

<b>Attributes</b>	<b>DSL</b>	<b>BB-PLC</b>	<b>UMTS</b>	<b>WiMAX</b>	<b>LTE</b>
<b>Data rate</b>	25 Mbps	100 Mbps	10 Mbps	70 Mbps	70 Mbps
<b>Range</b>	~1 km	~2 miles	~5 km	~4km	~4km
<b>Flexibility</b>	Medium	Medium	Medium	High	High
<b>Network Support</b>	Complex	Complex	Complex	Simple	Simple
<b>Cost</b>	~ 50US\$	~1000US\$	~100US\$	~400US\$	~400US\$

Table 2.1 Comparison of different communication standards [21]

WiMAX standard provides several frequency bands and describes the features provided by each of them, Table 2.2 describes some of their main characteristics [19].

<b>Frequency bands</b>	<b>Description</b>
<b>10 – 66 GHz Licensed Bands</b>	<ul style="list-style-type: none"> <li>• Due to short wavelengths the LOS is required and multipath interference is negligible;</li> <li>• Small office app are well served in this frequency range;</li> </ul>
<b>Below 11 GHz Licensed Bands</b>	<ul style="list-style-type: none"> <li>• LOS is not necessary and multipath interference is considered;</li> </ul>
<b>Below 11 GHz License Exempted Bands</b>	<ul style="list-style-type: none"> <li>• Typically using 5 - 6 GHz bands;</li> <li>• Similar to those of the 11GHz licensed bands;</li> <li>• License– exempt status introduces additional interference from the coexistence of other devices within the same range. This can be overcome by employing a mechanism such as dynamic selection of frequency, which is introduced in physical and Mac layer.</li> </ul>

Table 2.2 WiMAX Frequency bands [19].

IEEE 802.16 MAC recommends five categories of traffic scheduling: Unsolicited Grant Service (UGS), Real - Time Polling Service (rtPS), Extended Real - Time Polling Service (ertPS), Non - Real - Time Polling Service (nrtPS), Best Effort (BE). The Base Station performs the uplink request/grant scheduling in order to detect the bandwidth requirement for the uplink transmission and transmit it further to the subscriber station. Different scheduling types are associated with Quality of Service (QoS) parameters. The MAC layer provides five types of scheduling services and usage rules described as follows in Table 2.3:

<b>Scheduling Services</b>	<b>Description</b>	<b>Applications</b>
<b>UGS</b>	<ul style="list-style-type: none"> <li>• Used for Constant-Bit-Rate services like VoIP, real-time uplink flows with constant sized data packets;</li> <li>• Low latency and low jitter are very important;</li> <li>• UGS flows are given priority over the other scheduling services;</li> </ul>	<ul style="list-style-type: none"> <li>• TI/EI(overIP)</li> <li>• VoIP</li> </ul>
<b>rtPS</b>	<ul style="list-style-type: none"> <li>• Designated to support real-time service flows , variable size of packets; MPEG video;</li> <li>• The subscriber station defines the size of the desired grant;</li> <li>• This service had more request overhead than UGS;</li> </ul>	<ul style="list-style-type: none"> <li>• MPEG</li> </ul>
<b>ertPS</b>	<ul style="list-style-type: none"> <li>• Combination between UGS and rtPS, from UGS takes the allocation of base station with unicast grants in an unsolicited manner and from rtPS takes the variable grand allocation;</li> </ul>	<ul style="list-style-type: none"> <li>• VoIP</li> </ul>
<b>nrtPS</b>	<ul style="list-style-type: none"> <li>• Non-real-time service flows, variable size packets, minimum data rate;</li> </ul>	<ul style="list-style-type: none"> <li>• FTP</li> <li>• HTTP</li> </ul>
<b>BE</b>	<ul style="list-style-type: none"> <li>• Supports data streams that do not require minimum guaranteed rate;</li> <li>• BE packets take longer to be transmitted in congested networks ;</li> </ul>	<ul style="list-style-type: none"> <li>• E-mail</li> </ul>

Table 2.3 WiMAX Scheduling Services [20]

### **2.4.3 FDD, TDD**

The WiMAX standard provides two ways of separating the uplink stream from the downlink stream. The transmitted signal and the received signal needs to be separated in order to prevent situations when the station receives its own transmitted signal and is not able to select it from the received one. The duplex technique separates the received signal from the transmitted one. This can be obtained by using a Frequency Division Duplexing (FDD) or a Time Division Duplexing (TDD) [22].

FDD allows the transmission of the uplink and the downlink in different frequency bands. Since higher frequencies are more likely to be affected by attenuation than the lower frequencies, the latest are usually employed for the transmitting band of the mobile station and higher frequencies for the transmitting band of the base stations.

TDD separates the transmitted and received signals in time. The base station and the mobile station are transmitting alternatively. This technique allows a more efficient distribution of transmission capacity between the uplink and downlink and asymmetric data traffic.

### **2.4.4 Physical Layer**

IEEE 802.16 supports different physical layer specifications, which depend on the band of operation and duplexing modes. The following physical interfaces are supported by IEEE 802.16 air interface nomenclature and description [19]. Table 2.4 provides a description of the main physical interfaces defined in the WiMAX standard such as: Wireless Metropolitan Area Network Single Carrier (WirelessMAN-SC), Wireless Metropolitan Area Network Single Carrier Access (WirelessMan-SCa), Wireless High-speed Unlicensed Metropolitan Area Network (WirelessHUMAN), Wireless Metropolitan Area Network Orthogonal Frequency Division Multiplexing (Wireless-MAN OFDM), Wireless Metropolitan Area Network Orthogonal Frequency Division Multiplexing Access (WirelessMAN OFDMA).

In OFDMA mode the active subcarriers are divided into subsets of subcarriers, each of which is termed a subchannel. In uplink, several transmitters can transmit in the same time, with

the transmitter assigned to more than one subchannel. In downlink, a subchannel is used by different receivers.

<b>Designation</b>	<b>Band of Operation</b>	<b>Duplexing Mode</b>	<b>Notes</b>
<b>WirelessMAN-SC</b>	10-66 GHz	TDD, FDD	Single Carrier;
<b>WirelessMANSCa</b>	2-11 GHz Licensed Band	TDD, FDD	Single Carrier technique for NLOS;
<b>WirelessMAN OFDM</b>	2-11 GHz Licensed Band	TDD	OFDM for NLOS operation;
		FDD	
<b>WirelessMAN OFDMA</b>	2-11 GHz Licensed Band	TDD	OFDM Broken into subgroups to provide multiple access in a single frequency band;
		FDD	
<b>WirelessHUMAN</b>	2-11 GHz Licensed Band Exempt	TDD	May be SC, OFDM, and OFDMA. Must include Dynamic Frequency Selection to mitigate interference;

Table 2.4 WiMAX Physical Layers [23]

The standard IEEE 802.16e defines multiple subcarrier allocation types [23]:

1. FUSC- Fully Used Subchannelization, the subcarriers are distributed throughout the frequency channel range.
2. PUSC- Partially Used Subchannelization, several scattered clusters of subcarriers can be used to form a subchannel.
3. AMC- Adaptive Modulation and Coding, subchannel can be composed of contiguous groups of subcarriers.

Figure 2.8 shows the distributed and adjacent subcarrier allocation for two users that are using the AMC, FUSC and PUSC subcarrier allocation types.

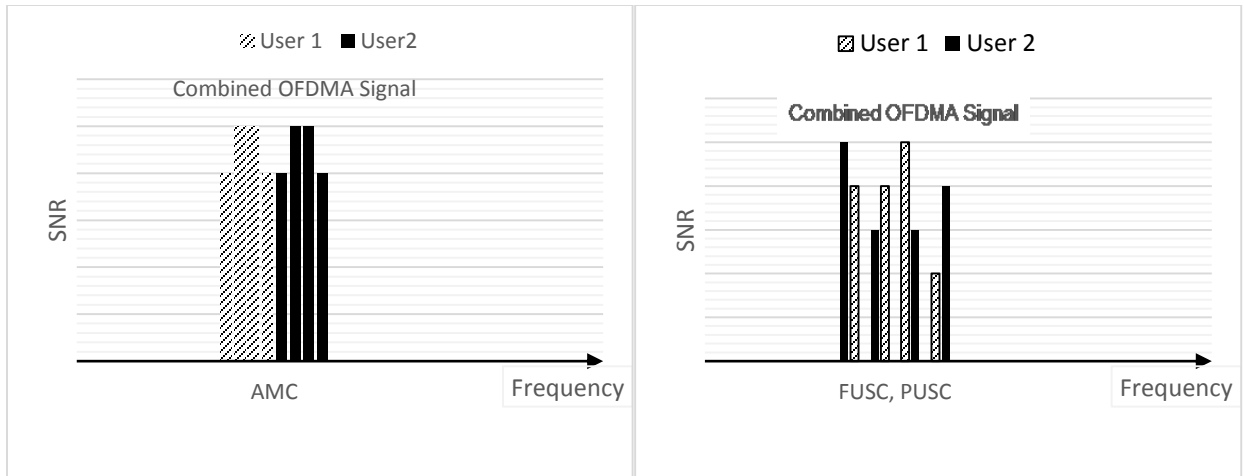


Figure 2.8 Distributed and adjacent subcarrier allocation [23]

#### 2.4.4.1 Specifications

The WiMAX Physical Layer offers broadcast access for both mobile and fixed applications. WiMAX was seen as an alternative to the DSL technologies that was able to offer a faster, more accessible and more reliable way of providing broadband access to internet at higher speeds and on a larger distances.

The fixed WiMAX specification requires a fixed WiMAX terminal and subscribers to a location, while the mobile WiMAX allows movement at different speeds. Usually OFDM is employed in fixed WiMAX and OFDMA is used for mobile WiMAX.

The fixed WiMAX system specification uses the standard IEEE 802.16d. The size of the cyclic prefix can take values from 1/4, 1/8, 1/16 and 1/32 and FFT size supported is only 256. The channel bandwidth can swing from 1.72MHz to 10MHz and the frame duration can take values from 2.5msec to 20 msec. Different types of modulations are supported by the fixed WiMAX system from which we can list BSPK, QPSK, 16/64 QAM [20].

The mobile extension of the standard IEEE 802.16e offers a wider range of specifications and selection for different types of applications, varying the system channel bandwidth, FFT size, modulation, overall code rate etc.



The parameters used by the mobile OFDMA for WiMAX are presented in Table 2.5

Parameters	Values			
System Channel Bandwidth (MHz)	1.25	5	10	20
Sampling Frequency ( $F_p$ MHz)	1.4	5.6	11.2	22.4
FFT Size ( $N_{FFT}$ )	128	512	1024	2048
Number of Sub-Channels	2	8	16	32
Sub-carriers Frequency Spacing	10.94 kHz			
Useful Symbol Time ( $T_b=1/f$ )	91.4 $\mu$ sec			
Guard Time ( $T_g=T_b/8$ )	11.4 $\mu$ sec			
OFDMA Symbol Duration ( $T_s= T_b + T_g$ )	102.9 $\mu$ sec			
Number of OFDMA Symbols ( 5ms Frame)	48			

Table 2.5 OFDMA Scalability Parameters [20]

By adding AMC, hybrid automatic repeat request and fast channel feedback, the coverage and capacity for WiMAX in mobile application was effectively increased. Many modulation types are supported for both uplink and downlink as well as several types of coding techniques such as Convolutional Coding (CC), Convolutional Turbo Coding (CTC) and repetition rates.

Table 2.6 provides a summary of the coding and modulations schemes supported by the Mobile WiMAX.

		Downlink	Uplink
<b>Modulation</b>		<b>QPSK, 16QAM, 64QAM</b>	<b>QPSK, 16QAM, 64QAM</b>
<b>Code Rate</b>	<b>CC</b>	1/2 , 2/3, 3/4, 5/6	1/2 , 2/3, 5/6
	<b>CTC</b>	1/2 , 2/3, 3/4, 5/6	1/2 , 2/3, 5/6
	<b>Repetition</b>	x2, x4, x6	x2, x4, x6

Table 2.6 Supported Codes and Modulation [20]

A complete set of specifications is provided in Table 2.7 along with the data rates for all modulations and coding technique used for data transmission.

Parameters		Downlink	Uplink	Downlink	Uplink
<b>System Bandwidth</b>		<b>5MHz</b>		<b>10MHz</b>	
<b>FFT Size</b>		<b>512</b>		<b>1024</b>	
<b>Null Sub-Carriers</b>		92	104	184	184
<b>Pilot Sub-Carriers</b>		60	136	120	280
<b>Data Sub-Carriers</b>		360	272	720	560
<b>Sub-Channels</b>		15	17	30	35
<b>Symbol Period</b>		102.9 $\mu$ sec			
<b>Frame Duration</b>		5 msec			
<b>OFDM Symbols/Frame</b>		48			
<b>Data OFDM Symbols</b>		44			
Mod.	Code Rate	5 MHz Channel (Mbps)		10 MHz Channel (Mbps)	
<b>QPSK</b>	$\frac{1}{2}$ CTC, 6x	0.53	0.38	1.06	0.78
	$\frac{1}{2}$ CTC, 4x	0.79	0.57	1.58	1.18
	$\frac{1}{2}$ CTC, 2x	1.58	1.14	3.17	2.35
	$\frac{1}{2}$ CTC, 1x	3.17	2.28	6.34	4.7
	$\frac{3}{4}$ CTC	4.75	3.43	9.50	7.06
<b>16QAM</b>	$\frac{1}{2}$ CTC	6.34	4.57	12.67	9.41
	$\frac{3}{4}$ CTC	9.50	6.85	19.01	14.11
<b>64QAM</b>	$\frac{1}{2}$ CTC	9.50	6.85	19.01	14.11
	$\frac{2}{3}$ CTC	12.67	9.14	25.34	18.82
	$\frac{3}{4}$ CTC	14.26	10.28	28.51	21.17
	$\frac{5}{6}$ CTC	15.84	11.42	31.68	23.52

Table 2.7 Mobile WiMAX Physical Layer Data Rates with PUSC Sub-Channel [20]

WiMAX configuration permits a TDD framing that can be done adaptively, in such way that the bandwidth ratio between uplink and downlink can vary with time. In [24] studies the effects of an adaptive bandwidth allocation for uplink and downlink channels in WiMAX. Another method of allocation bandwidth efficiently for real-time services is developed in [25].

## 2.4.5 OFDM

### 2.4.5.1 Working Principle

OFDM is a modulation format used in several wireless and telecommunication standards that provides immunity to multipath fading and efficient use of the frequency spectrum [23]. By multiplexing the frequencies orthogonally with each other, the spectral efficiency of OFDM is superior compared with the Frequency Division Multiplexing Access (FDMA). OFDM allows the arrangement of carriers in such way that the sidebands of the individual subcarriers overlap without affecting or creating adjacent carrier interference. The separation of signals is facilitated by the maintenance of the orthogonality between the subcarriers at the receiver side.

The principle behind OFDM is based on the division of a given high-bit-rate data stream into several parallel lower bit-rate streams and modulating each stream on separate carriers, often called sub-carriers or tones [23].

OFDMA is the multiuser version of the OFDM, which assigns subsets of subcarriers to individual users, and allows simultaneous transmissions of data while sharing the physical medium. Figure 2.9 provides a graphical comparison of the OFDM and OFDMA allocation of sub-channels and sub-carriers.

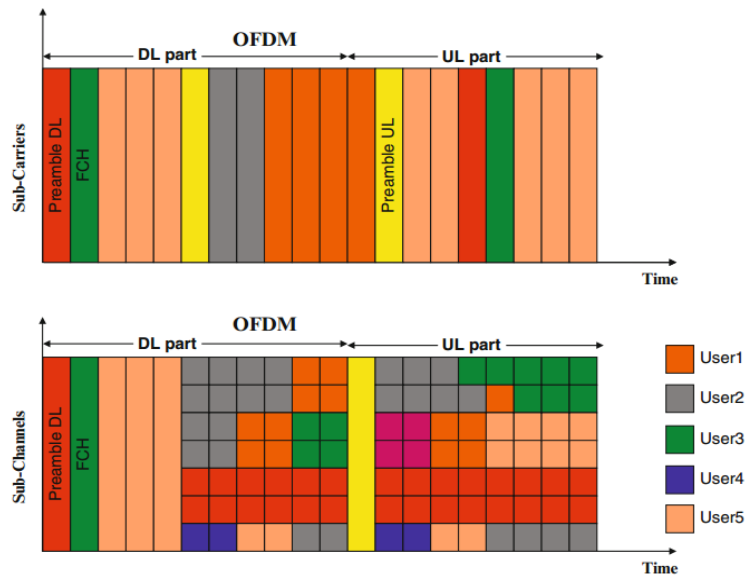


Figure 2.9 OFDMA versus OFDM: sub-channels and sub-carriers [23]

The advantages brought by OFDM are the following [23]:

- It does not use inter-carrier guard bands, and thus uses the spectrum more efficiently in comparison with FDM;
- It handles multipath effects better by using the Fast Fourier Transform (FFT) and the Inverse Fast Fourier Transform (IFFT);
- Robustness against narrowband interference;
- OFDM transmitter is easy to implement and cost efficient;
- The capacity can be enhanced as the data rate can be adapted for each subcarrier depending on the SNR at a certain transmission;
- More robust to fading;
- Can be used for high speed applications;
- Can be adapted for a Multiple Input Multiple Output (MIMO) system;

The disadvantages of using OFDM are the following [23]:

- Strict synchronization requirements, as OFDM is very sensitive with errors involved in frequency and time synchronization;
- Peak to Average Power Ratio depends on the number of subcarriers used by OFDM. An increased number of subcarriers will trigger a higher peak-to-average power ratio. A larger peak-to-average power ratio makes the design of the radio-frequency amplifier much difficult;
- Co-channel interference mitigation in Cellular OFDM;

#### 2.4.5.2 Transmission

The transmitter of the OFDM-WiMAX system combines the following blocks:

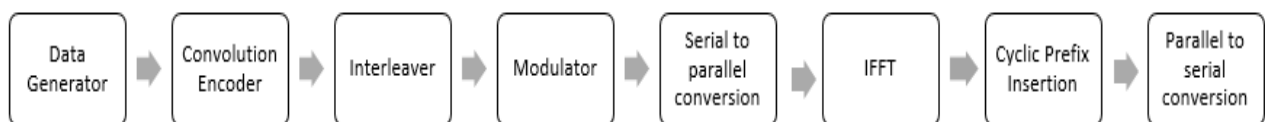


Figure 2.10 Transmitter for OFDM-WiMAX System [26]

The information is generated by the information source, which is further on encoded by the convolutional encoder. Depending on the desired code rate of 1/2, 2/3, 3/4, 5/6 and 7/8, the code might require puncturing the coded output bits. In our case however, the desired code rate will use QPSK 1/2 which does not require puncturing. The binary values resulted after interleaving will be modulated into the desired modulation.

Each OFDM symbol contains  $N$  subcarriers, with duration of  $T_u$  seconds [27]. The subcarrier spacing is:

$$\Delta\omega = \frac{2\pi}{T_u}. \quad (2.1)$$

The OFDM system sees the source symbols as they are in frequency domain. Using this assumption, the duration of the  $s^{th}$  OFDM symbols is [27]:

$$X_s(\omega) = \sum_{k=-N/2}^{\frac{N}{2}-1} X_s[k] \delta_c(\omega - k\Delta\omega). \quad (2.2)$$

The Inverse Fourier Transform (IFFT) is used to convert the symbol from frequency domain to time domain. The time-domain signal,  $\tilde{x}_s(t)$ , is given by [27]:

$$\tilde{x}_s(t) = F\{X_s(\omega)\} \Xi_{T_u}(t) = \begin{cases} \frac{1}{\sqrt{T_u}} \sum_{k=-\frac{N}{2}}^{\frac{N}{2}-1} X_s[k] e^{j\Delta\omega kt}; & 0 \leq t < T_g \\ 0 & ; \textit{otherwise} . \end{cases} \quad (2.3)$$

where,  $\Xi_{T_u}$ , is the unity amplitude rectangular pulse of duration  $T_u$ .

After converting the symbol to time domain, the cyclic prefix needs to be added. The cyclic prefix adds a duration  $T_g$  to the total symbol time  $T_s = T_u + T_g$ . The extended signal after adding the cyclic prefix has the following relation [27]:

$$\tilde{x}_t'(t) = \begin{cases} \tilde{x}_s(t + T_u + T_g); & 0 \leq t < T_g \\ \tilde{x}_s(t - T_g); & T_g < t < T_s \\ 0; & \textit{otherwise} . \end{cases} \quad (2.4)$$

After concatenating all OFDM symbols in the time domain, the transmitted complex base-band signal is the following [27]:

$$\tilde{s}(t) = \sum \tilde{x}'_t(t - sT_s). \quad (2.5)$$

The transmitted radio frequency signal is up converted to a carrier frequency [27]:

$$s(t) = \Re\{\tilde{s}(t)e^{j2\pi f_c t}\}. \quad (2.6)$$

### 2.4.5.3 AWGN Channel or Impulsive Channel

The input signal processed by the composing blocks of the transmitter is sent through an AWGN channel that might include or not impulsive noise components as it can be seen in Figure 2.11 . The impulsive channel was chosen in order to examine the effects of the impulsive noise over transmitted data using WiMAX specifications.

Equation (2.7) provides the expression for the received signal,  $R$ , which depends on the input signal,  $S$ , impulsive noise,  $In$ , and AWGN noise.

$$R = S + In + N. \quad (2.7)$$

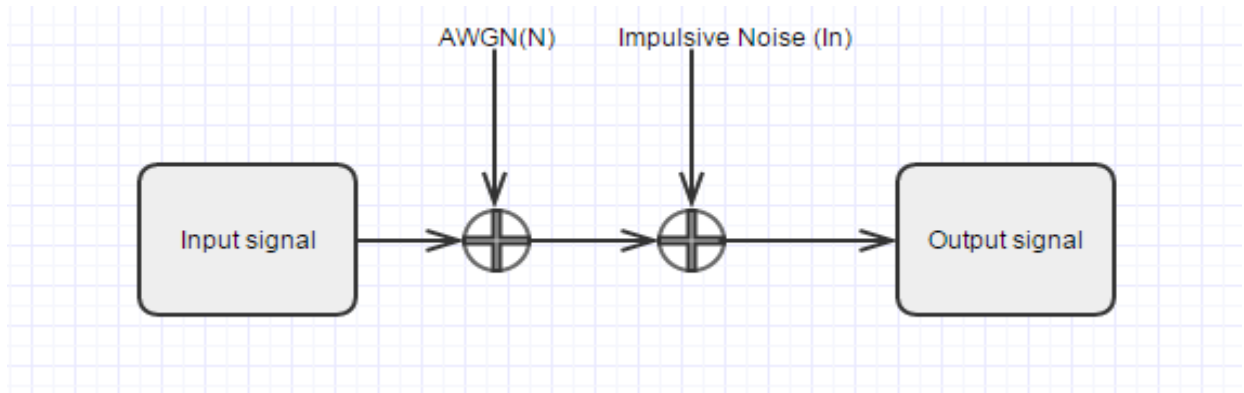


Figure 2.11 Impulsive Channel system

#### 2.4.5.4 Reception

At the receiver side all the operations performed in the transmission side are reversed, by employing the following blocks:

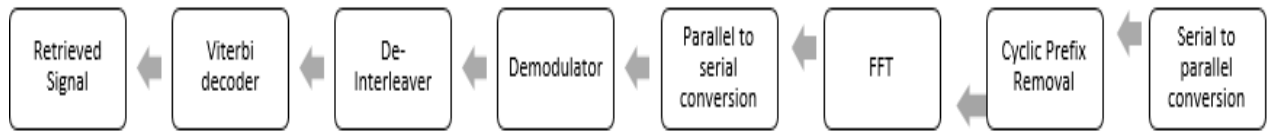


Figure 2.12 Receiver for OFDM-WiMAX System [26]

The serial signal resulted after passing through the channel is converted into several parallel streams. The cyclic prefix is removed from the received signal. The FFT block will convert the time-domain signal into frequency domain signal, which is afterwards demodulated back into its binary form. The signal will be de-interleaved and Viterbi hard decoding will be applied. On hard decision operation, the decoding is explained with  $\pm 1$  using only one bit of precision, while the soft decision uses multibit quantization and three or four bits of precision.

#### 2.4.5.5 WiMAX in Smart Grid

The design of the wireless network and the selection of communication technology are essential when the smart grid is built. Starting with the requirements of the smart grid in the electrical power generation areas and ending with the requirements in the consumer area, all these segments need to have appropriate standards. A smart grid is expected to have a large number of sensors, meters, and other devices that need to transmit and receive constant information from the base station. Creating connectivity for so many entities can prove challenging. In [28], a WiMAX Base Station is used to create a two way connectivity between the entities from the smart grid and the utility station, carrying information on consumption, price rates, cycle time, load control etc.

In order to select the best solution for the implementation of the smart grid, important factors need to be considered, namely the cost, the availability of the technology and whether the

environment is rural, urban, indoor, and outdoor. WiMAX is presented in numerous papers as a reliable solution to fulfill the challenges imposed by the smart grid.

1. **Home Area Network (HAN).** Is composed of electrical appliances and devices that need to communicate with the AMI. AMI's purpose is to collect the information from smart meters installed in households and to share it to the utility company. This type of communication could be wireless or wired. Wireless communication offers some advantages compared to the wired technology, such as low cost, ease of implementation, widespread access, rapid deployment. The HAN does not require a large bandwidth at 1 – 10 kbps with a coverage of 1000 square feet. Technologies such as ZigBee, Wi-Fi and PLC would satisfy the above requirements.

2. **NAN.** The communication structure supporting the NAN is responsible with meter reading, demand response, remote disconnect for load control or local command messages [21]. The NAN needs to cover a few square miles to interconnect hundreds of smart meters, which are installed in residential and businesses areas. A collector node connects a group of smart meters and forwards the traffic between them and the control center. Another requirement concerns the end to end latency which has to be between 1 and 15sec. The technologies that should support this list of constraints are WiMAX, BB-PLC.

3. **DAN.** It handles the cumulative metering traffic from the collector in the uplink, while for the downlink, it handles the load control messages for distribution automation. For distribution sub-station, it manages the video surveillance traffic in the uplink. The DAN requires a larger bandwidth and coverage, 500kbps-10Mbps and the latency has to be less than milliseconds. The publication [29] presents a study on the smart meter infrastructure implemented using WiMAX in the DAN. The authors of [30] provide a characterization of the link quality when the DAN is implemented with WiMAX through different applications.

Table 2.1 describes the characteristics offered by different wired and wireless technologies that could be implemented for the DAN. The wired communication including PLC and DSL can use existing electrical and telephone conductors as a transmission media. By comparing it to the wireless technologies, we can observe smaller data rates for DSL, a smaller coverage range but with a far lower cost than the others. BB-PLC is a PLC technique that offers a high speed data transmission over the public electric wiring. Its drawbacks are that is a very expensive technology, requiring repeaters for long distance and it does not have a very large coverage area. On the other



hand, a wireless implementation would provide a less expensive solution that does not require employing a new infrastructure. Having very low data rates, EDGE/UMTS is excluded and for further analysis the table displays a WiMAX and LTE comparison. These two technologies offer, according to [21], the same attributes in terms of data rate, range, flexibility, network support and cost. In [21], WiMAX is selected for a more in-depth discussion as it is preferred by other communities and has been deployed in several fields of practice.

In [28], different variables are analyzed in a WiMAX network that have to serve a smart grid. The simulations were conducted by increasing the number of users up to 1000 in a 2 Km cell with random distribution. The results displayed the capability of this type of network to overcome the challenges brought by the smart grid, the whole while providing high QoS performance at decent levels of cost. Further on in [21], the simulations are conducted in the DAN and the access network. The attributes simulated where the packet loss, the bandwidth, latency and smart metering capacity and scalability.

In [31], the scenarios are designed and simulated in OPNET using a WiMAX communication model. Three scenarios are evaluated: the first of which takes 50 smart meters per cell in a coverage radius of two kilometers; the second scenario increases the number of users to 500 per cell in the same two kilometer radius, and the third one takes 50 smart meters per cell for a coverage radius between two and five kilometers. The service class selected is nrtPS, standing for non-real time polling service, which provides a guaranteed minimum rate. By using this method, we cannot however have any assurance that the packets are received. The base station and the subscriber station control the resources allocation on the downlink and uplink. By using the nrtPS class all the subscriber stations are polled after every Interpolling Time (IPT). Every mobile station has the option of transmitting a bandwidth request when the poll arrives to it. In this simulation, WIMAX square cells are used with a circular distribution of the nodes. The total number of subchannels is asymmetrically distributed for downlink and uplink and two applications are considered to detect the traffic model, File Transfer Protocol (FTP) over Transmission Control Protocol (TCP) and single message User Datagram Protocol (UDP).

## 2.5 OPNET

The simulations performed in Chapter 3 were obtained using the OPNET Modeler software Suite, now known under Riverbed Modeler. This software is a network simulation tool that comprises several protocols and technologies that help analyzing networks and compare different technologies [32]. OPNET contains a large library of commercial models and offers support for many wireless communications technologies such as Wi-Fi, WiMAX, LTE, Zigbee, and Bluetooth as well as for other wired technologies. OPNET simulations operate at packet-level and, depending on the standard used, it also offers support for simulating both fixed and mobile networks.

The structure of OPNET is divided in three main domains, outlined as the network domain, the node domain and the process domain. The network domain represents the high level description of the objects defined in the model, such as topology, the employed technology, the geographical location, interconnections and configuration. The node domain defines the objects in network domain. In this domain, nodes such as workstations and base stations, terminals, and substations will have their internal functions defined. The process models define the behavior of processes that exist in the node domain.

In order to model traffic using OPNET software, an application profile needs to be defined following the architecture described in Figure 2.13.

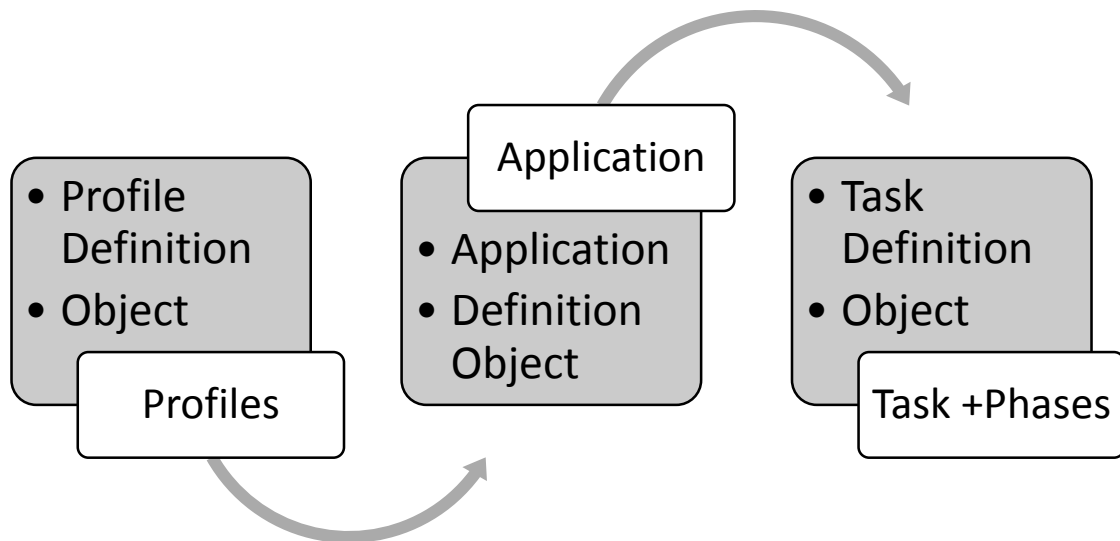


Figure 2.13 The Application Model Hierarchy [33]

### 1) Profile Configuration

Profiles include a list of applications and they are assigned to different users representing a traffic pattern that they are assigned with. Many profiles can run simultaneously in the same network. A profile describes user activity over a time frame and all the applications that are assigned within a profile may have certain characteristics such as start time, duration, and repeatability and operation mode. Even the profiles for different users are defined by the same characteristics.

The software offers the possibility of defining the operation mode, start time, duration and repeatability for each profile.

### 2) Application Configuration

A user profile is built using different applications. OPNET Modeler offers the description for a limited list of standard applications, notably database, email, FTP, HTTP, Print, Remote Login, Video Conferencing, and Voice as well as custom applications where one can define the Task Description, Transport Protocol and the Type of Service.

### 3) Task Configuration

Multiple tasks define a custom application. The tasks are a basic unit of user activity within the context of applications. The task behavior can be configured automatically or manually.

### 4) Phase Configuration

If we choose to configure the task behavior manually then we also need to define the list of phases that are included in a task. The phase is an interval in which a certain activity that contained within a task is occurring. For each phase, one needs to define the start time, source, destination, source/destination traffic and the pattern of responses and answers between source and destination. The source/destination traffic includes elements such as the initialization time, inter-request time, request count, request packet size and inter-packet time.

The results obtained after running the simulations in OPNET include global statistics, node statistics and link statistics. The global statistics include performances of the overall network for each standard that was used, for example for WiMAX one can see the network's delay, load and

throughput. Node statistics offer the results for each node in the topology for the same characteristics as the global statistics. The link results give the outcomes of the accomplishments at the link level such as point to point delay, throughput, utilization on the uplink and downlink. The manual [34] provides a comprehensive description of OPNET Modeler and includes the necessary information in order to use this software at its full capacity.

## **2.6 Impulsive Noise**

The impulsive noise is described by random, uncorrelated and unwanted noise peaks of high amplitude [35]. It is caused by external electromagnetic disturbances and it can be separated into two categories: natural and man-made. Usually the natural causes of impulsive noise are lightning and thunderstorms, while the artificial causes include ignition system of motor vehicles, power lines, industrial machinery, electric tools and domestic equipment.

The influence of the impulsive noise was first observed when digital data started to be sent through telephone lines. In voice communication, the impulsive noise manifests itself as of temporary disturbances, such as sharp noises and clicks during a phone conversation. The impulsive noise is seen more like noise bursts that eventually degrade very much the digital communication through commercial telephone lines [35].

Over long-haul transmissions, the impulsive noise is considered to be a major source of interference. In digital communication, the effects of the impulsive noise can transform into bursts of errors. This type of noise is more frequent in lower frequency bands and even microwave bands.

Usually the effects of the impulsive noise in the ultra-wide band systems are ignored. This is due to the use of the thermal noise as a frequent model to define the effects of the ambient noise over the communication channel.

### 2.6.1 Literature Review

Many papers are analyzing the effects of the impulsive noise over PLC networks, such as [36], [37]. Some of the effects of impulsive noise over digital data transmission are analyzed in [35]. Article [38] uses the effects of the ignition noise to present the characteristics of the impulsive noise and design equipment to measure these parameters.

Usually, the effects of the impulsive noise in the ultra-wide band systems are ignored and only the thermal noise is used to define the effects of the ambient noise over the communication channel. The influence of the impulsive noise in wide bands is analyzed in [39] where they are measured and studied indoors and outdoors. They choose environments with higher degrees of electromagnetic radiation such as a hospital room and a computer lab for the indoor case, and a bus terminal for the outdoors model. Household appliances and devices that require a lot of power are considered sources of impulsive noise, which also manifests itself in parking lots with a considerable number of cars. In [39], the results are generated by performing electromagnetic frequency measurements both indoors and outdoors to observe the impulsive noise at different frequencies.

Substation impulsive noise can affect the quality of wireless data. Article [40] compares three different models of impulsive noise: Middleton, Bernoulli Gaussian and Markov Chain model. The authors of the paper propose a partitioned Markov Chain model for the impulsive noise. This model proves to have the closest resemblance of impulsive noise distribution measured at different substations. The measurements are done at different substations located in Quebec and for different frequency bands ranging from 200MHz to 4GHz.

Research literature offers many solutions to minimize the effects of the impulsive noise over wireless communication systems. [41] proposes a solution that involves decomposing the noisy signal adaptively into oscillatory components, operation called shifting, which are further on filtered and to which a threshold is applied, while being reconstructed subsequently at the receiver. [42] proposes an algorithm that can mitigate impulse noise which uses the guard band null subcarriers. Other suppression solutions to minimize the influence of the impulsive noise over the communication system are proposed in [43], [44] and [45].

## 2.6.2 Characteristics of the Impulsive Noise

Intensive research was conducted to determine the nature of the impulsive noise in the electromagnetic environment of the power substations. The results of these studies show that the impulsive noise is created by partial discharges, corona noise and electrical arcs that are introduced by high-voltage equipment such as transformers, bushing, power lines, circuit breakers and switch-gear [40].

The impulsive noise has a random nature with uncorrelated bursts of noise that have a relatively short duration and high amplitude with respect to the Gaussian noise. The impulsive noise is considered to be one of the main causes of burst error occurrence in data transmission, which generates temporary loss of signal. At the beginning, the impulsive noise was seen as a noise source that could alter data transmission for shorter bands, but as the digital communication emerged, research showed that wide bands can also be influenced by impulsive noise.

The impulsive noise can be generated by either natural or artificial causes. Manmade noise is generated by automotive ignition, power transmission lines, household appliances and electrical tools [41]. Impulsive noise [41] can be divided into the following categories:

**Middleton Class A.** In this case, the impulsive noise is stationary over time and usually seen as background noise considered coherent. The noise has a similar or lesser bandwidth that the one of the receiving system.

The probability density function is [41]:

$$f_x(x) = e^{-A} \sum_{m=0}^{\infty} \frac{A^m}{m! \sqrt{2\pi\sigma_m^2}} e^{-\frac{x^2}{\sigma_m^2}} \quad (2.8)$$

m- Different impulsive sources [6]:

$$\sigma_m^2 = \frac{m+\Gamma}{1+\Gamma}, \text{ is the noise variance} \quad (2.9)$$

$A = \nu_i T_s$  is the impulse index,  $\nu_i$  is the mean impulse rate and  $T_s$  is mean impulse duration.

**Middleton Class B.** The noise pulses produce short time changes in the receiver. The noise bandwidth is greater than the one of the receiving system

**Middleton Class C.** This type is a linear sum of Class A and Class B.

The impulsive noise is defined by three major characteristics, pulse amplitude, time-duration and inter-arrival time of pulses.

The mathematical model used in this thesis to describe impulsive noise is the Bernoulli-Gaussian model of Poisson arriving delta Rayleigh probability density function [46].

The Bernoulli distribution is discrete, taking the value 1 (“success”) with the probability  $p$  or the value 0 (“failure”) with the probability  $q=1-p$  [8].  $X$  is a discrete random variable that assigns a number to each outcome of  $S$  that can take values from  $\{0, 1\}$ .

The probability mass function (*PMF*) of a random variable  $X$  takes the following values [47]:

$$P_r(X = 1) = 1 - P_r(X = 0) = 1 - q = p; \quad 0 \leq p \leq 1 \quad (2.10)$$

$$P_r(X = 0) = 1 - p = q; \quad 0 \leq p \leq 1$$

The expected value of a Bernoulli random variable  $X$  is [47]:

$$E[X] = p \quad (2.11)$$

the variance of Bernoulli random variable  $X$  is:

$$\sigma^2 = p(1 - q) = pq \quad (2.12)$$

The input signal,  $S$ , is transmitted through the channel with impulsive noise,  $In$ , and AWGN,  $N$ . The resulted signal,  $R$ , is processed at the receiver and takes the following mathematical form [46], where both input and output,  $S$  and  $R$ , are complex values:

$$R = S + In + N \quad (2.13)$$

Figure 2.14 shows the impulsive noise occurrence with regard to the AWGN. The impulse occurrence is represented by the values equal to ‘1’ in impulse states and background noise is represented by samples equal to ‘0’.

The impulsive noise is the product of real Bernoulli process,  $b$ , and complex Gaussian process,  $g$  [46]. This means that the probability of having impulsive noise is given by the probability of occurrence  $p$  and the random amplitude  $g$ .

$$In = bg . \quad (2.14)$$

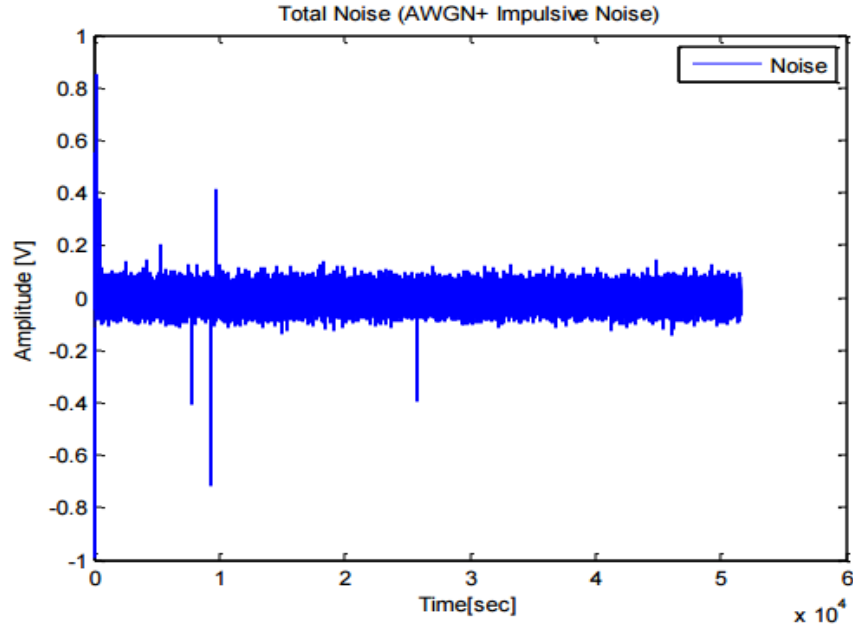


Figure 2.14 Impulsive Noise Amplitude

The Gaussian distribution  $g$  and the Bernoulli distribution  $b$  are defined by the following parameters:

Distribution	Attributes	Values
Gaussian	Mean	$\mu = 0$
	Variance	$\sigma_{\omega}^2$
	Characteristic Function	$\phi_g(\omega_1) = e^{-\frac{\sigma_{\omega}^2 \omega_1^2}{2}}; \sigma_{\omega}^2 > 0$
Bernoulli	Mean	$p$
	Variance	$p(1 - p) = pq$
	Characteristic Function	$\phi_b(\omega_2) = 1 - p + pe^{-i\omega_2};$ $0 < p < 1, \quad p \in R$

Table 2.8 Parameters of the Gaussian and Bernoulli distribution [46]:

The characteristic function of the impulsive noise is provided by the following Equation (2.15) with mean zero and variance  $\sigma_i^2 = p\sigma_{\omega}^2$  [46].



$$\phi_{In}(\omega_1, \omega_2) = (1 - p + pe^{-i\omega_2})e^{-\frac{\sigma_\omega^2 \omega_1^2}{2}}. \quad (2.15)$$

The characteristic function of the total noise is then:

$$\begin{aligned} \phi_{Nt}(\omega_1, \omega_2) &= (1 - p + pe^{-i\omega_2})e^{-\frac{(\sigma_\omega^2 + \sigma_i^2)\omega_1^2}{2}} \\ &= (1 - p)e^{-\frac{(\sigma_\omega^2 + \sigma_i^2)\omega_1^2}{2}} + pe^{-i\omega_2 - \frac{(\sigma_\omega^2 + \sigma_i^2)\omega_1^2}{2}}. \end{aligned} \quad (2.16)$$

# Chapter 3

## Smart Grid Applications

The traffic collected from the power grid devices has to contain information related to the most relevant power consumers in a community. Research papers propose the development of various applications that simulate the sent and received traffic from different consumers in the power grid at the network level. Devices that use most of the bandwidth in the power smart grid are defined through the following applications: Advanced Metering, Demand Response pricing control, Electric Car, Power Monitoring, Substations Control Systems, Distribution Automation/Grid Management, Distributed Energy Resources and Storage Control, Video Surveillance, Data maintenance and Telephony for workforce [21].

Many of these applications are associated with the household power consumption such as the Advanced Metering, Demand Response and the Electric Car applications. Another relevant category of applications are related to the operation and control of the substations, while others are used to ease the access of workforce by providing constant access through video surveillance of the grid and voice service.

In this chapter, we present the implementations and simulations of several applications, such as metering and pricing, voice, video surveillance and electric car. The main performances

investigated are the data throughput, packet loss ratio and the latency of the applications. The study of the simulation's results contains both individual and comparative interpretations.

An extensive section of this chapter is dedicated to the examination of the maximum collector's capacity supported by a DAN. In this section we analyze the segment of traffic between the NAN and DAN. Figure 3.1 shows the architecture of information flow in the smart grid. At the end-mile, the smart meters are sending periodic information which is gathered by a local collector. The collector from the NAN will forward the information to a base station in the DAN. The base stations from each DAN will afterward send the information to the utility company.

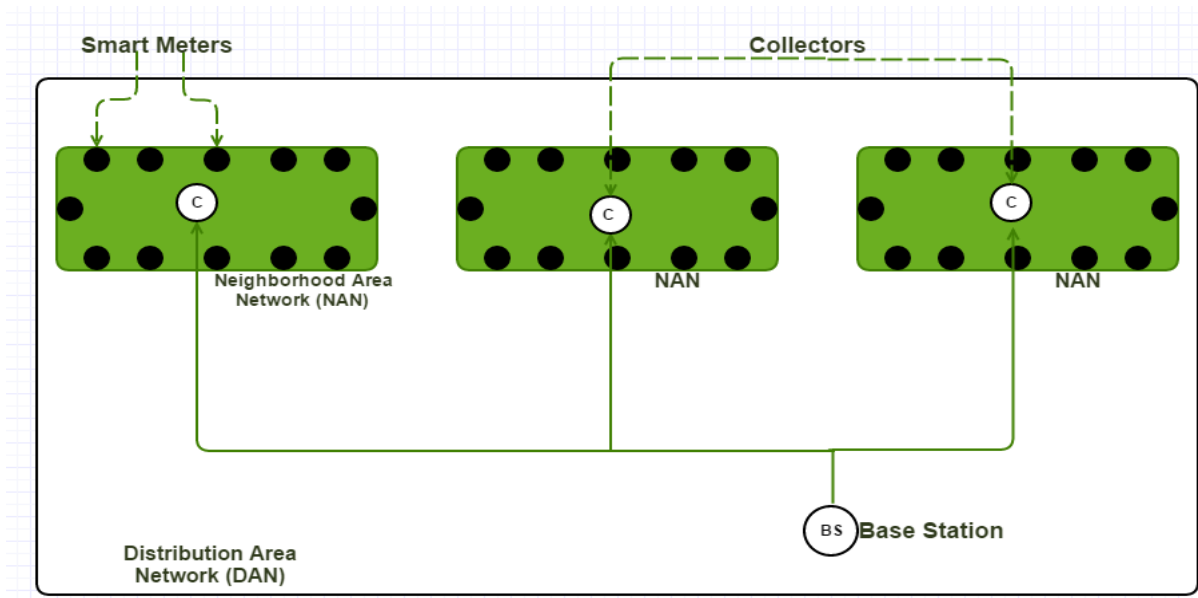


Figure 3.1 Smart Grid Infrastructure between NAN and DAN

### 3.1 Metering and Pricing Application

An essential attribute of the smart grid is the ability to receive periodical information regarding electrical consumption in residential and business areas. Power consumption information is employed to better manage resources so that the electrical grid is not overused and can be exploited for a longer period of time. AMI proposes a complex way of reading the electrical meters and processes the information. It provides a two-way wireless communication between the smart me-

ters and the utility station. The uplink traffic represents the information gathered from the household, such as power consumption at a certain time, voltage, current, power factor and user identification ID [28]. The downlink traffic represents the updated electricity price after examining the information received on the uplink. The traffic generated is periodic, every 30 minutes, and has a constant bit rate with a difference of 5 minutes between the uplink and downlink collection times. Frequent updates on power consumption provide the utility company the necessary knowledge to better estimate power utilization at different hours of the day. This is reflected in the price paid by the customer. Higher rates will be imposed for above average consumption and lower rates for the time of the day when the electrical consumption does not exceed a certain threshold. This information will be broadcasted by the utility company to all smart meters on a timely basis.

We are considering a scenario where every collector combines the traffic from 4000 smart meters in a NAN. The collectors will send information on the uplink to the utility company with a data rate of 500kbps and a packet size of 125bytes. The inter-arrival time of incoming packets is 0.002sec, such that there is enough time to send this amount of information on the available link. The downlink will not get congested due to lower data rates of 100kbps and packet size of 25bytes. The scheduling service used to employ this application is BE within the bronze class. A detailed classification of the traffic scheduling classes can be found in Table 2.3. The WiMAX parameters used for the simulation of both uplink and downlink traffic models are presented in Table 3.1.

<b>Metering and Pricing Application Parameters</b>	<b>Values</b>
<b>Data rate / collector (kbps)</b>	Uplink: 500; Downlink:100
<b>Packet size(bytes)</b>	Uplink: 125; Downlink:.25
<b>Inter-arrival packet time (sec)</b>	0.002
<b>Type of Service</b>	BE
<b>Destination Name</b>	Server
<b>Traffic type</b>	Periodic (every 30 minutes)
<b>Latency (msec)</b>	1000

Table 3.1 Metering and Pricing Application Configuration [21]

The metering and pricing application is a custom application implemented using OPNET. It contains a single task which defines the traffic flow from the collectors to the server and backward. The custom application is designed when the standard applications offered by OPNET are not appropriate. The traffic originates from collectors and is forwarded to the application server. The metering and pricing application message transmission is presented in Figure 3.2.

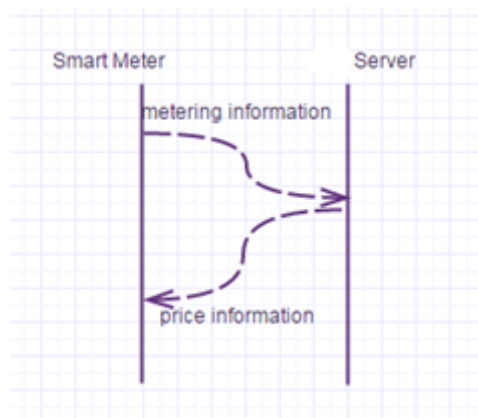


Figure 3.2 Metering and Pricing application message transmission

Figure 3.3 illustrates the total metering and pricing application's throughput that collects the information sent and received by the base station. The uplink data rate is first sent by smart meters and received by the base station and is afterwards followed by a price response from the utility company after 5 minutes. This sequence is repeated periodically every 30 minutes. The downlink data rate is significantly lower than the uplink, representing only price information, whereas the uplink information contains a set of multiple outputs establishing price rates by the electrical company. The traffic sent by the base station periodically has a limited influence to the capacity of data transmission of the base station.

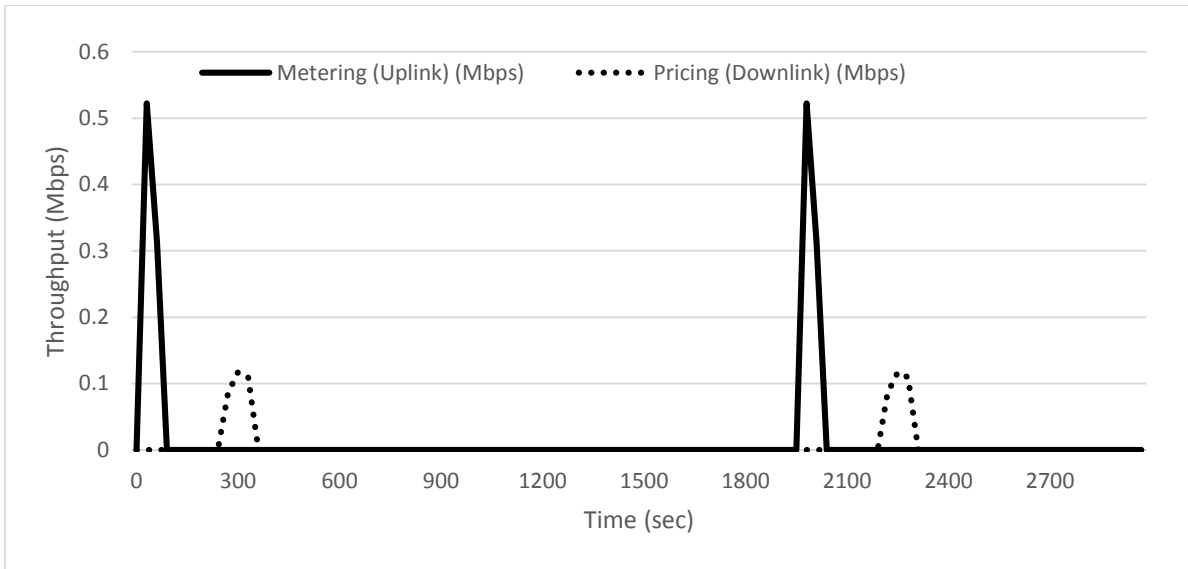


Figure 3.3 Throughput (kbps) generated by 1 collector which uses the Metering and Pricing Application over 1 hour

We are interested in finding the number of meters that can be supported by the base stations without affecting the requirements of the system. Every collector accumulates the loads from 4000 smart meters and acts as a small base station, which represents the connection between the neighborhood and the distribution network.

The Figure 3.4 shows the capacity of the system when only the uplink traffic is taken into consideration, as it is significantly larger than the downlink one.

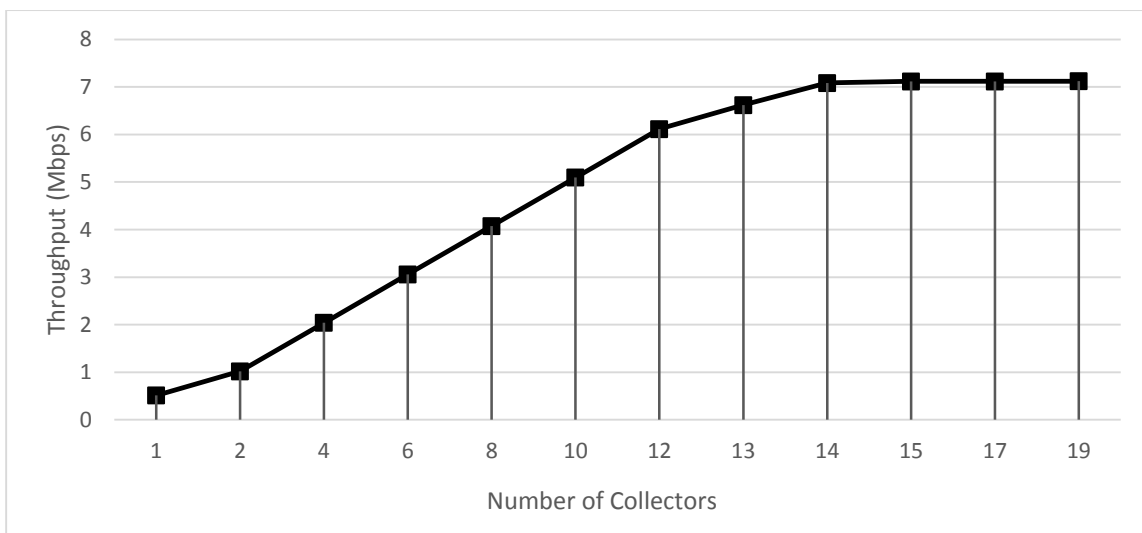


Figure 3.4 Capacity performance when Metering and Pricing application is employed (UPLINK)

The packets will start to drop when the number of collectors in the DAN reaches a certain threshold. In the case of the metering and pricing application, the threshold is reached at 14 collectors. The threshold is imposed by the capacity of the WiMAX base station, which is 7.8 Mbps and is detailed in Table 2.7. If the capacity is reached, despite an increase in the number of collectors beyond this threshold, the throughput will remain constant and remaining packets will be dropped.

### **3.2 Video Surveillance**

The power grid can be a possible target for hardware and software threats such as terrorism, vandalism and tampering. Monitoring the most important elements of the grid, namely the substations, power lines and neighborhood areas is a critical measure that would facilitate identifying the source of attack. The article [49] provides the design requirements of the video surveillance service when the WiMAX standard is used.

This application continuously feeds the base station with real-time video capture from different areas of the network being an uplink only application. In every NAN, 12 cameras will record and supply images from specific points to a collector, which will further transmit to the utility company. Each collector has a 256kbps data rate with a packet size of 600bytes. The scheduling service selected for this application is BE, bronze class. This outgoing stream inter-arrival time is 2 msec. This application has to generate continuous uplink traffic. The latency for the video application needs to be medium, while the security and reliability of the applications need to be high despite high volume of data at the endpoint.

The video surveillance application is developed by modifying the standard application video conference. The main characteristics of the video application are listed in Table 3.2. The inter-arrival time for the incoming frames is selected as “none” since the traffic for a video monitoring application is only on the uplink. This is why the frame size for the incoming stream is considerably smaller compared with the outgoing stream frame size.

Video Surveillance Application Parameters	Value
Inter-arrival packet time (sec)	Incoming: None; Outgoing: 0.02
Frame size information (bytes)	Incoming: 1; Outgoing: 600
Destination Name	Video Server
Type of Service	BE
Traffic type	Continuous
Data rate / collector (kbps)	256
Latency (msec)	200
Packet size(bytes)	200,400

Table 3.2 Video Surveillance Application Configuration [21]

Figure 3.5 displays the capacity reached by the base station when the video surveillance application is employed. The threshold obtained is 29 collectors by measuring the throughput acquired when all collectors are sending 256kbps. The increase of the number of collectors beyond this point results in an increased packed loss.

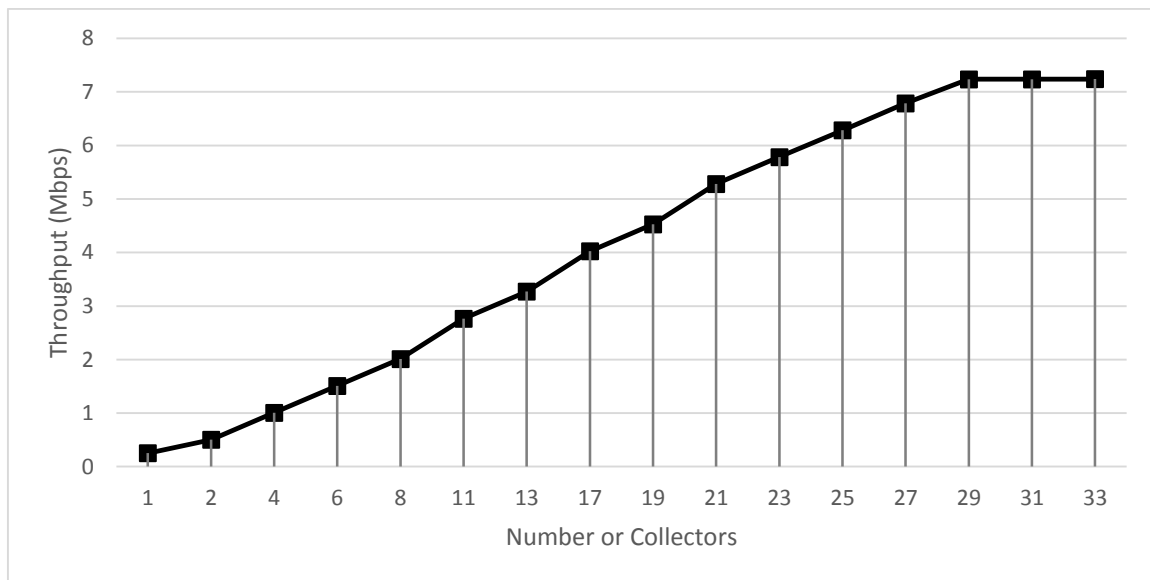


Figure 3.5 Capacity performance when Video Surveillance application is employed



### 3.3 Electric Car Application

This renovation of the power grid requires accessibility for the incoming trend of electric cars. The increasing popularity of electric cars is triggered by the awareness towards environmental changes. Plenty of car brands are joining the project in having more environment friendly methods of transportation. The authors of [50] are describing why is so important to integrate electric vehicles in the smart grid platform.

The amount of electricity necessary to charge an electric car or a plug-in hybrid electric vehicle (PHEV) is substantially larger than the one needed for general household appliances. Also, the time necessary to charge an electric car varies from half an hour to a day depending on the battery capacity, state of charge, and the type of charging infrastructure. The electric car needs to be in contact with the grid often because it can be a source of consumption that could unbalance the power grid and eventually produce a power collapse. A high percentage of population will charge their cars after 6pm, once consumers arrive home from work. The electric cars could also be charged when the grid has an excess of power or the batteries could discharge back the electricity when the grid needs more to keep it stable [50].

The results obtained when the Electric Car Application is active assumes that six charging venues that are randomly online across a two kilometer radius neighborhood. These locations could be either located at home or at random locations such as the gas stations or municipal parking spots. The purpose of these applications is to send information when the electric car commenced the charging process. Table 3.3 presents the parameters required to employ the electric car application

<b>Electric Car Application Parameters</b>	<b>Value</b>
<b>Data rate (Mbps) / collector</b>	1 Mbps
<b>Packet size(bytes)</b>	125
<b>Type of Service</b>	BE
<b>Traffic type</b>	Random
<b>Latency (msec)</b>	1000
<b>Inter-arrival packet time (sec)</b>	0.005

Table 3.3 Electric Car Application Configuration [21]

The capacity performance when the electric car application is used is displayed in Figure 3.6. The threshold obtained is seven collectors.

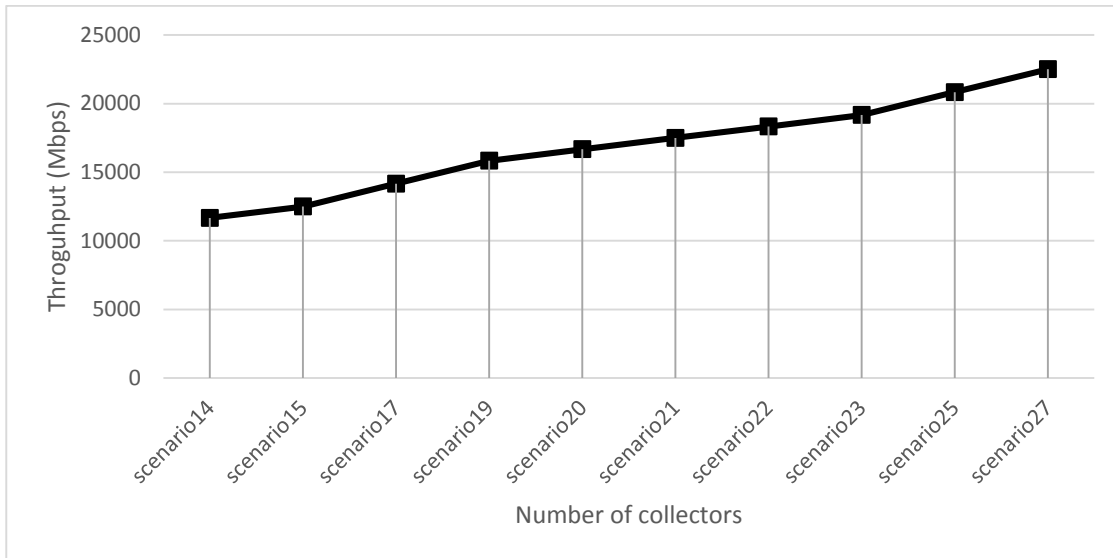


Figure 3.6 Capacity performance when Electric Car application is employed

### 3.4 Voice Application for Workforce

The Voice application is provided for the workforce on the field and makes communication possible between employees of the utility company. This voice application is one of the standard applications provided by OPNET. The parameters from Table 3.4 are used to employ the voice application.

Voice Application Parameters	Value
Data rate (Kbps) / collector	32
Data rate (Kbps) / user	8
Type of Service	Interactive Voice
Type of Scheduling	UGS
Service class name	Gold
Latency(msec)	50
Traffic type	Random

Table 3.4 Voice Application Configuration [21]

The throughput is directly proportional with the number of collectors. In Figure 3.7 we can see the evolution of the WiMAX throughput for different scenarios. Since the voice application requires both uplink and downlink traffic, the throughput contains both these traffics. Taking into account that the data rate needed to employ this application is too low, a threshold for this application was not reached. With a data rate that is 30 times lower than the metering and pricing application, it was not necessary to obtain a maximum number of users in the DAN, since it exceeds by a considerable number of users the threshold imposed for the Metering and Pricing and Electric Car applications. Figure 3.7 shows the relationship between the throughput and the number of collectors. In [51] are described several codec and encoder schemes required by the voice application.

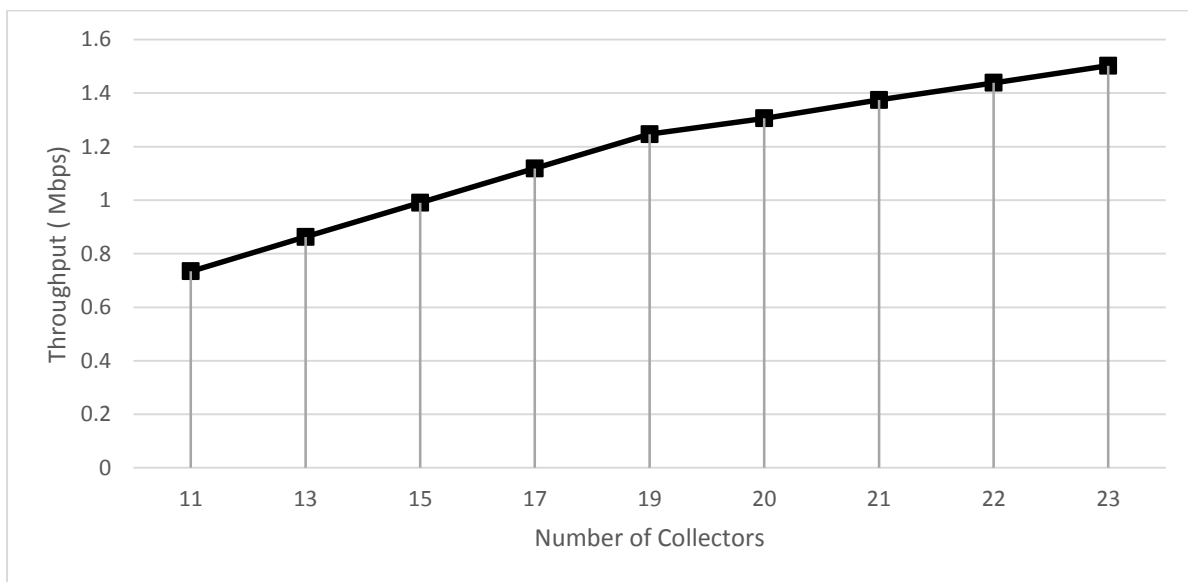


Figure 3.7 Capacity performance when Voice application is employed

### 3.5 Comparative Analysis between Applications

#### 3.5.1 Packet Loss Performance

The packet loss ratio indicates the amount of packets that did not reach the destination compared with the number of packets sent. Many reasons can cause packet loss, such as signal degradation over network medium, channel congestion, corrupted packets rejected in-transit, faulty hardware,

faulty network drivers and the distance between the transmitter and receiver. The packet loss performance is computed by using the following formula and is analyzed with respect to the packets sent:

$$\text{packet loss ratio} = \frac{\text{packets sent} - \text{packets dropped}}{\text{packets sent}} \quad (3.1)$$

Figure 3.8 shows the packet loss performance of DAN when the number of collectors is varied and different applications are employed. A better performance is obtained by the Voice application and the Video Surveillance application. The Voice application has an errorless transmission with no packet loss for the 33 collectors that were simulated in this scenario. The scheduling service employed influences the packet loss performance for the simulated applications. The scheduling type BE was used for all applications except the voice application. The results of using this WiMAX QoS mapping could be seen in a congested network where the data transmitted using this method would be the least to be sent. The voice applications does not experience packet loss, since it has a smaller data rate compared with other applications and it uses UGS scheduling service and gold class. The Video Surveillance application has no packet loss up to 29 collectors and when the number of collector is increased beyond this threshold a percentage of packets start dropping.

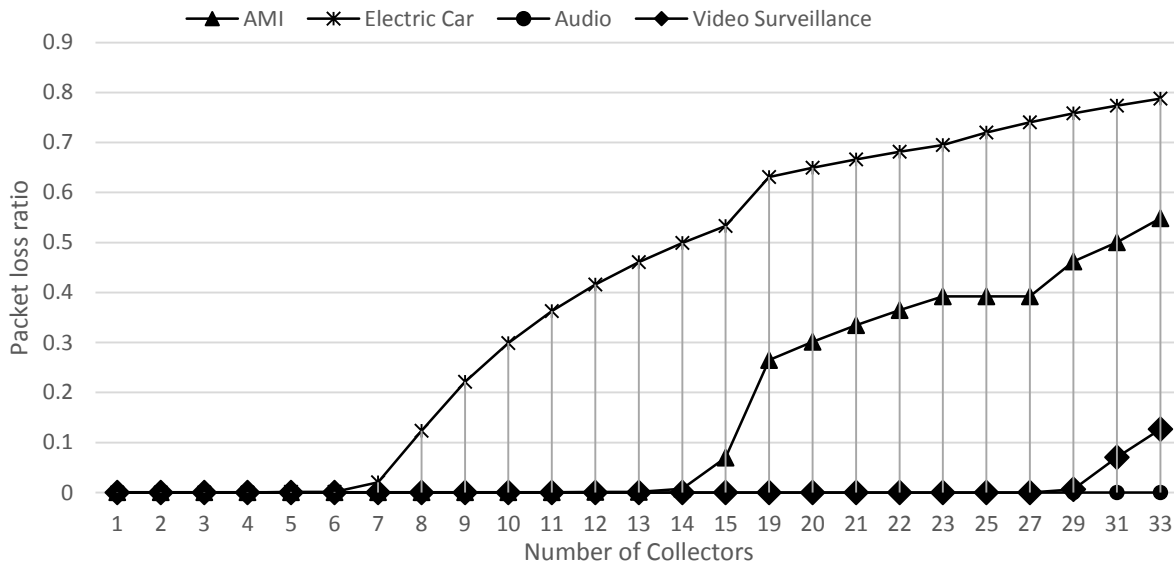


Figure 3.8 Packet Loss Performance when the number of collectors is increased

### 3.5.2 Latency Performance

Latency provides the total time needed to send a packet from source until it arrives at destination. The metering application has a shorter duration of the profile compared to other applications, since its traffic is being periodically transmitted and the respective packets are being held in line for scheduling which increases the overall latency.

Figure 3.9 indicates the average latency results of the smart grid from the DAN. The latency exceeds the maximum value defined in the WiMAX configuration once the threshold of collectors is surpassed. The maximum latency recommended for the metering and pricing application is one second and this value is exceeded when the number of collectors reached is 15. The latency required for the video application is significantly smaller than the ones for the electric car and metering and pricing applications. This value is overpassed before the threshold was reached at 29 collectors. For the amount of collectors assessed, the latency for the audio application was not outdone. In the case of the electric car application, the maximum latency imposed was overstepped only after 14 collectors.

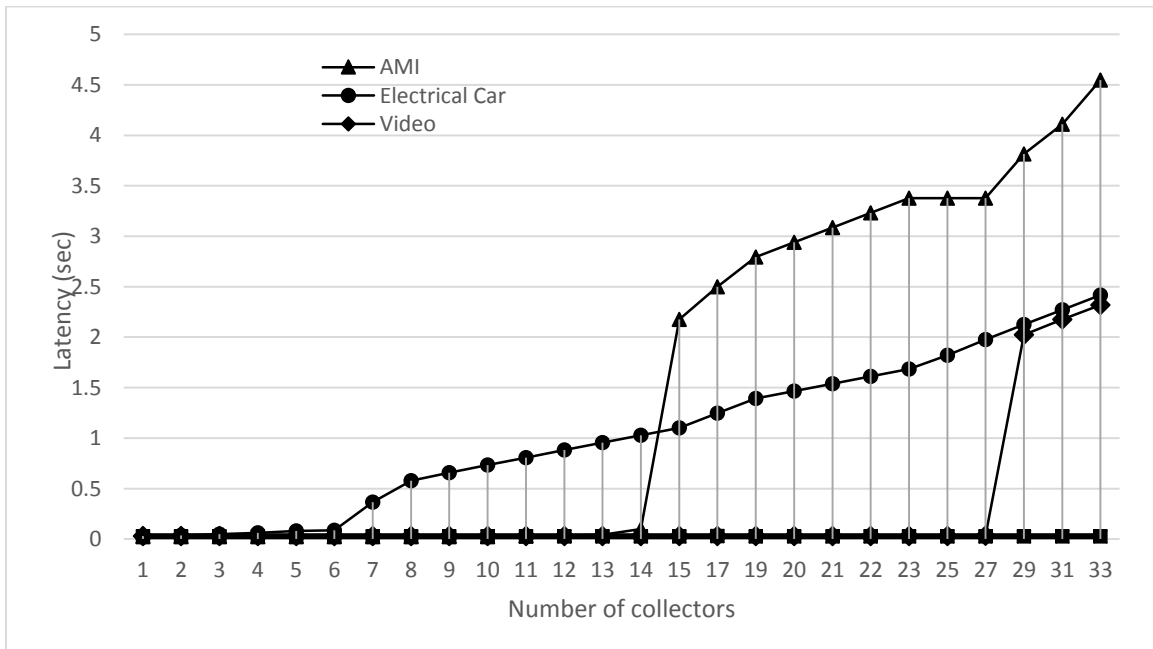


Figure 3.9 Latency performance when different applications are employed

### 3.6 Simulations

The test bed consists of a simulated WiMAX network which is interconnected with real devices defined as nodes. The cell has coverage of four kilometers and we evaluate the communication requirements for the DAN. The fixed nodes are arranged in a random manner. The total bandwidth is 10MHz divided into 1024 subcarriers.

The project design contains a base station, an application server and several scenarios where the number of neighborhoods is increased from one to twelve for the random traffic, and from one to six for the fixed traffic. The application, profile and WiMAX configurations are defined along with the network. A résumé of the system configuration is presented in Table 3.5 including the characteristics of the subscriber stations (collectors), base station.

Parameter	Value
Number of collectors	1 to 12
Max Tx Power (W)	Collectors: 0.5W; BS: 5W
Modulation and codification	QPSK $\frac{1}{2}$
Antenna Gain (dB)	Subscriber Stations: 14dB; BS: 15dB
Path loss Parameters	Disabled
Path loss Model	Erceg, Type A -suburban

Table 3.5 Base station and subscriber stations configuration

The parameters of the WiMAX profile are presented in Table 3.6.

Parameter	Value
Frame duration	5msec
Symbol duration	102.86 $\mu$ sec
Frequency	2.5GHz
Bandwidth	10MHz
Number of Subcarriers	1024
Uplink : Downlink Ratio (UL:DL)	75:25

Table 3.6 WiMAX configuration parameters

### 3.6.1 Constant Distribution of Applications' Profiles

In this section, we analyze the capacity of the channel when all the applications are active at the same time. This helps understanding the total throughput that can be sent in worst case scenario.

This scenario assumes that the start time for all application is the same. We can observe around 120 seconds during which all applications are sending uplink information to the base station in the same time. The values obtained are the highest amount of data that would be received by a base station from 4000 smart meter, 6 electric cars, 12 video cameras and 4 work phones.

Figure 3.10 shows the throughput from a single NAN, which is aggregated by a collector. In this situation all applications are active over 15 minutes.

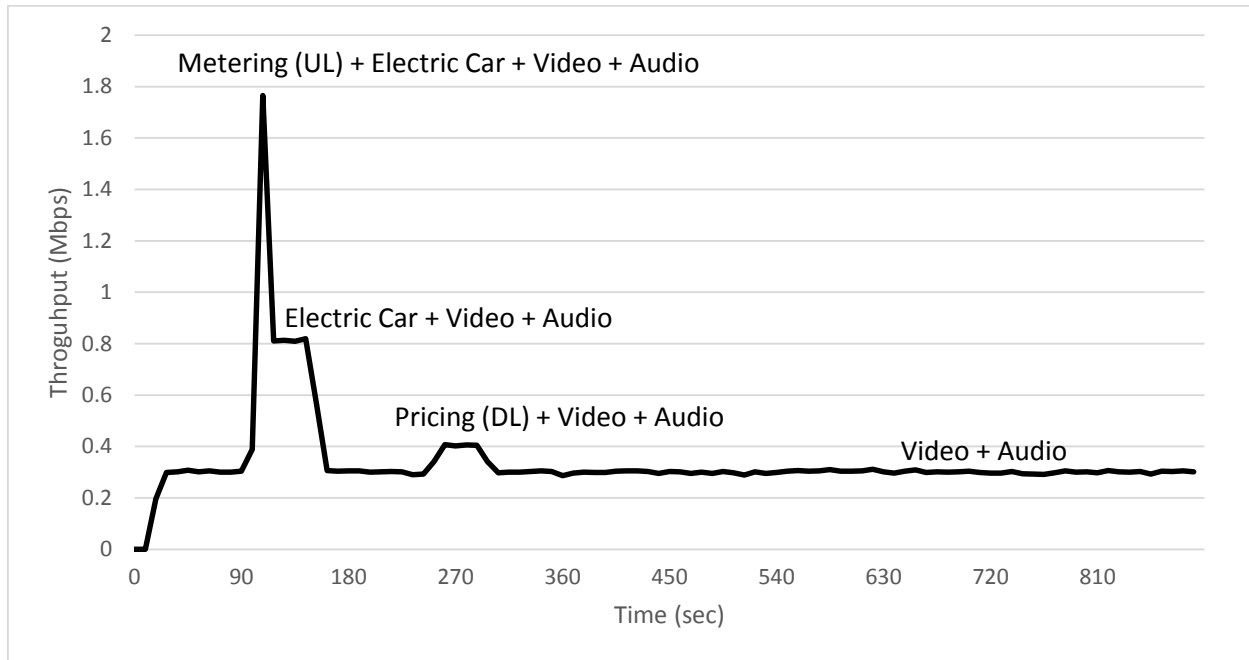


Figure 3.10 Throughput Performance for 1 Collector over 15 minutes, when all the applications are using the same constant start-time distribution.

We can observe that the highest data rate is experienced once both metering and pricing application and Electric Car are sending information. The maximum load that a collector could send to the main server is 1.788 Mbps. This result is obtained when a constant distribution is ap-

plied for the start time of the used applications. The traffic profiles of these applications are described in the Smart Grid Applications Section. The Video and Audio Applications have a significantly lower flow of data sent compared with the other two applications.

Figure 3.11 displays the throughput of the network over one hour simulation for multiple collectors. All applications have the same constant start-time distribution, which helped congesting the network when the load reached 7Mbps. The maximum number of collectors reached is 4, under the worst possible scenario when all applications are sending information at the same time. Compared to the previous figure, in this case, the simulation is run for an hour. We can observe that during the first five minutes, a very high amount of data is being sent. Since the Electric Car application is not run more than once per hour, the other applications are either constant, either periodic or with a load that is too small to affect or congest the network as the Voice Application.

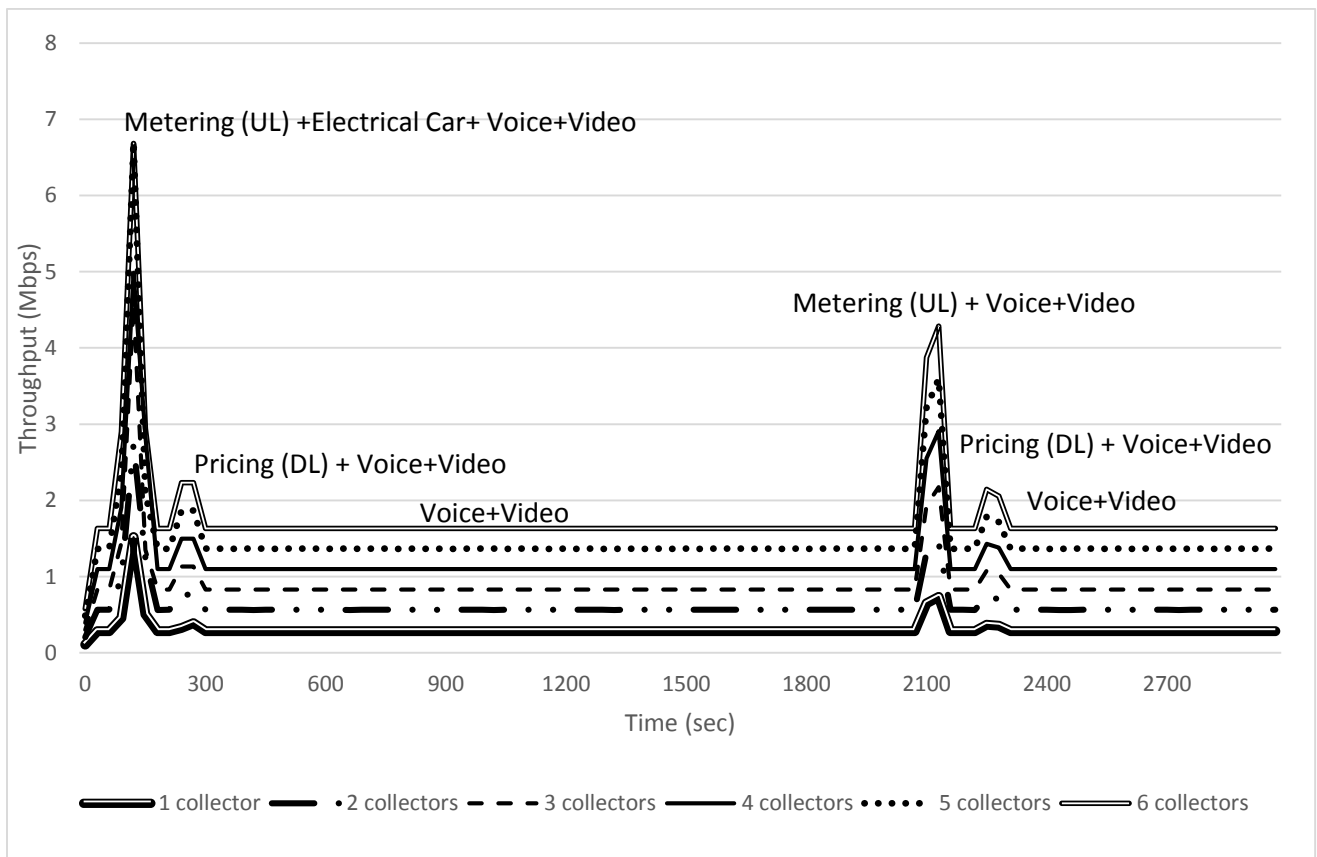


Figure 3.11 Throughput Performance for up to 6 collectors over 1 hour, when all the applications have the same start time



### 3.6.2 Random Distribution of Applications' Profiles

### 3.6.3 Single Collector

In this section the results of one collector are examined when the start-time distribution is selected to be Poisson. The Poisson distribution is used to express the probability of a given number of independent events occurring in a fixed interval of time, space, volume with an average rate. Figure 3.12 shows the topology of one neighborhood, which is positioned over  $1 \text{ km}^2$  area.

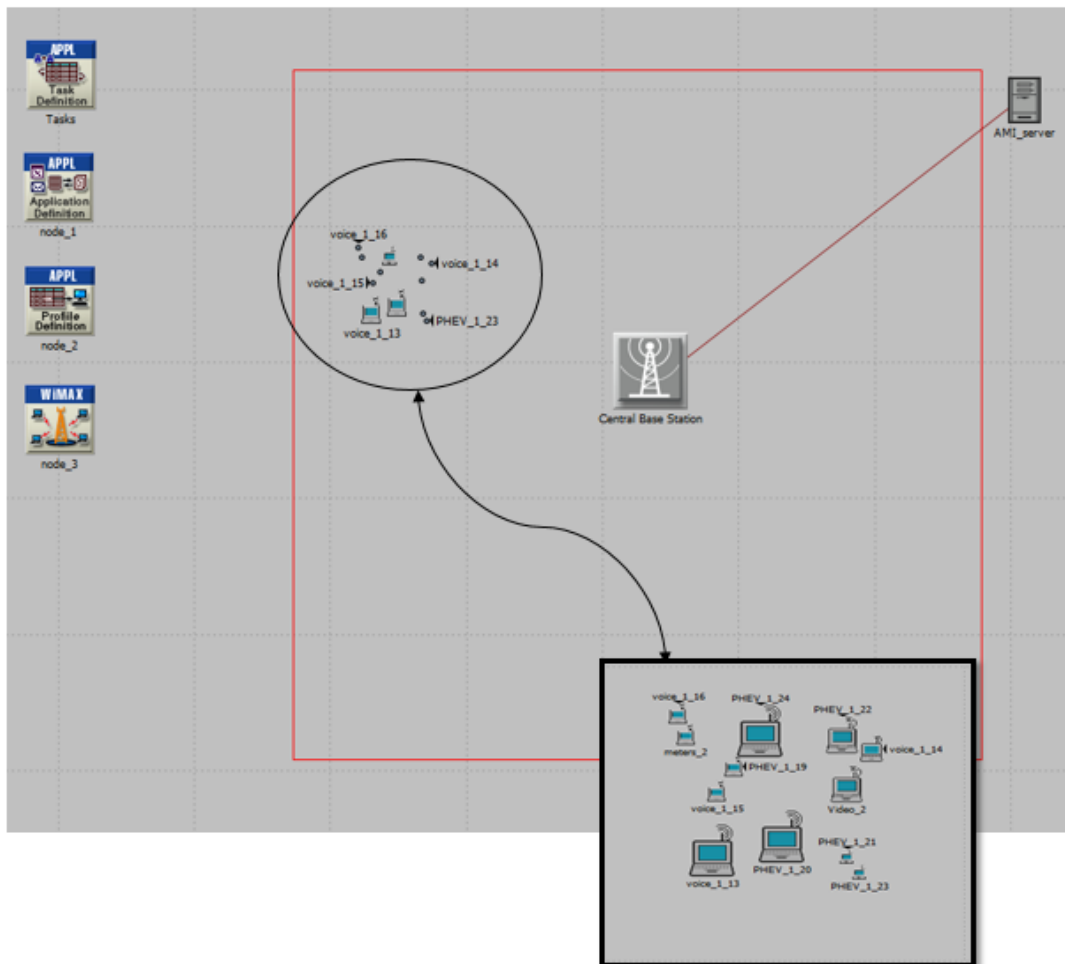


Figure 3.12 Network Topology of 1 Collector: 1 node which aggregates the information from 4000 smart meters, 4 nodes- Voice Application, 6 nodes- Electric Car Application, 1 node - Video Application.

One collector aggregates data from different types of subscriber stations that are presented in Table 3.7.

No. of Collectors	No. of Smart Meters	No. of Electric Cars	No. of Surveillance Cameras	No. of Telephones
1	4000	6	12	4

Table 3.7 Distribution of subscriber stations in one neighborhood

In order to ease the design, the meters are combined into one subscriber station with a data rate of 500kbps on the uplink and 100kbps on the downlink. This will not affect the performances and the accuracy of the simulation since the smart meters' traffic is periodical with a constant bit rate. The same pattern is used also for the video surveillance cameras since their traffic is continuous throughout the simulation. The subscriber stations with random traffic are distributed across the neighborhood as the following six electric cars and four work phones.

Figure 3.13 shows the throughput performance of one collector over a one hour simulation. In comparison with Figure 3.11, both electric car and voice applications have a random traffic. The main alteration was achieved by the change in the electric car profile, since it has a large data rate being sent in comparison with the voice application that has the lowest load being sent.

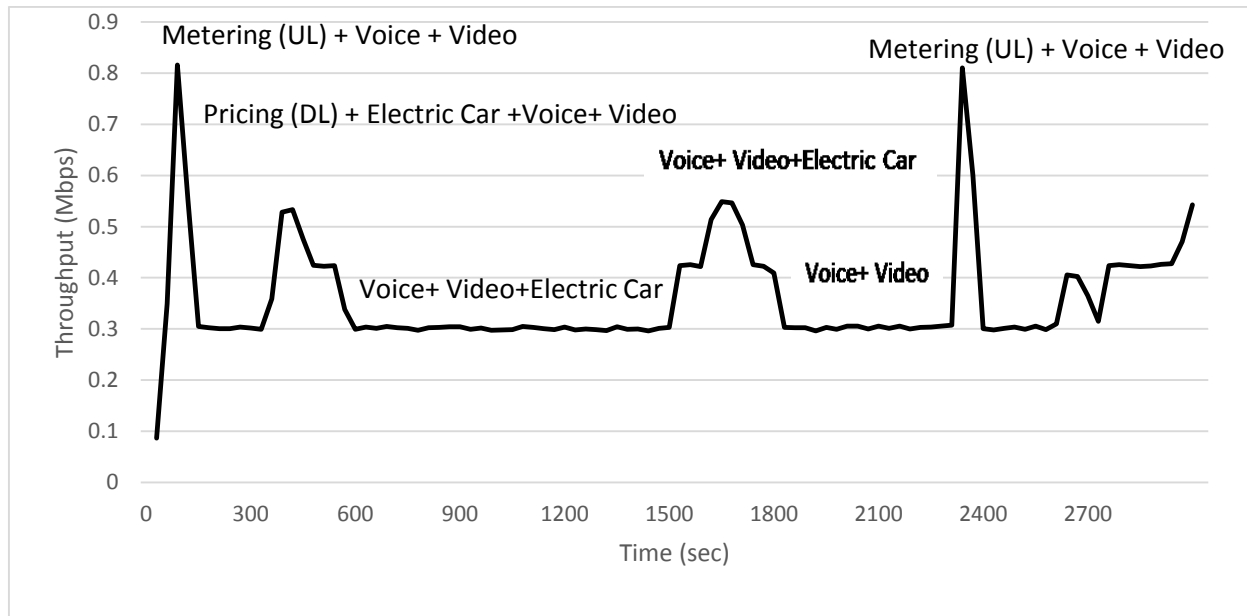
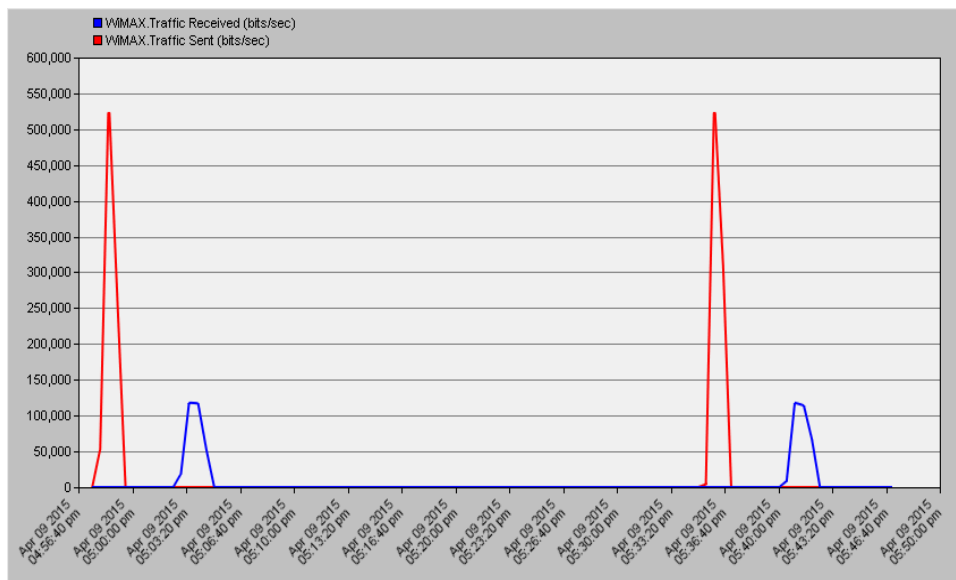
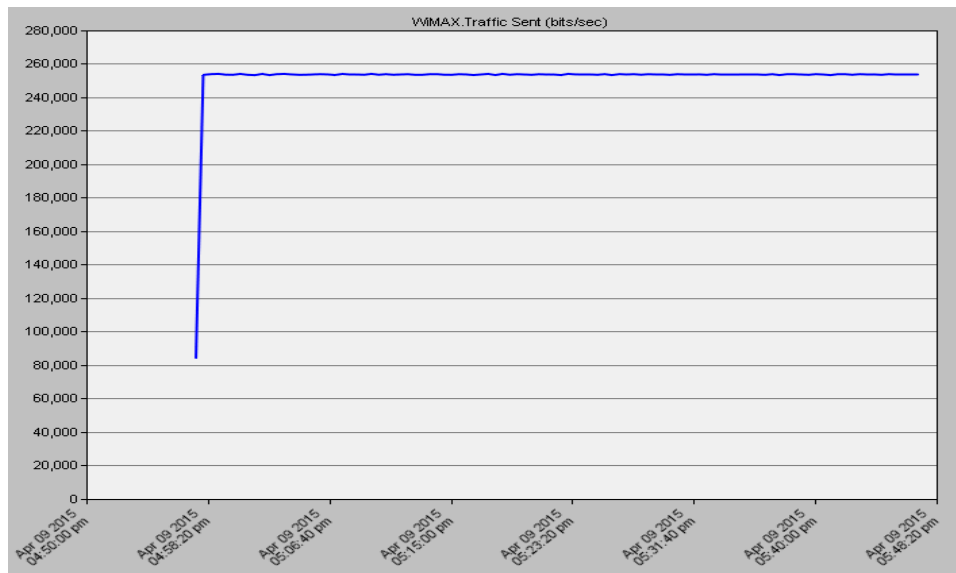


Figure 3.13 Throughput (Mbps) of 1 collector over 1 hour simulation

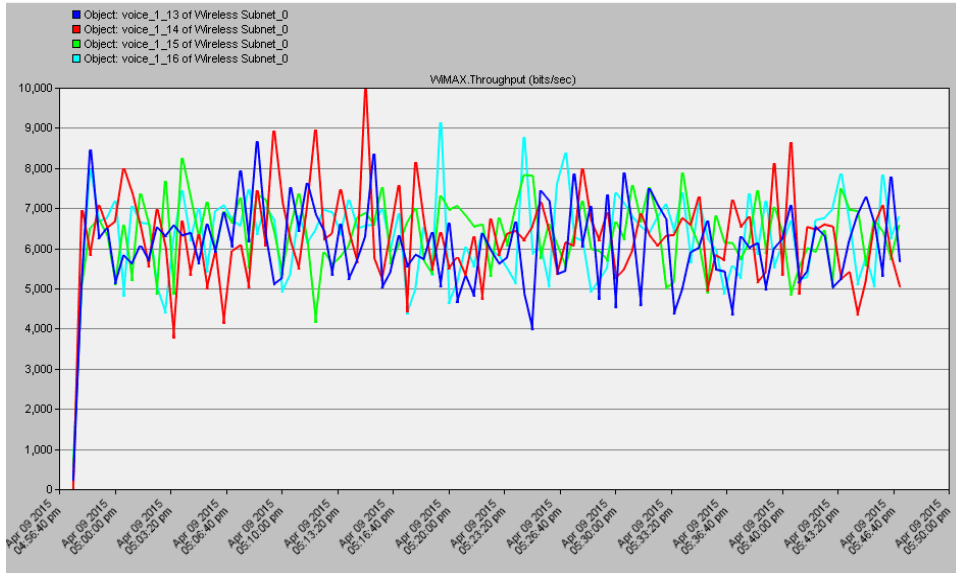
The data bursts related to each application are described in the Figure 3.14 where we can observe the sent traffic distribution over time from different devices. During an hour simulation a collector is receiving data from different consumers across the network. The traffic sent by the metering and pricing application (a) is periodical, with a constant bit rate and includes both uplink and downlink type of traffic. The traffic sent by the video surveillance cameras installed across a NAN is uniform with a constant bitrate. We assumed four devices spread across the NAN that would offer voice service for workforce and whose traffic pattern would be as in Figure 3.14 (c), random and without a constant bit rate. In a neighborhood are assumed to be six electric cars that are use electricity, at random start time as in Figure 3.14 (d).



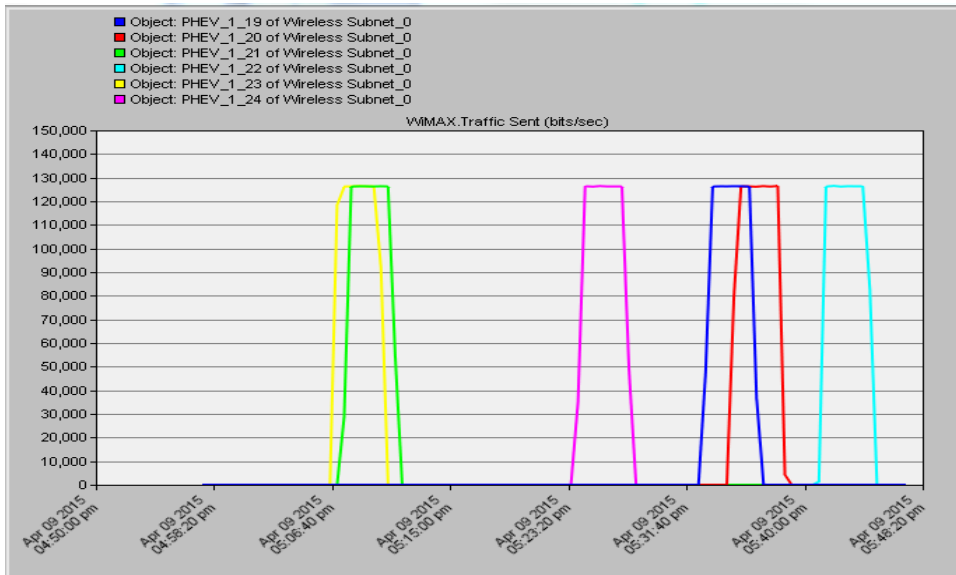
a)



b)



c)



d)

Figure 3.14. Throughput of all applications from 1 collector over 1 hour simulation: a) Metering + Pricing Application, b) Video Surveillance Application, c) Voice Application, d) Electric Car Application

### 3.6.4 Multiple Collectors

In this section, the results of several collectors are examined when the start-time distribution is selected to be Poisson. Figure 3.15 shows the topology of 8 neighborhoods on a total surface of  $4 \text{ km}^2$ . This surface represents the coverage range of the DAN which aggregates the traffic from several NANs.

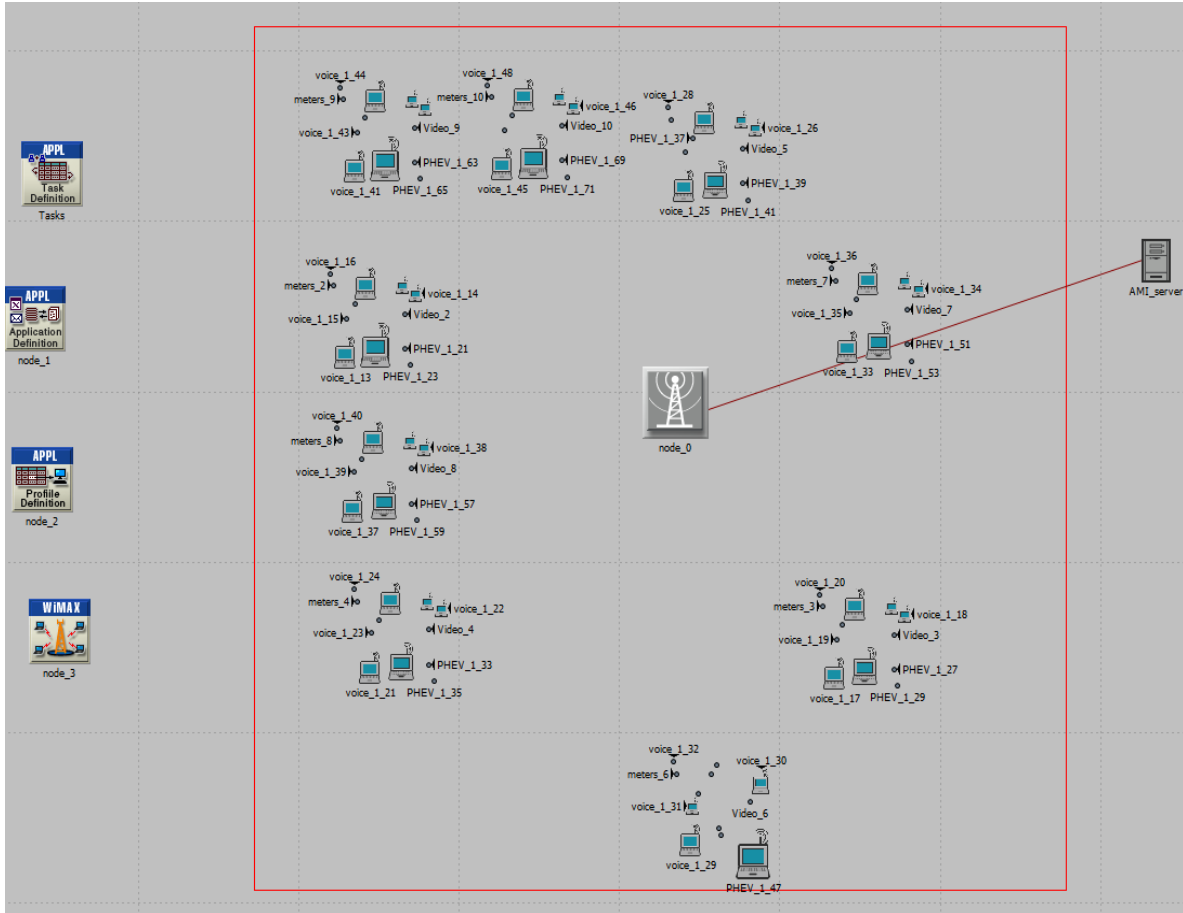


Figure 3.15 Network topology for 9 collectors

The maximum number of NAN that a DAN can collect is determined in this section. Several parameters are analyzed and simulated such as the throughput, packet loss ratio and the latency for 12 neighborhoods.

Figure 3.16 and 3.17 show the throughput of several collectors over a one hour simulation, when the voice and the electric car applications are randomly distributed. The maximum number

of NAN that a DAN can aggregate while maintaining the quality and reliability parameters imposed for the smart grid is eight. These results are closer to reality than the ones from Figure 3.17. Those results are obtained under critical conditions when all applications are deployed in the same time, while these are randomly distributed using Poisson distribution.

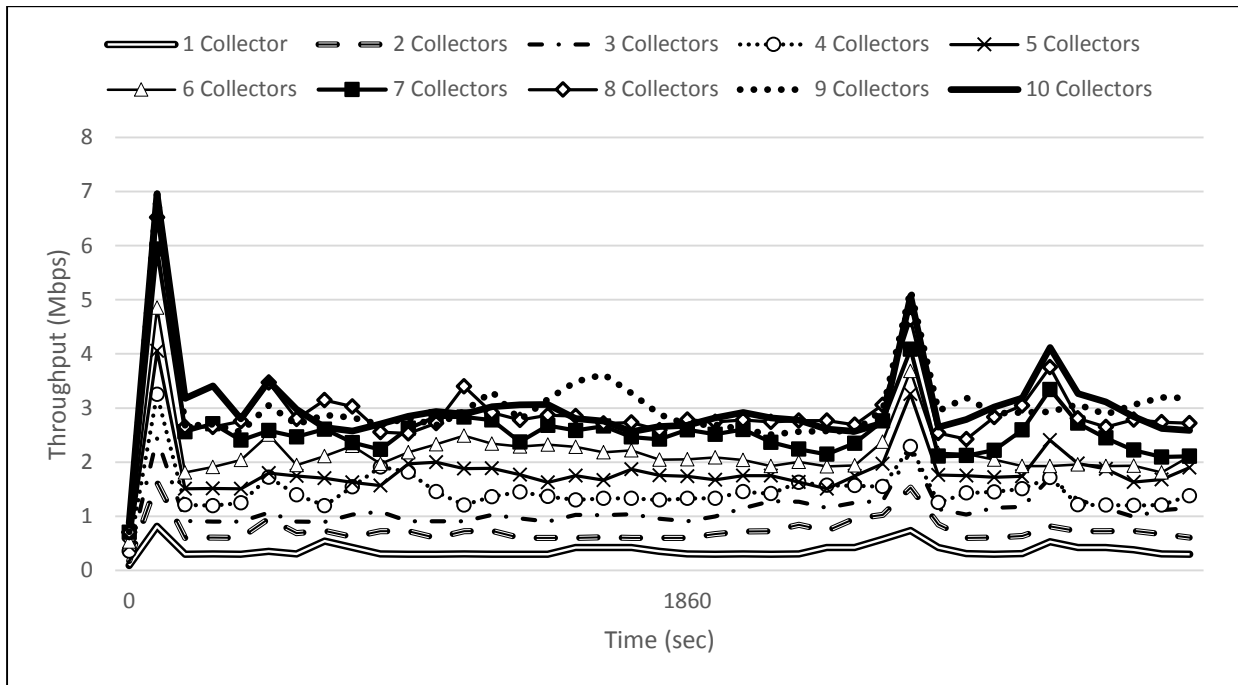


Figure 3.16 Throughput performance for different number of collectors over 1 hour simulation

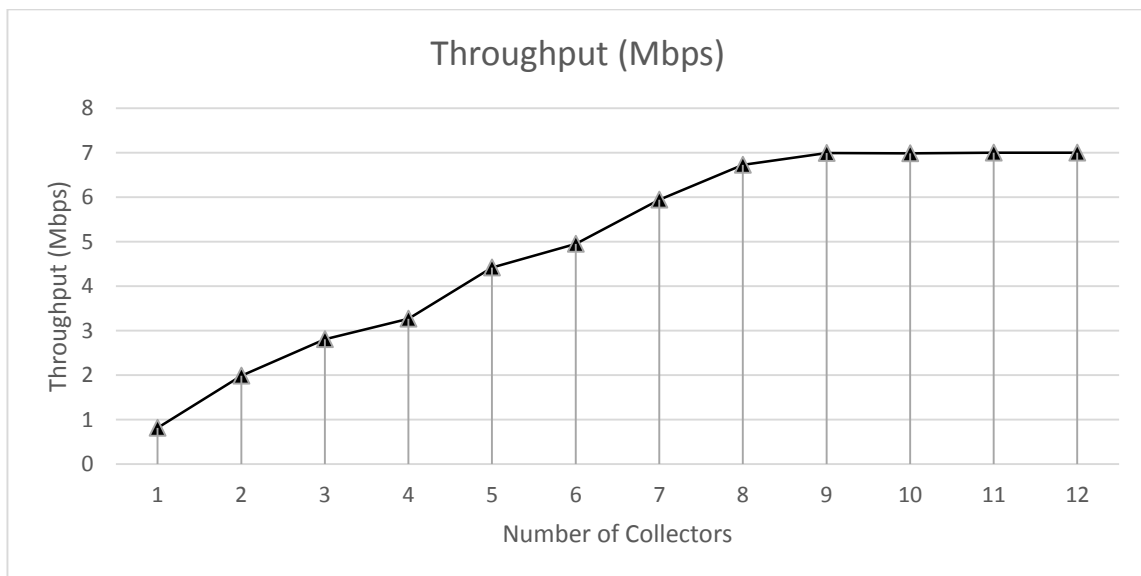


Figure 3.17 Throughput performance vs Number of Collectors, random traffic

In Figure 3.18 the packet loss ratio performance and the latency performance are presented. From both plots we can observe a decrease in the transmission quality, as the number of collectors exceeds the threshold of eight collectors. Both plots are overall plots including all applications that are being evaluated throughout the simulation.

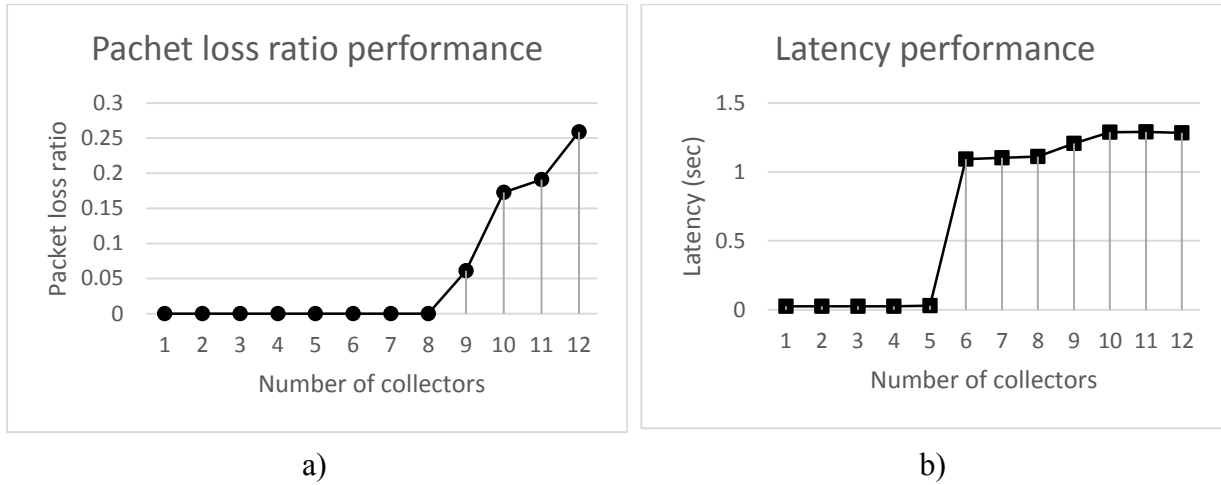


Figure 3.18 a)Packet loss ratio performance, random traffic b)Latency performance, random traffic

# Chapter 4

## Effects of Impulsive Noise over the Communication Layer

This chapter contains a detailed analysis on the impulsive noise effects over the smart grid's communication layer. The results were obtained after simulating an OFDM implementation of the WiMAX physical layer. This implementation of the WiMAX physical layer includes most of the defining parameters of the standard and is presented in detail in Section 2.4.5. All the smart grid applications are implemented individually according to the parameters indicated in Section 4.1. The implementation of the impulsive noise channel is made pursuant to the theoretical concepts developed in Section 2.6. This chapter highlights the effects of the impulsive noise over the following performances: BER, PER, throughput and the overall capacity of the network. For a better understanding, the outcomes are presented with and without the presence of impulsive noise.



## 4.1 Applications Requirements

The smart grid applications presented in Chapter 3 are employed to describe the effects of the impulsive noise over the WiMAX communication of the smart grid. All the applications considered have different data rates and most of them are uplink types of applications. The utility company collects and processes information from NANs and afterwards broadcasts a price update along with other information to the smart meters and other wireless devices that communicate with the utility station. In this section, we are interested in providing the implementation characteristics required to simulate the OFDM system used by the WiMAX standard.

The subcarrier allocation needed by the OFDM system is made by following the theoretical concepts described in the section 2.4.5 and adapted to the WiMAX specifications from section 2.4. Table 2.4 offers the specification required to simulate the system in MATLAB. However, because most of the applications contain uplink type of traffic, which is why Table 2.4 provides information mostly for the uplink implementation.

System Attributes	Values
System Bandwidth	10 MHz
FFT Size	1024
Null sub-Carriers UL	184
Pilot Sub-carriers UL	280
Data sub-carriers UL	560
Sub-channels	35
Symbol Period, $t_s$	102.9 microseconds
Frame Duration	5 milliseconds
Downlink : Uplink Ratio	25:75
Number of OFDM symbols	48
Number of OFDM Uplink Symbols	36
Cyclic Prefix (CP)	1/8
CP Length	$FFT * CP = \frac{1024}{8} = 128$
Sampling Rate	$OFDM\ symbols * \frac{CP\ Length + FFT}{frame\ duration}$ $= 48 * \frac{128 + 1024}{0.005} = 11.059\ MHz$
Modulation	QPSK
Coding Technique	CC 1/2

Table 4.1 System Attributes

Table 4.2 presents the algorithm used to generate the subcarrier allocation. The number of subcarriers increases along with the data rate related to each application. Because the data rates are very different, different allocations are used for all applications, translating into different length codes processed by the convolutional encoder. The values obtained for the bit/frame rate are due to the fact that QPSK modulation is employed, signifying that two bits are required to send a symbol.

Application	Data rate	Bits/frame=frame duration*data rate	Subcarrier allocation
Voice	18kbps	68	32 symbols*2 subcarriers+4 symbols*1 subcarriers=68
Video	256kbps	960	12 symbols*28 subcarriers+24 symbols*26 subcarriers=960
Metering	500kbps	1876	4 symbols*53subcarriers+32symbols*52 subcarriers=1876
Electric Car	1 Mbps	3750	6symbols*105subcarriers+30symbols*104subcarriers=3750

Table 4.2 Subcarrier Allocations for the employed applications

## 4.2 Simulations Results

The simulated scenario provides the effects of the impulsive noise over the OFDM physical layer with settings that are usually assigned in a WiMAX setup. This section provides an analysis on results such as BER, PER, throughput, and the base station capacity. These results are obtained when SNR, Signal to Interference Ratio (SIR) and probability of having impulsive noise are varied. The representation of the impulsive channel in MATLAB takes into consideration the impulse amplitude, duration, probability of having impulse and inter-arrival time.

The simulations are performed by assuming an OFDM configuration with 1024 subcarriers, QPSK modulation with the allocation of the used subcarriers given in Table 4.2. The average power of the real and imaginary signal components are normalized to 1 in all simulations.

The amplitude of the impulsive noise is controlled through the SIR:

$$SIR = \frac{E[|a_k|^2]}{E[|g_k|^2]} = \frac{\sigma_a^2}{2\sigma_i^2}. \quad (4.1)$$

$\sigma_a^2$  is the variance of the signal

$\sigma_i^2$  is the variance of the impulsive noise

The values of SIR chosen to deliver all the simulations from these sections are: -15dB, -10dB and -5dB. The probabilities of having impulsive noise used to generate the simulations are the following: 0.5, 0.1, 0.05, 0.01, 0.005, 0.001, 0.0005, 0.0001, 0.00005 and 0. The width of the impulsive noise sample was selected to have the same duration of as the OFDM symbol. For a higher impact of the impulsive noise over the symbol, the duration of the impulsive noise should be decreased, such that an OFDM symbol would be affected by more than one sample of the impulse noise. The inter-arrival time between impulses is given by the probability of impulse appearance.

#### 4.2.1 BER Performance

The influence of the impulsive noise over the bit error probability is analyzed in this section when  $E_b/N_0$  is increased from 0 to 15db and the probability of the impulsive noise is varied.

The results obtained from the simulations are presented in Figures 4.1 – 4.12 as the BER curve over  $E_b/N_0$ . The curves represent the number of bit errors divided by the number of total bits in a certain time frame and at a certain SNR. The bit error probability represents the expectation of having an error at a certain SNR.

The purpose of this section is to analyze the performance difference of the OFDM system when the channel considered is AWGN or the channel considered presents both AWGN and Impulsive Noise. As expected, for all applications the performance obtained when impulsive noise is added is worse than for the channel that has only AWGN.

Table 4.2 describes the way the subcarriers are assigned in the OFDM scheme. Theoretically, by increasing the number of subcarriers a better transmission performance is obtained. When a single-carrier high speed system is employed means that the delay spread will be larger than the symbol duration. The principle of OFDM is to divide a high data rate channel over a multiple number of subcarriers. Since the symbol duration of a multicarrier system is proportional to the number of subcarrier used, this means that having a larger number of subcarriers translated into longer symbol duration. With longer symbol duration this means that the delay will be smaller

relative to the symbol length. As expected, the BER performance related to each application is better for applications will larger number of subcarriers used.

Table 4.3 provides the values for BER when  $E_b/N_0$  is set to 8dB, the probability of having impulsive noise is  $p=0.0005$  and the SIR is varied between -15dB, -10dB and -5dB. The BER performance obtained when the AWGN is used is better for applications with a larger traffic. We can observe that for all the applications the gain between the BER curve obtained with an AWGN channel and the one obtained with an impulsive channel decreases as the SIR is increased. This means that when the power of the impulsive signal is decreased then the probability of bit error gets smaller. This leaves a smaller difference in performances between the two cases. A smaller gain between the two BER results means that the influence of the impulsive noise is decreasing.

<b>Application</b>	<b>BER for AWGN</b>	<b>SIR</b>	<b>BER for Impulsive Noise</b>	<b>Gain</b>
<b>Electric Car</b>	3.19E-07	-15dB	2.73E-03	2.73E-03
		-10dB	1.16E-06	8.41E-07
		-5dB	1.60E-07	1.60E-07
<b>Metering</b>	3.46E-07	-15dB	3.08E-03	3.08E-03
		-10dB	1.49E-06	1.14E-06
		-5dB	5.16E-07	1.70E-07
<b>Video Surveillance</b>	6.25E-07	-15dB	3.20E-03	3.20E-03
		-10dB	3.12E-06	2.50E-06
		-5dB	8.16E-07	1.91E-07
<b>Voice</b>	1.10E-06	-15dB	4.60E-03	4.60E-03
		-10dB	3.67E-06	2.57E-06
		-5dB	2.35E-06	1.25E-06

Table 4.3 BER values when  $E_b/N_0=8$  dB,  $p=0.0005$  and the gain of BER between the results with AWGN and Impulsive noise

Figures 4.1 – 4.3 show the BER performance of the electric car application when the  $E_b/N_0$  is increased from 0 to 15dB and also the SIR is varied from -15db,-10dB and -5dB. These results show that while the power of the impulsive noise is diminished, the BER curves tend to

merge to the AWGN case, leaving a smaller gain between the two curves. We can also observe the performance degradation when the probability of sending erroneous bits is increased.

Figures 4.4 – 4.6 display the performance for the metering applications when different characteristics are modified throughout the simulations. The BER curve gets worsen when the probability of having erroneous bits sent is higher, as well as when their power amplitude is increased.

The BER results for the Video surveillance applications are displayed in Figures 4.7– 4.9. With a traffic of 256kbps, the video applications have the subcarrier allocations presented in Table 4.2. All applications simulated in this section follow the same algorithm adapted for each of them, such that their characteristics from Table 4.2 are matched. With the lowest traffic required from all applications the Voice for workforce application illustrates the performances from Figures 4.10 - 4.12.

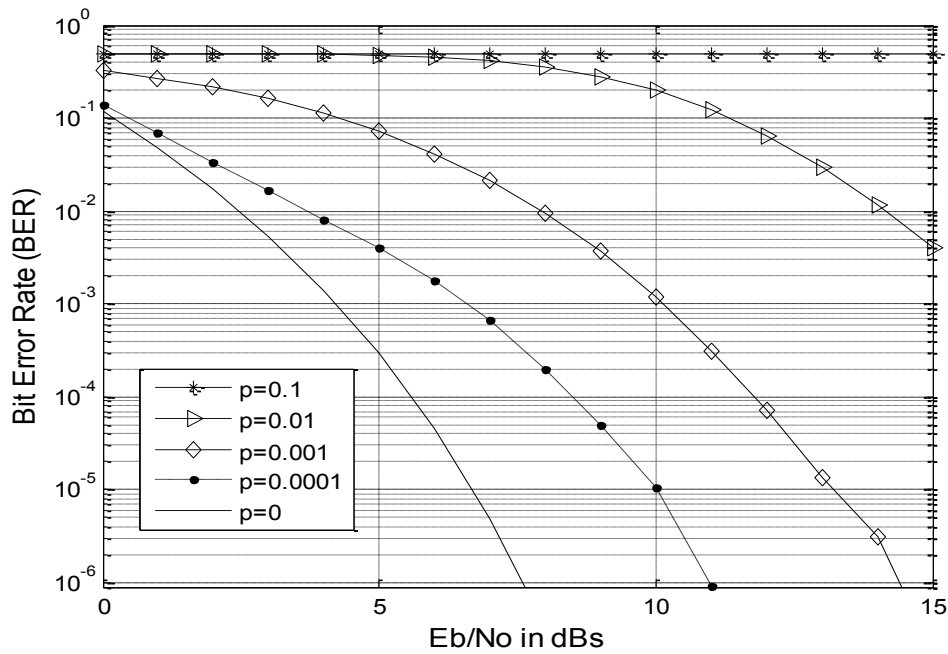


Figure 4.1 BER vs  $E_b/N_0$ , SIR= -15dB, Electrical Car Application

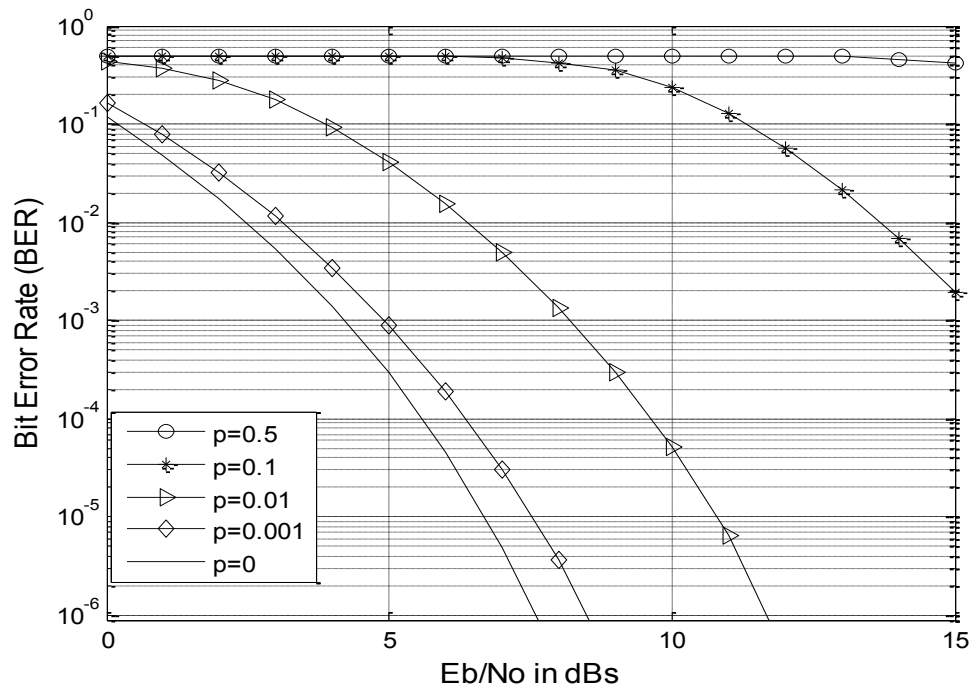


Figure 4.2 BER vs  $E_b/N_0$ , SIR=-10dB, Electric Car Application

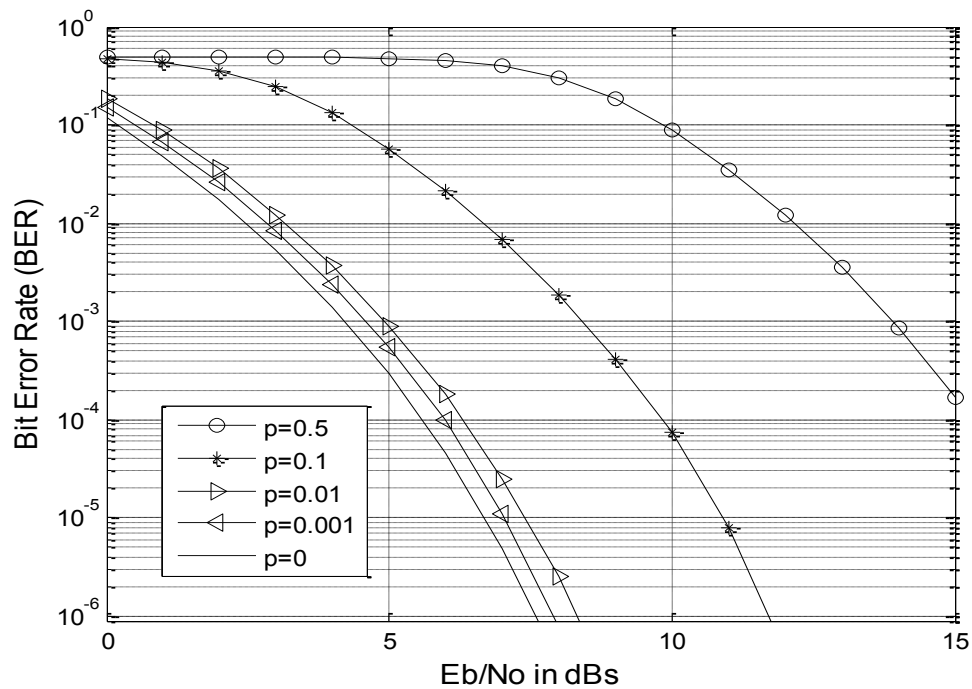


Figure 4.3 BER vs  $E_b/N_0$ , SIR=-5dB, Electric Car Application

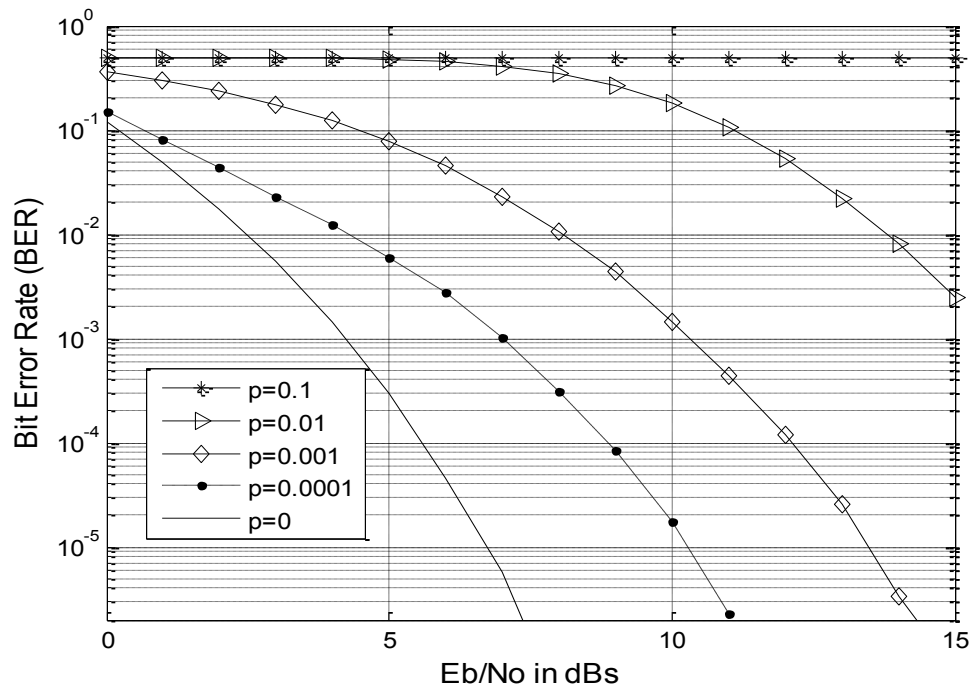


Figure 4.4 BER vs  $E_b/N_0$ , SIR=-15dB, Metering Application

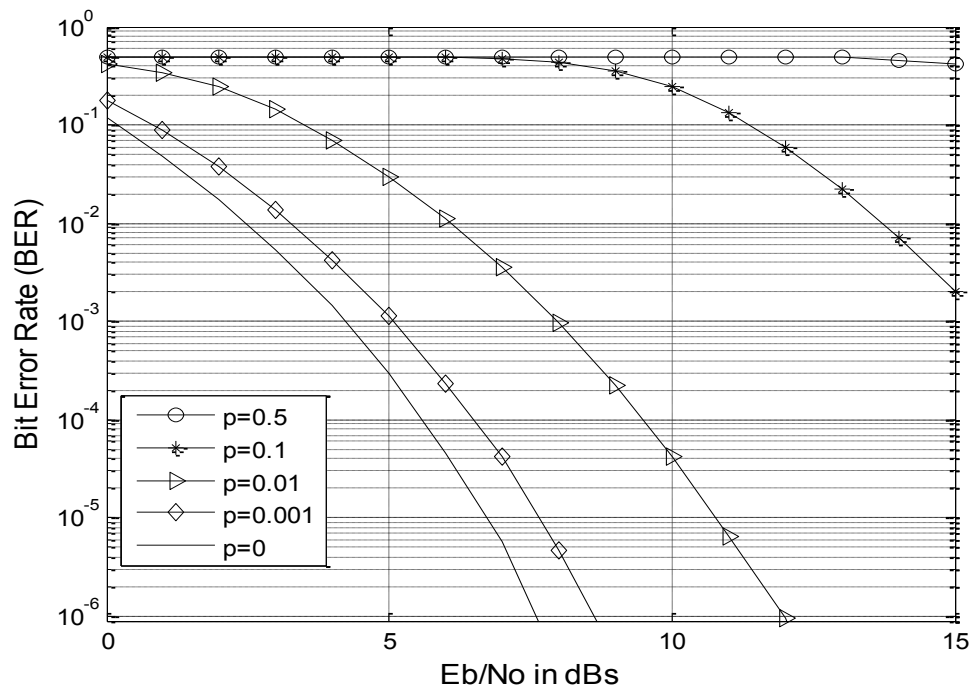


Figure 4.5 BER vs  $E_b/N_0$ , SIR=-10dB, Metering Application



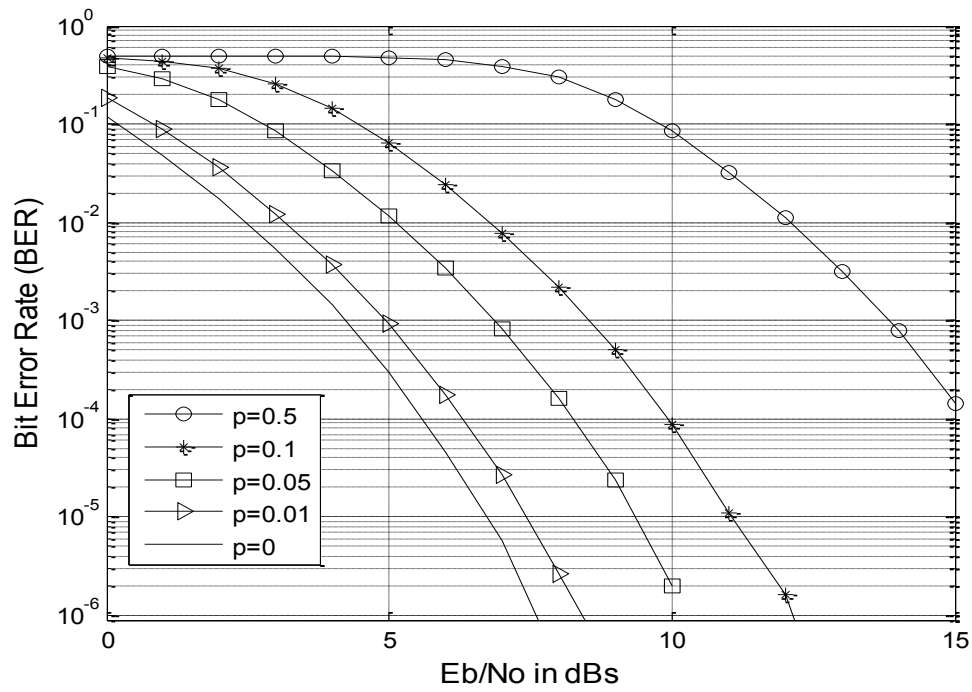


Figure 4.6 BER vs  $E_b/N_0$ , SIR=-5dB, Metering Application

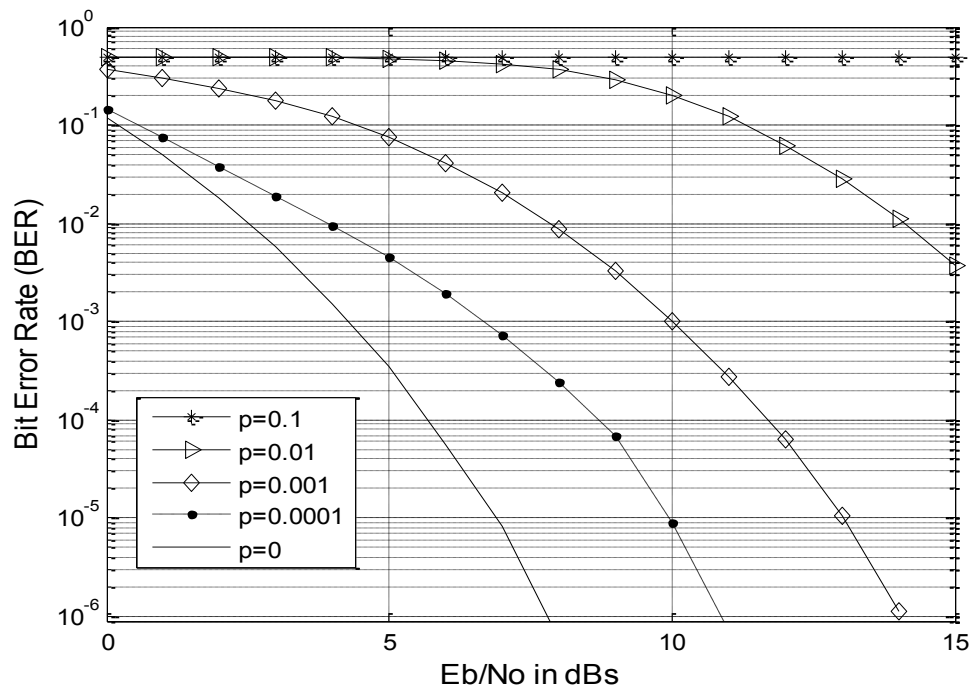


Figure 4.7 BER vs  $E_b/N_0$ , SIR=-15dB, Video Surveillance Application

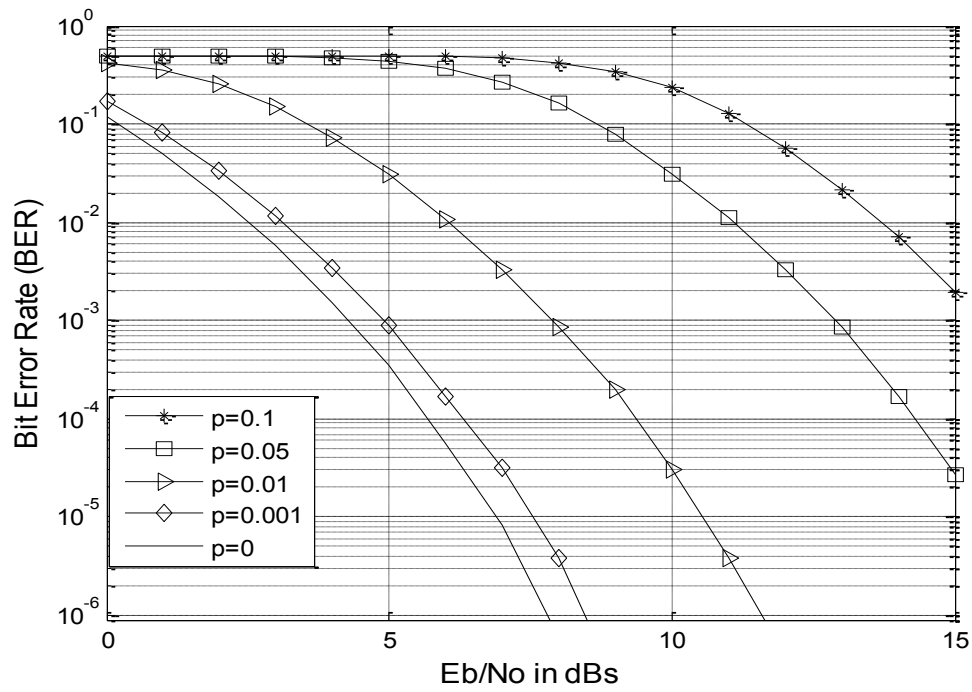


Figure 4.8 BER vs  $E_b/N_0$ , SIR=-10dB, Video Surveillance Application

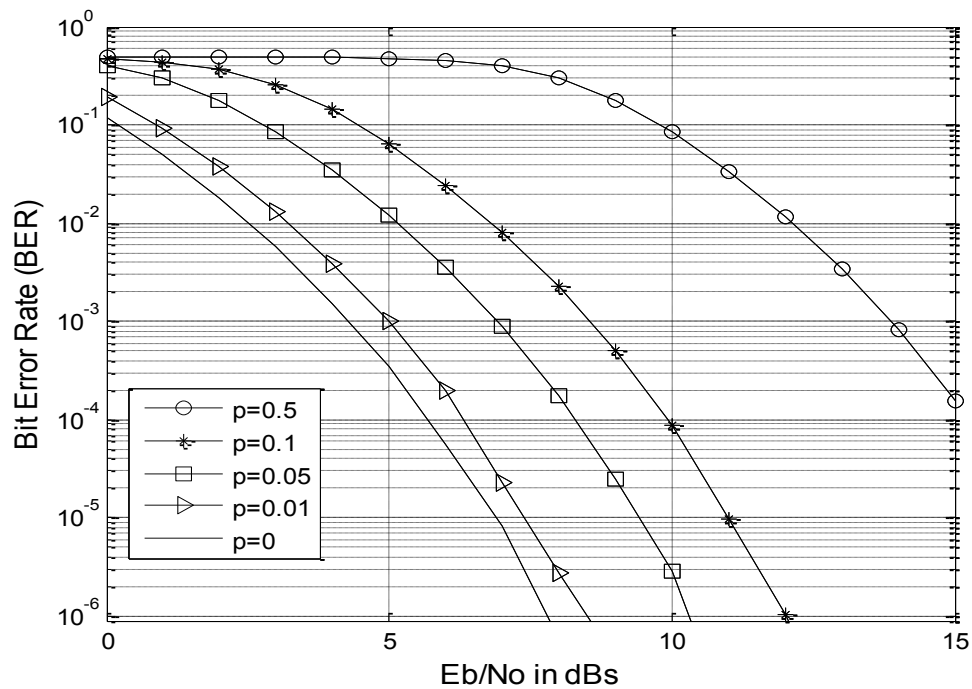


Figure 4.9 BER vs  $E_b/N_0$ , SIR=-5dB, Video Surveillance Application

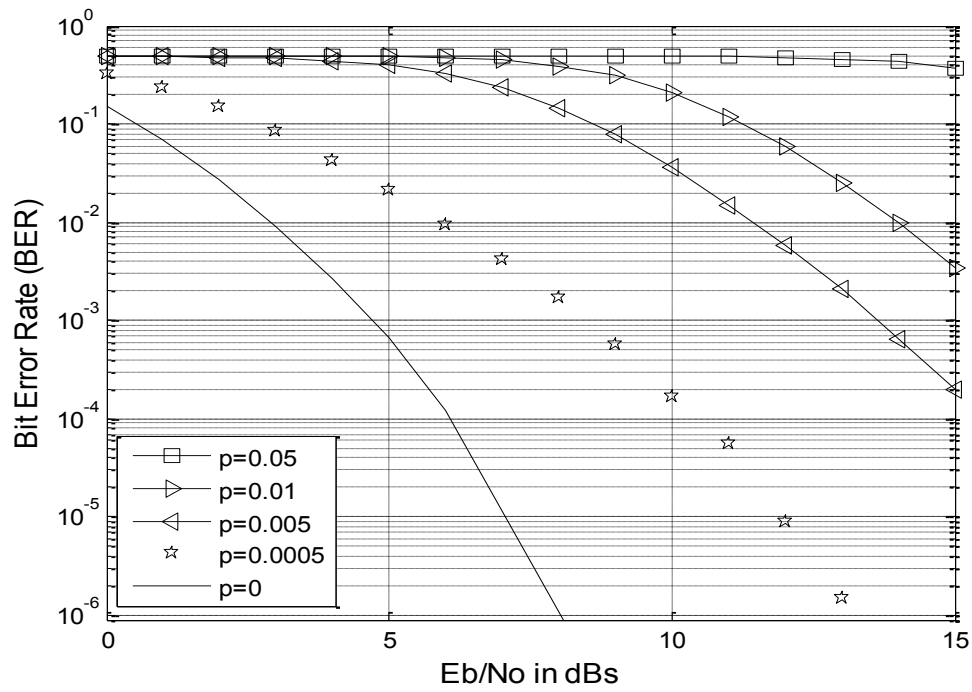


Figure 4.10 BER vs  $E_b/N_0$ , SIR=-15dB, Voice Application

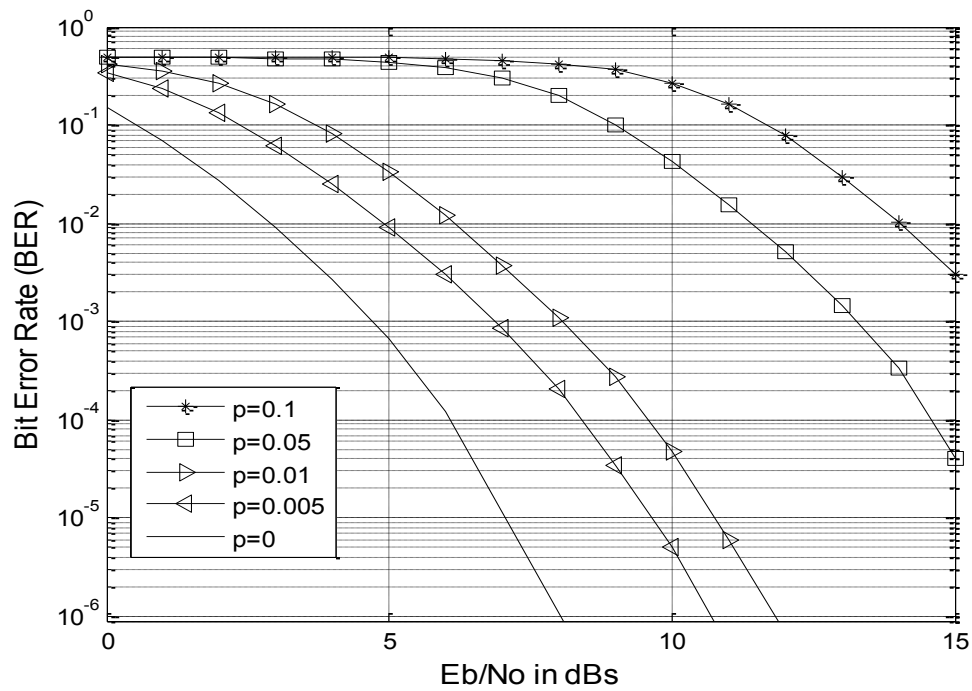


Figure 4.11 BER vs  $E_b/N_0$ , SIR=-10dB, Voice Application

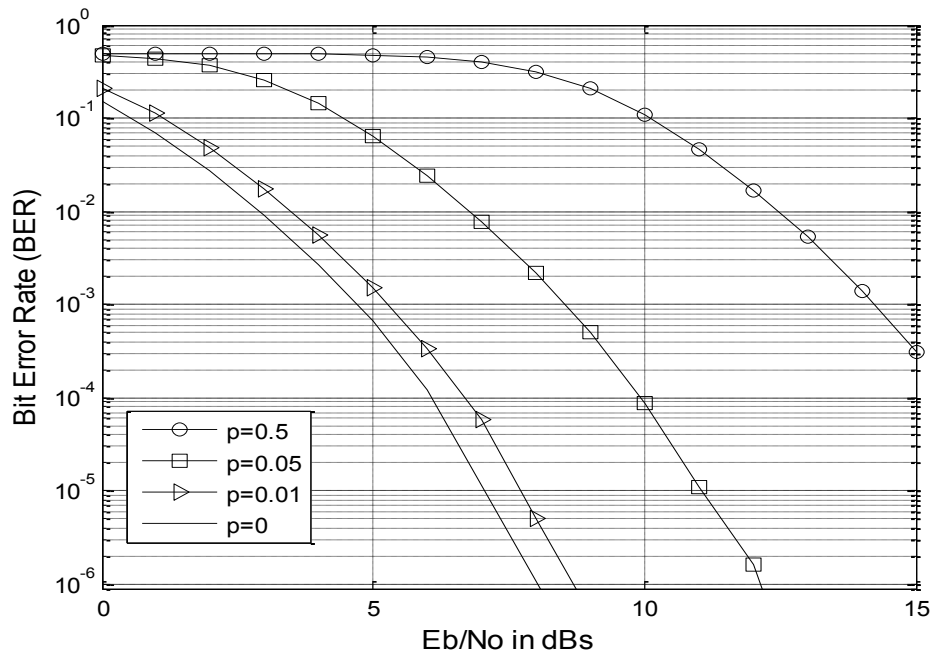


Figure 4.12 BER vs  $E_b/N_0$ , SIR=-5dB, Voice Application

#### 4.2.2 PER Performance

The packet loss ratio indicates the amount of packets that did not reach the destination in comparison with the number of packets that were sent. Among the causes of packet dropping we can list signal degradation, channel congestion, corrupted packets, faulty hardware, poor SNR, etc. The values of PER are similar to the ones of the BER. However, in this situation the size of the packet sent for each application can also influence the results, taking into account that the formula for the PER is the following:

$$PER = 1 - (1 - BER)^n; \quad n = \text{size of the packet} \quad (4.2)$$

Application	Size of the UPLINK Packet
Electric Car	125 bytes
Metering	125 bytes
Video Surveillance	600 bytes
Voice	32 bytes

Table 4.4 Uplink Packet sizes for all applications

Table 4.5 shows the PER values for all applications when the probability of having impulsive noise is  $p=0.001$  or  $p=0.0001$ ,  $SIR=-15\text{dB}$  and  $\frac{E_b}{N_0} = 12\text{dB}$ . As expected, when the influence of the impulsive noise is lower, the probability of having dropped packets diminishes.

Application	$p=0.001$	$p=0.0001$
Electric Car	0.268	0.0009
Metering	0.35	0.0022
Video Surveillance	0.58	0.0023
Voice	0.04	0.0001

Table 4.5 PER,  $\frac{E_b}{N_0} = 12\text{dB}$ ,  $SIR=-15\text{dB}$   $p=0.001$  and  $p=0.0001$

Figures 4.13 – 4.20 show the PER for all applications that were used to simulate and analyze the characteristics of the smart grid. The PER gain difference for all applications between the AWGN case and the Impulsive Noise case, where the probability of having impulsive noise is  $p=0.001$  or  $p=0.0001$  and the SIR is varied from  $-15\text{dB}$ s to  $-5\text{dB}$ s. As expected, when the influence of the impulsive noise is lower, the probability of having dropped packets diminishes as well.

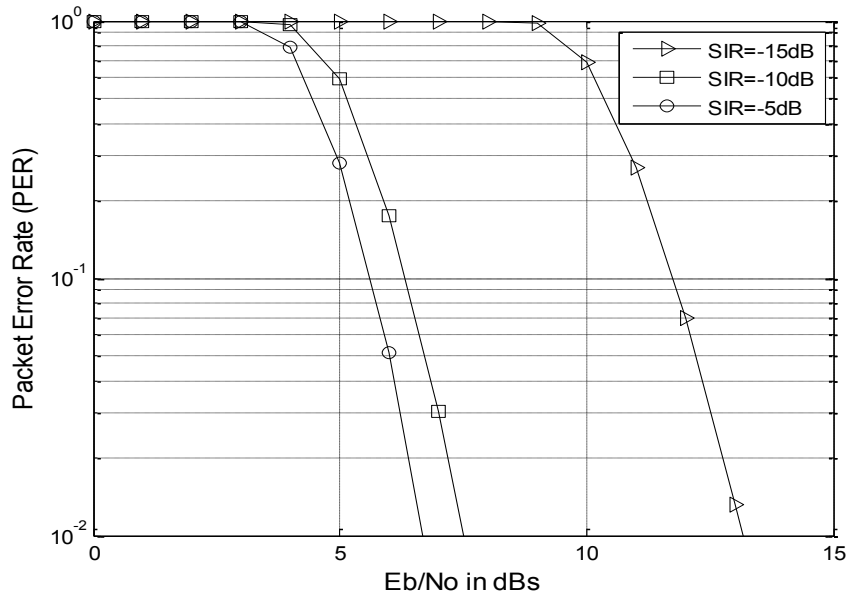


Figure 4.13 PER vs  $E_b/N_0$ ,  $p=0.001$ , Electric Car Application

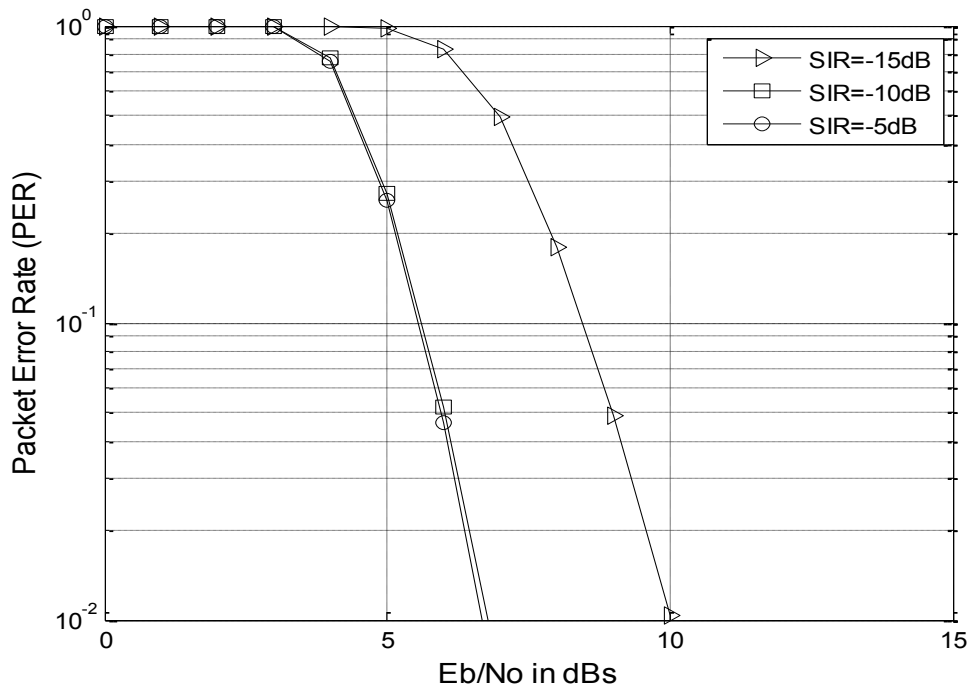


Figure 4.14 PER vs  $E_b/N_0$ ,  $p=0.0001$ , Electric Car Application

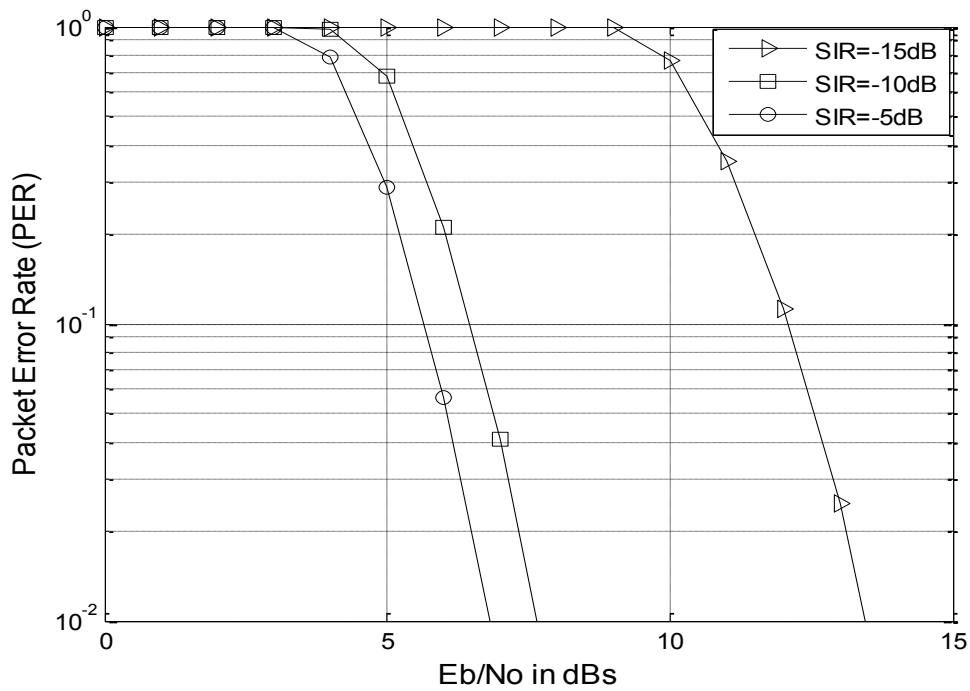


Figure 4.15 PER vs  $E_b/N_0$ ,  $p=0.001$ , Metering Application

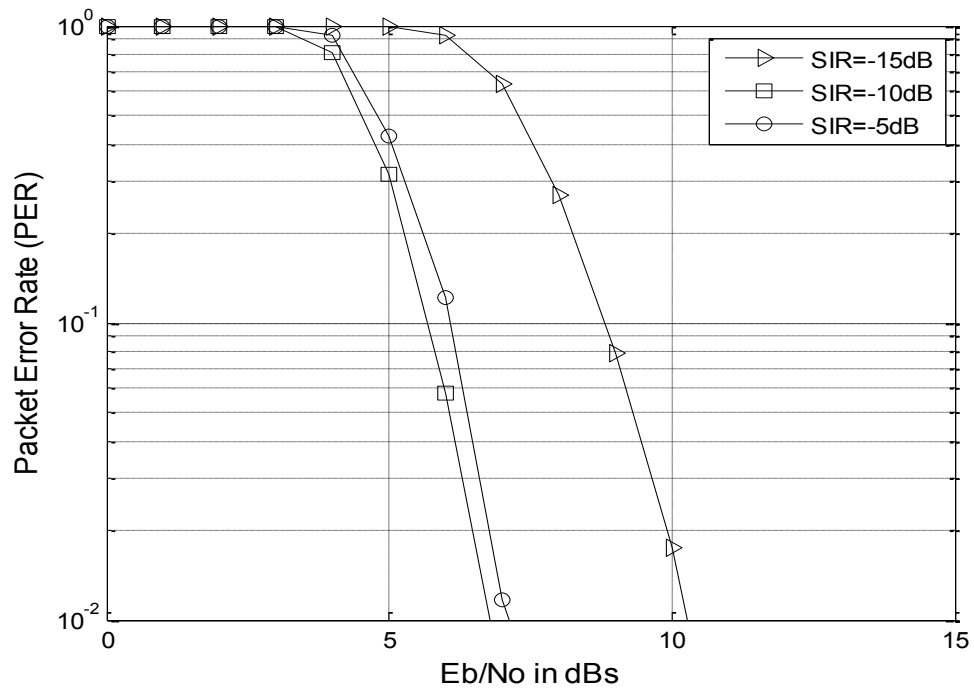


Figure 4.16 PER vs  $E_b/N_0$ ,  $p=0.0001$ , Metering Application

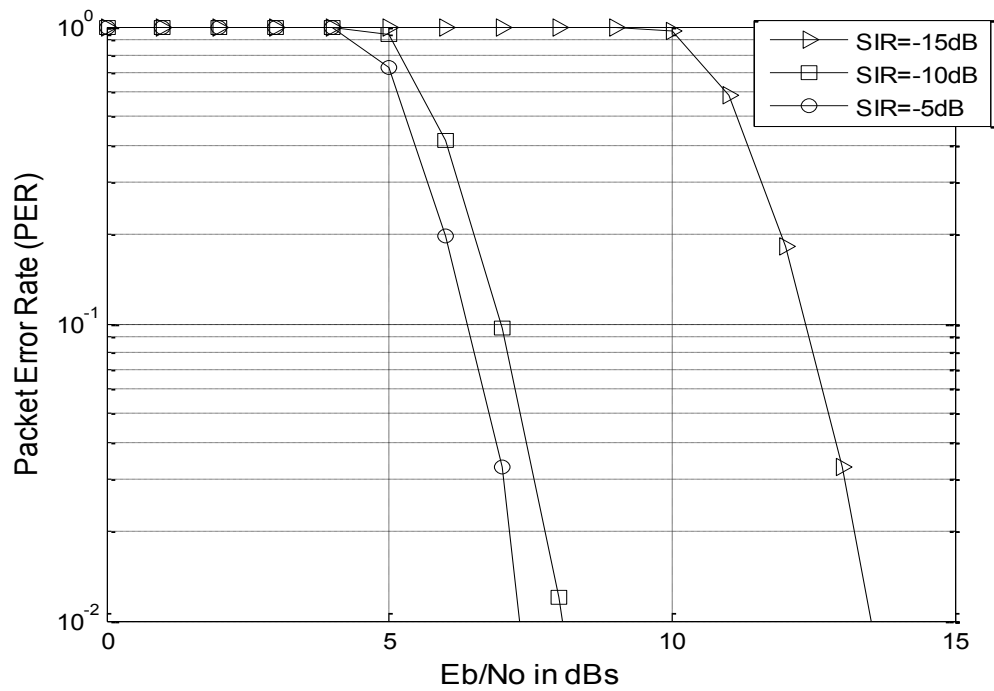


Figure 4.17 PER vs  $E_b/N_0$ ,  $p=0.001$ , Video Surveillance Application

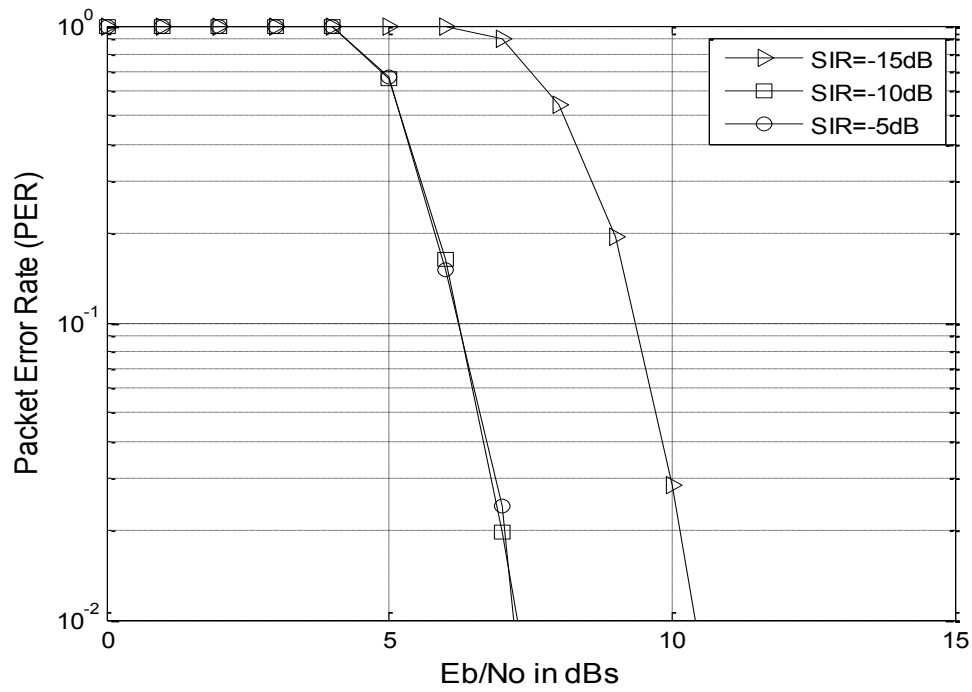


Figure 4.18 PER vs  $E_b/N_0$ ,  $p=0.0001$ , Video Surveillance Application

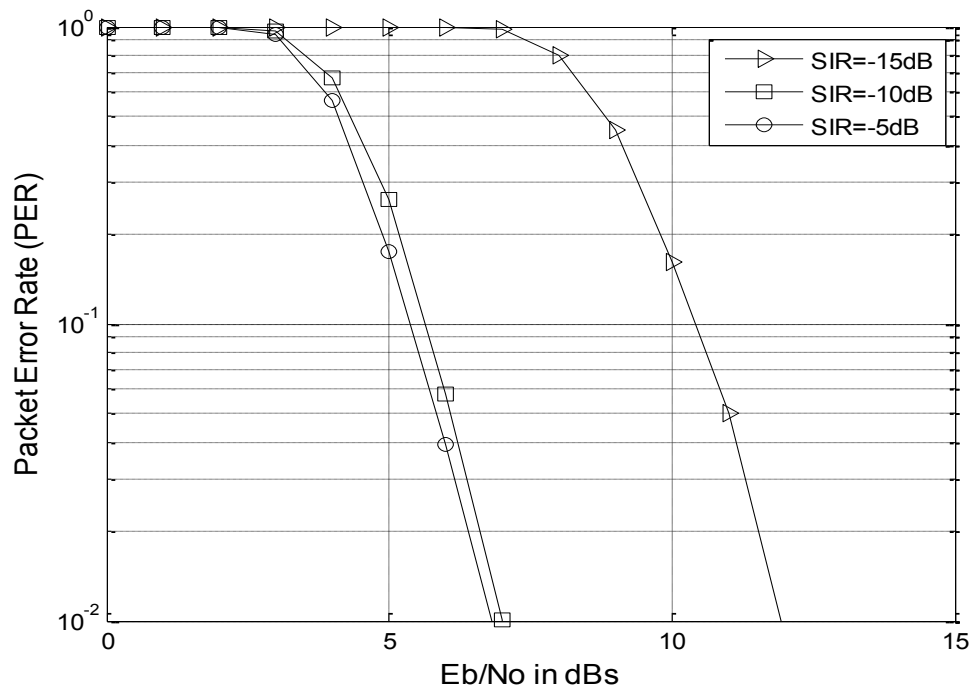


Figure 4.19 PER vs  $E_b/N_0$ ,  $p=0.001$ , Voice Application



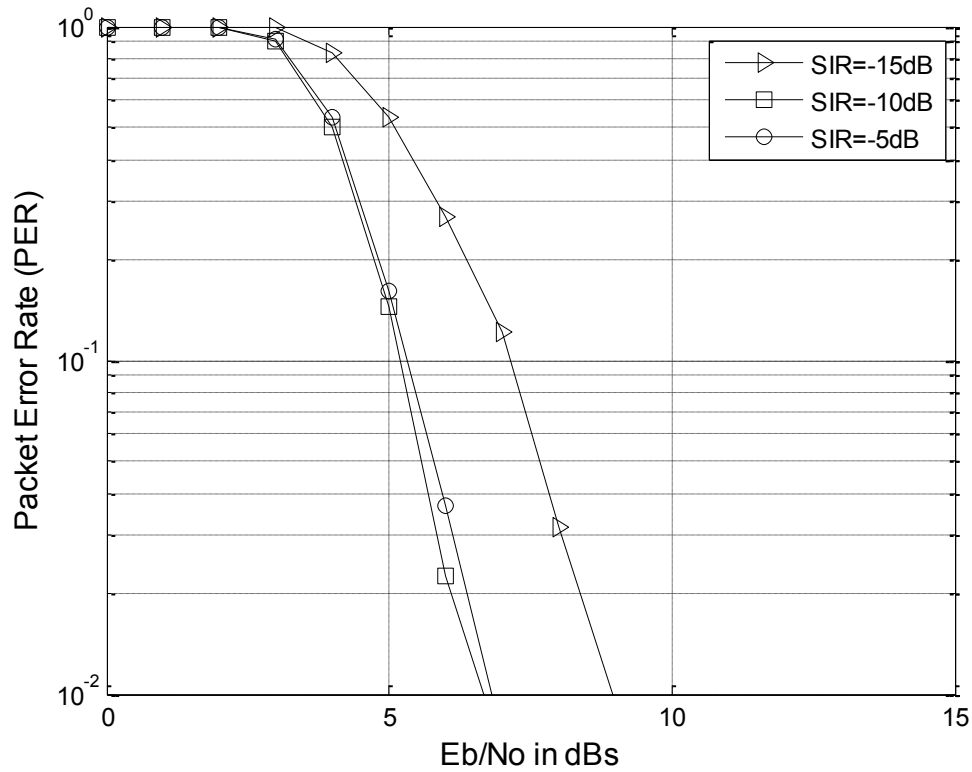


Figure 4.20 PER vs  $E_b/N_0$ ,  $p=0.0001$ , Voice Application

### 4.2.3 Throughput Performance

The throughput represents the number of messages that were successfully delivered over one unit time. The values of the throughput are influenced by the bandwidth, SNR, hardware latency etc. The throughput is computed using:

$$\text{Throughput} = (1 - \text{PER})^n \cdot \text{Data Rate}; \quad n = \text{size of the packet}. \quad (4.3)$$

Figures 4.21 – 4.24 show the throughput performance when  $E_b/N_0$  is varied for the both types of channels that are considered in this chapter, AWGN and AWGN with impulsive noise. The throughput depends on the values of BER, this means that when the  $E_b/N_0$  ratio increases the throughput increases as well. In the impulsive noise case the throughput performance is worse because the BER values obtained are poorer than in the AWGN case.

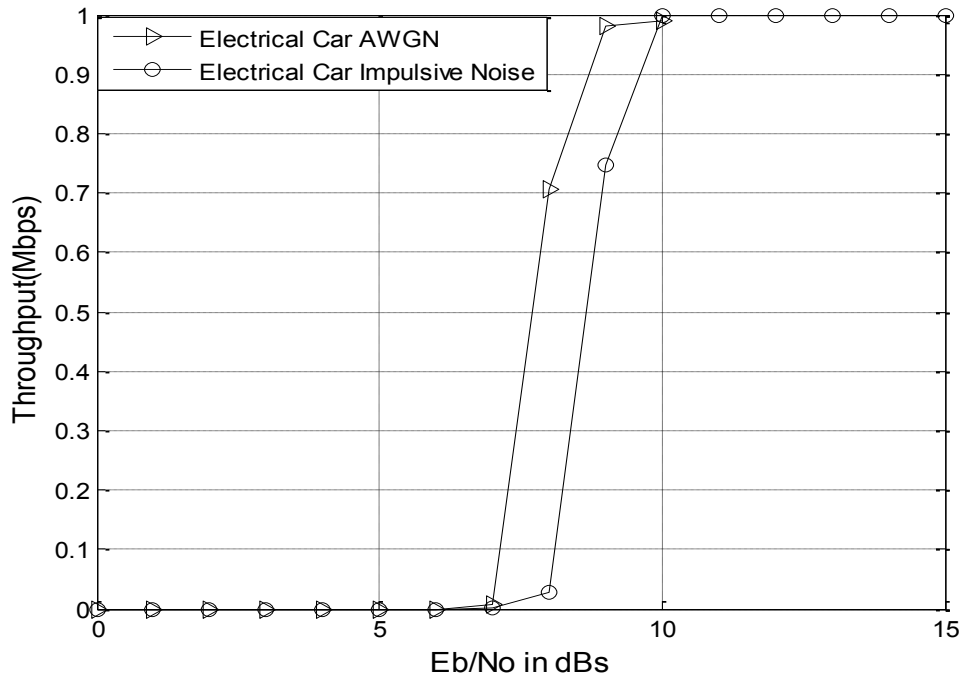


Figure 4.21 Throughput Performance vs  $E_b/N_0$  for AWGN and Impulsive Noise Channels for the Electric Car Applications

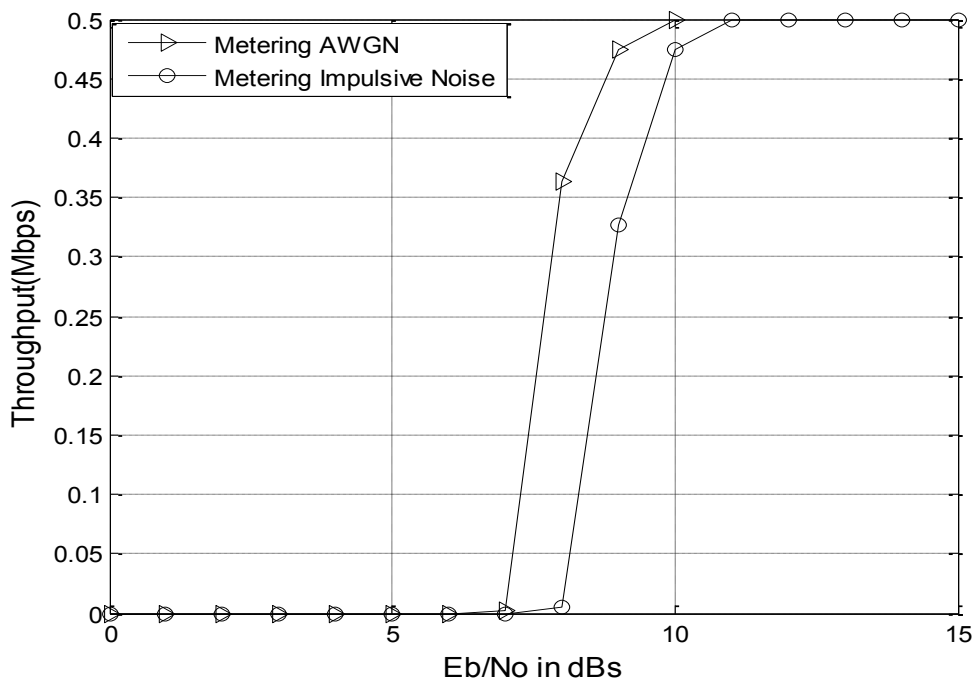


Figure 4.22 Throughput Performance vs  $E_b/N_0$  for AWGN and Impulsive Noise Channels for the Metering Application

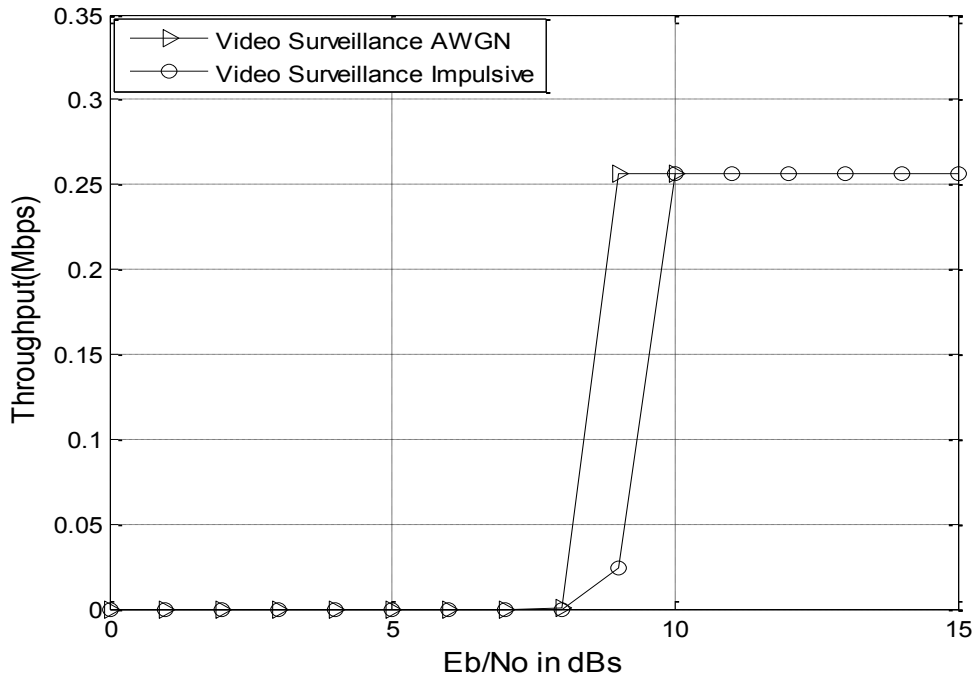


Figure 4.23 Throughput Performance vs  $E_b/N_0$  for AWGN and Impulsive Noise Channels for Video Surveillance Application

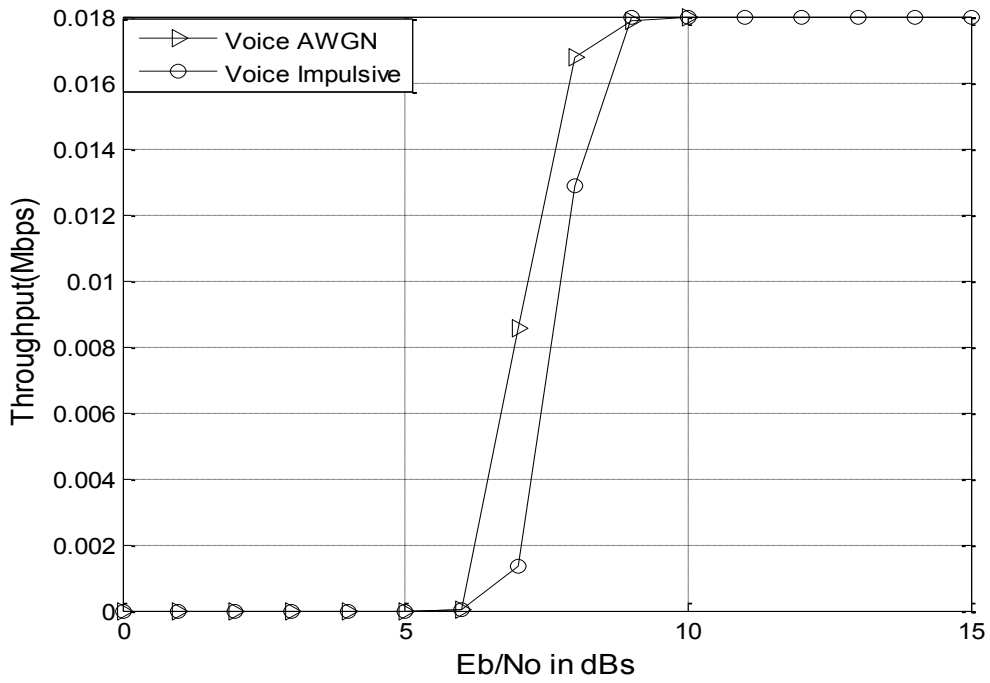


Figure 4.24 Throughput Performance vs  $E_b/N_0$  for AWGN and Impulsive Noise Channels for Voice Application

#### 4.2.4 Capacity of the Base Station

#### 4.2.5 Throughput Performance for Fixed traffic

Figure 4.25 shows the maximum number of collectors reached for  $E_b/N_0=8\text{dBs}$ . The uplink threshold imposed for the base station of 7.8Mbps is the value obtained after the simulations performed in OPNET. The maximum number of collectors that a base station can support is larger for impulsive channel due to the poorer performance of bit error.

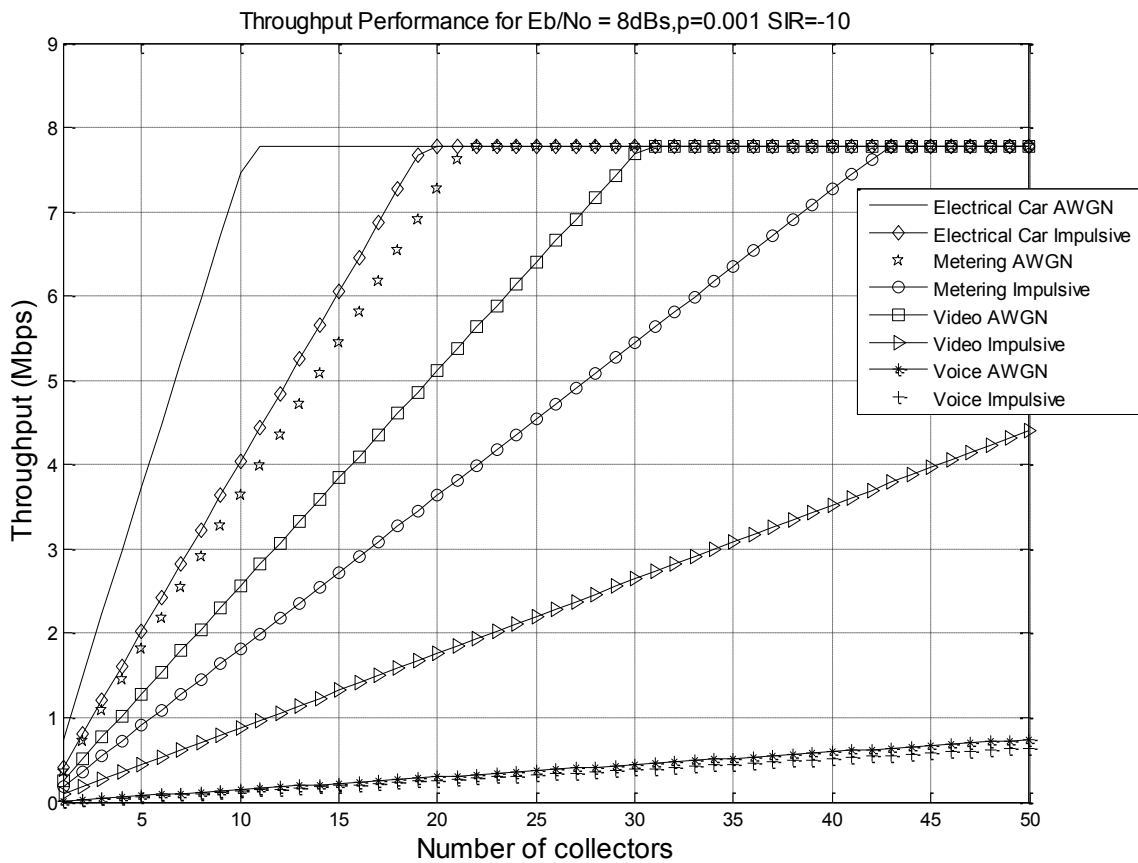


Figure 4.25 Number of collectors for each application that can be supported by the Base Station (AWGN and Impulsive Noise) when the start time is fixed

The maximum number of collectors for each application that a WiMAX base station can support given the parameters set in OPNET are provided in Table 4.6. The impulsive noise added to channel creates a very obvious difference in throughput performance.

Application	AWGN	Impulsive noise
Electric car	10 collectors	18 collectors
Metering	16 collectors	21 collectors
Video surveillance	21 collectors	87 collectors
Voice	Not reached	Not reached

Table 4.6 Maximum number of Collectors for fixed start-time distribution

Figure 4.26 shows the maximum number of collectors supported by the base station when all applications are sending information at the same time. The results are given for an  $E_b/N_0$  values of 8dBs. The difference of performance between the AWGN curve and the Impulsive Noise curve is noticeable. The maximum number obtained when only AWGN is present is 7 collectors while when having the impulsive noise added the number of collectors that can sent is 13. The difference is that when impulsive noise is considered, a large number of errors due to the burst of noise considerably affect the wireless communication leading to a difference of 6 collectors between the two types of channels.

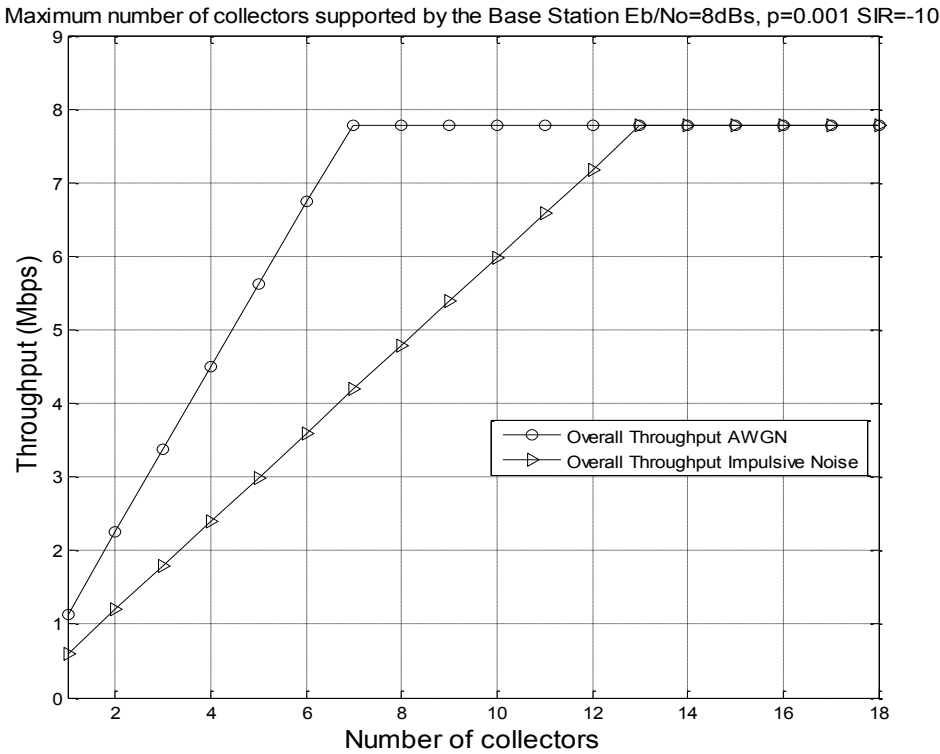


Figure 4.26 Number of collectors that can be supported by the Base Station (AWGN and Impulsive Noise) when all applications are sending information in the same time.

# Chapter 5

## Conclusions and Future Work

### 5.1 Conclusions

This thesis presents the performances of a WiMAX implementation of the smart grid's communication layer. Firstly, in the background chapter, we introduced the theoretical concepts of the traditional power grid along with its challenges. Subsequently, general concepts of smart grid were outlined while focusing on the communication layer, followed by WiMAX specifications and ending with a detailed discussion over OFDM and impulsive noise.

Chapter 3 introduced four smart grid applications, metering and pricing, video surveillance, electric car and voice support for workforce. The software OPNET was employed to simulate the send and received traffic by each of the applications. Their characteristics were assigned through profiles, applications, tasks and phases configurations. The topology of the network along with the characteristics of the base station and workstations were set according to the WiMAX specifications. The results obtained after simulating the WiMAX network layer used to implement the smart grid applications comprise the following categories: throughput analysis, total capacity of the base station, packet loss and latency.

At first, each application was individually simulated, thus determining the related capacity of the DAN base station. Due to a larger traffic sent on the uplink, the base station collecting traffic

from the electric car application is the first one to reach the capacity threshold, followed by the metering and pricing application, video surveillance and lastly voice support. When the packet loss is analyzed, the base station starts to drop packets after its capacity is reached. Similarly, the first application that experiences packet loss is the electric car followed by metering and pricing, video surveillance and voice. Moreover, the applications are experiencing latency in the same order as they are experiencing packet loss and capacity limitation. Each application has a maximum latency parameter that was added to their configuration and that assures a good functioning of the application without disturbing the performances. The electric car and metering application experience a level of latency beyond the maximum admitted by their configuration for the same number of collectors, with a high increase of latency. This is due to the high traffic generated for a short period of time for which the data waits in queue to be scheduled.

Chapter 4 investigates the effects of the impulsive noise over the smart grid's communication layer. The communication layer was implemented in MATLAB using the OFDM physical layer with WiMAX specifications. The traffic generated by each smart grid application was implemented through the subcarrier allocation. Changing the impulsive noise amplitude and probability of appearance varies the effect of the impulsive noise. The following performances were analyzed: BER for all applications, PER, throughput and the total capacity of the base station with and without the addition of impulsive noise. As expected, the performances are diminishing once the impulsive noise is affecting the transmission. The possibility of receiving erroneous symbol increases with the implication of impulsive noise. When the base station is not able to receive everything that is being sent, the level of packet drops is increased, resulting in the WiMAX base station being able to support a larger number of collectors.

## **5.2 Future work**

The following could be topics for future studies:

- 1) The implementation of different smart grid applications could be done using other communications standards such as LTE or other hybrid implementations making use of other available technologies. Also, several parameters of the application could be varied, such as the QoS class for different applications, and for better results, the AMC could be implemented. The

implementation of WiMAX from this thesis does not include mobility in the network, and future work could assign mobility trajectories.

- 2) The OFDM implementation using WiMAX physical layer characteristics was made without including the Forward Error Correction, interleaving and de-interleaving blocks. By including these blocks an improvement in the BER performance will be noticed.
- 3) The implementation from Chapter 4 assumed an AWGN channel with or without impulsive noise. Usually, the WiMAX standard is based upon the Stanford University Interim (SUI) Channel Model, which includes 6 sets of different channels featuring elements such as: terrain types, Doppler spreads, delay spreads, LOS – NLOS conditions. By implementing this type of channel the results from Chapter 4 will be comparable with the results from Chapter 3, since a SUI channel was selected in the OPNET implementation.



# Chapter 6

## References

- [1] Canadian Electricity Association, “Canada’s Electricity Industry”, June 10, 2014.
- [2] Canadian Electricity Association, “Key Canadian Electricity Statistics”, June, 2014.
- [3] Colorado Senate Bill 10-180, “Deploying Smart Grid in Colorado, Recommendation and Options”, Meridian Institute, December 2010.
- [4] Smart Grid, IESO Independent Electricity System Operator. [Online].  
Available (9/21/2015):  
<http://www.ieso.ca/Pages/Ontario's-Power-System/Smart-Grid/default.aspx>
- [5] M. E. Kantarci, H. T. Mouftah, “Wireless Sensor Networks for Smart Grid Application”, IEEE Ottawa Section Seminar, November 22, 2010.
- [6] M. E. Kantarci, H. T. Mouftah, “Wireless Networks for Domestic Energy Management in Smart Grids”, 25th Biennial Symposium on Communications, 2010.
- [7] E. W. Gunther, “Smart Grid 101 – Presentation”, IEEE Smart Grid, 2010.
- [8] Canadian Electricity Association, “Power for the future”. [Online].  
Available (9/21/2015):  
<http://powerforthefuture.ca/electricity-411/electricity-today/reliable-electricity/>
- [9] V. C. Gungor, G. P. Hancke, “Opportunities and Challenges of Wireless Sensor Networks in Smart Grid”, IEEE Transactions on Industrial Electronics, Vol.57, No.10, October 2010.
- [10] M. El Brak, M. Essaïdi, “Wireless Sensor Network in Smart Grid Technology: Challenges and Opportunities”, 6th International Conference on Sciences of Electronics, 2012.

[11] J. Girvan, "Consumer Council of Canada", March 2009. [Online].

Available (9/21/2015):

<http://www.consumerscouncil.com>.

[12] T. Bean, J. McGrory, "The Integration of Smart Meters Into Electrical Grids to Ensure Maximum Benefit for Consumers, Generators and Network Operators", Dissertation, Dublin Institute of Technology, May 2010.

[13] G. Rajalingham, Q.Ho, T. Le-Ngoc, "Random Linear Network Coding for Converge-Cast Smart Grid Wireless Networks", IEEE Communications (QBSC), 27th Biennial Symposium, June 2014.

[14] S. Panchadcharam, G.A Taylor, I. Pisica, M.R.Irving, "Modeling and Analysis of Noise in Power Line Communication for Smart Metering", Power and Energy Society General Meeting, 2012 IEEE.

[15] B. Sivaneasan, K.N. Kumar, P.L So, E. Gunawan, "A Hybrid PLC-WiMAX based Communication System for Advanced Metering Infrastructure", IPEC, 2012 Conference on Power & Energy, 2012.

[16] R. H. Khan, J. Y. Khan, "A heterogeneous WiMAX-WLAN network for AMI communications in the smart grid", IEEE SmartGridComm 2012 Workshop – Wireless Infrastructure for Smart Grid.

[17] V. C. Gungor, D. Sahin, T. Kocak, S. Ergut, C. Buccella, C. Cecati, G. P. Hancke, "Smart Grid Technologies: Communication Technologies and Standards", Industrial Informatics, IEEE Transactions on (Volume: 7, Issue: 4), 2011

[18] A. Mahmood, N. Javaid, S. Razzaq, "A review of wireless communications for smart grid", Renewable and Sustainable Energy Reviews, Vol. 41, January 2015, Pages 248–260

[19] IEEE Standard for WirelessMAN-Advanced Air Interface for Broadband Wireless Access Systems, 7 September 2012.

[20] WiMAX Forum, Mobile WiMAX – Part I: A Technical Overview and Performance Evaluation August, 2006.

[21] Rengaraju, C. H. Lung, A. Srinivasan, "Communication Requirements and Analysis of Distribution Networks Using WiMAX Technology for Smart Grids", Wireless Communications and Mobile Computing Conference (IWCMC), 2012 8th International.

[22] B. H. Walke, P. Seidenberg, M. P. Althoff, "UMTS the Fundamentals", Wiley, pp.111- 114, June 2003.

- [23] R. Prasad, F. J. Velez, “WiMAX Networks: Techno-Economic Vision and Challenges”, Springer Science & Business Media, June 2010.
- [24] C. H. Chiang, W. Liao, T. Liu, “Adaptive Downlink/Uplink Bandwidth Allocation in IEEE 802.16 (WiMAX) Wireless Networks: A Cross-Layer Approach”, IEEE GLOBECOM 2007.
- [25] Eun-Chan Park, “Efficient Uplink Bandwidth Request with Delay Regulation for Real-Time Service in Mobile WiMAX Networks”, IEEE TRANSACTIONS ON MOBILE COMPUTING, VOL. 8, NO. 9, 2009.
- [26] N. Dhillon, K. Sharma, J. Kaur Bisla, “Performance Evaluation of Punctured Convolutional Codes for OFDM – WiMAX System”, International Journal of Electrical and Electronics Research, Vol. 2, Issue 3, pp 142-148, September 2014.
- [27] N. Marchetti, M. Imadur Rahman, S. Kumar, R. Prasad, “New Directions in Wireless Communications Research”, Chapter 2 OFDM: Principles and Challenges, 2008.
- [28] G. D. Castellanos, J. Y. Khan, “Performance Analysis of WiMAX polling Service for Smart Grid Meter Reading Applications”, Communications Conference (COLCOM), 2012 IEEE Colombian.
- [29] M. Islam, M. M. Uddin, Md A. Al Mamun, M.A. Kader, “Performance Analysis of AMI Distributed Area Network using WiMAX Technology”, Strategic Technology (IFOST), 2014.
- [30] J. F. Aguirre, F. Magnago, “Viability of WiMax for Smart Grid Distribution Network, European International Journal of Science and Technology Vol. 2, No. 3, April 2013.
- [31] P.P.S. Priya, V.Saminadan, “Performance Analysis of WiMAX based Smart Grid Communication Traffic Priority Model”, Communications and Signal Processing (ICCSP), 2014 International Conference
- [32] OPNET Modeler 14.5 – OPNET Technologies, [Online]. Available : <http://www.opnet.com>
- [33] OPNET Modeler Suite, “Configuring Application and Profiles”. [Online]. Available (9/21/2015): [http://aetos.it.teithe.gr/~ziochr/network\\_lab/configuring\\_applications.pdf](http://aetos.it.teithe.gr/~ziochr/network_lab/configuring_applications.pdf)
- [34] A. S. Sethi, V. Y. Hnatyshin, “The Practical OPNET User Guide for Computer Network Simulation”, CRC Press, Taylor & Francis Group, 2013.
- [35] A. Bodonyi, “Effects of Impulse Noise on Digital Data Transmission”, Communications Systems, January 2003.
- [36] M. Nassar, K. Gulati, Y. Mortazavi, B. L Evans, “Statistical Modeling of Asynchronous Impulsive Noise in Powerline Communication Network”, Global Telecommunications Conference (GLOBECOM 2011), 2011 IEEE.

- [37] M. Mahbubur, R. S. P. Majumder, “Performance Improvement of a Power Line Communication System Using OFDM under the Effect of Fading and Impulsive Noise with Diversity Reception”, *Broadband and Biomedical Communications (IB2Com)*, 2011
- [38] J. D Parsons, A.U.H. Sheikh, “The characterization of impulsive noise and considerations for a noise-measuring receiver”, *Radio and Electronic Engineer*, January 2010.
- [39] O.Z. Batur, M. Koca, G. Dundar, “Measurements of impulsive noise in broad-band wireless communication channels”, *Research in Microelectronics and Electronics*, 2008.Prime 2008.
- [40] F. Sacuto, F. Labeau, B.L. Agba, “Wide Band Time-Correlated Model for Wireless Communications under Impulsive Noise within Power Substation”, *Wireless Communications, IEE Transactions on Volume 13, Issue 3*, March 2014.
- [41] E. Pérez Rodenas, “QAM and PSK Modulation Schemes under Impulsive Noise”, *University of Gävle, Faculty of Engineering and Sustainable Development*, 2012.
- [42] T. Y. Al-Naffouri, A. A. Quadeer, G. Caire, “Impulse Noise Estimation and Removal for OFDM Systems”, *IEEE TRANSACTIONS ON COMMUNICATIONS*, VOL. 62, NO. 3, 2014.
- [43] S. V. Zhidkov, “Impulsive Noise Suppression in OFDM Based Communication Systems”, *IEEE Transactions on Consumer Electronics*, Vol. 49, No. 4, NOVEMBER 2003
- [44] K. Khalil, P. Corlay, F. X. Coudoux, M. G. Gazalet, M. Gharbi, “Analysis of the Impact of Impulsive Noise Parameters on BER Performance of OFDM Power-Line Communications”, *7th International Symposium on Signal, Image, Video and Communications (ISIVC 2014)*
- [45] H. Yasui, A. Nakamura, M. Itami, “Reducing Impulsive Noise in OFDM Transmission Using Higher Order Modulation”, *IEEE International Conference on Consumer Electronics (ICCE)*, 2015
- [46] S. Ghadimi, J. Hussian, T. S. Sidhu, S. Primak, “Effect of Impulse Noise on Wireless Relay Channel”, *Wireless Sensor Network*, June 2012.
- [47] Alberto Leon-Garcia, “Probability, Statistics, and Random Processes for Electrical Engineering”, *Prentice Hall*, 2008.
- [48] V. K. Jain, S.N. Gupta, “Digital Communication Systems in Impulsive Atmospheric Radio Noise”, *Aerospace and Electronic Systems*, February 2007.
- [49] N. Ababneh, J. L. Rougier, “High Utility Guarantee Video Surveillance System Using IEEE 802.16 WiMAX Networks”, *Wireless Days (WD)*, 2012.
- [50] Silver Spring Networks, “How the Smart Grid Enables Utilities to Integrate Electric Vehicles”, June 2010.

[51] A. Shrestha, K. M. Elleithy, and S. S. Rizvi, "Investigating the effects of Encoder Schemes, WFQ & SAD on VoIP QoS," International Joint Conferences on Computer, Information, and Systems Sciences, and Engineering (CISSE 07), Bridgeport, CT, USA. December 3 - 12, 2007.